MINISTRY OF EDUCATION

THE ANNALS OF "DUNAREA DE JOS" UNIVERSITY OF GALATI

Fascicle IX
METALLURGY AND MATERIALS SCIENCE

YEAR XXXIX (XLIV)
June 2021, no. 2

ISSN 2668-4748; e-ISSN 2668-4756

2021
GALATI UNIVERSITY PRESS

EDITORIAL BOARD

THE ANNALS OF "DUNAREA DE JOS" UNIVERSITY OF GALATI
FASCICLE IX. METALLURGY AND MATERIALS SCIENCE
Nº. 2 - 2021, ISSN 2668-4748; e-ISSN 2668-4756
Volume DOI: https://doi.org/10.35219/mms.2021.2

Table of Contents

THE ANNALS OF "DUNAREA DE JOS" UNIVERSITY OF GALATI
FASCICLE IX. METALLURGY AND MATERIALS SCIENCE
Nº. 2 - 2021, ISSN 2668-4748; e-ISSN 2668-4756
Volume DOI: https://doi.org/10.35219/mms.2021.2

THE ANNALS OF "DUNAREA DE JOS" UNIVERSITY OF GALATI
FASCICLE IX. METALLURGY AND MATERIALS SCIENCE
Nº. 2 - 2021, ISSN 2668-4748; e-ISSN 2668-4756
Article DOI: https://doi.org/10.35219/mms.2021.2.01

MATHEMATICAL MODELING IN VIEW OF PROPERTY PREDICTION OF DD11 STEEL LAMINATED IN LBC LIBERTY GALATI

Marian-Iulian NEACȘU
"Dunărea de Jos" University of Galaţi, Romania
e-mail: uscaeni@yahoo.com

ABSTRACT

The paper presents a mathematical model for predicting the mechanical properties of hot rolled strips. The realization of this mathematical model relied on statistical measurements of the mechanical properties (R_m, $R_{p0,2}$ and A_5) for the laminated strip in the LBC rolling mill from the Liberty Steel Galati steel plant. To achieve this mathematical model, there has been used the active experiment method.

By means of this mathematical model, significant time and material savings can be made in the process of testing the mechanical properties for hot rolled tape.

KEYWORDS: mathematical model, statistical measurements, active experiment, mechanical properties

1. Introduction

Located in south-eastern Romania, Liberty Galati is the largest integrated plant in the country and a leader in the manufacture of steel products, with a current production capacity of 2 million tons of steel, with the possibility of increasing it. It is known that the current demand of the hot and cold rolled products market is decreasing, which makes the producers of low carbon rolled steel strips and sheets, to permanently increase the research on the way of elaboration, casting and their processing, thereby strengthening the values of mechanical properties necessary for appropriate machinability with beneficial results on the costs of the finished product.

Modeling in general and mathematical modeling in particular, is a basic tool in the design phase but also in the execution phase as well as in the analysis of the functioning of processes. To determine the optimum in a metallurgical process, mathematical modeling is used with the help of computers by using specialized programs [1].

Development of mathematical models in general and statistical data processing methods, in particular, recorded in a technological process made it possible for the optimal decision to be approached on the one hand as a matter of technical efficiency and on the other hand as a matter of high economic efficiency [2].

In the metallurgical industry, the mathematical model of that process can be used to calculate the optimal conditions for that process, but it can also be used to provide information on the optimal management of metallurgical processes [3].

Mathematical modeling by statistical methods has two important stages of realization:

- the first stage is called a preliminary experiment and has the role of solving the problem of selection of process factors as well as the interactions that may occur;
- the second stage called the experiment on which the operator relies to perform real modeling and statistical analysis of the model [4].

The variation of process factors is assessed in the preliminary experiment by performing a series of determinations based on programs (dispersion analysis, correlation analysis, etc.) which allow the selection of factors that significantly influence and highlight the links between factors and their contribution to the process [3, 5].

The paper aims to create a mathematical model for predicting the values of mechanical properties of hot rolled strips in LBC from the Liberty Steel Galati plant.

By using this mathematical model, a saving of time and material will be obtained by not performing the operations of effective mechanical tests to establish the values of the mechanical properties pursued.

THE ANNALS OF "DUNAREA DE JOS" UNIVERSITY OF GALATI
FASCICLE IX. METALLURGY AND MATERIALS SCIENCE
No. 2 - 2021, ISSN 2668-4748; e-ISSN 2668-4756
Article DOI: https://doi.org/10.35219/mms.2021.2.01

2. Experimental conditions

Slabs intended for the rolling process from DD11 quality are heated in propulsion furnaces. Heating is performed in order to transform the polyphasic structure of steel into a single-phase austenite structure and dissolve in its mass the carbides [6].

Three different chemical compositions (EC) for hot-rolled DD11 steel were taken into account: 1-CE = 0.1%; 2-CE = 0.09%; 3-CE = 0.08%.

The experimental data had as parameters besides the chemical composition, the rolling end temperature (T_{f1} = 900 ºC, T_{f2} = 870 ºC, T_{f3} = 840 ºC) and the winding temperature (T_{w1} = 606 ºC, T_{w2} = 600 ºC, T_{w3} = 594 ºC), hot rolled rolls. The hot rolling of the strips is done in a wide temperature range and is accompanied by phase transformations and structure transformation. The paper presents the elaboration of the equations of the mathematical model with the help of which the mechanical properties of the hot rolled strips in LBC Liberty Galati can be predicted.

Mathematical modeling was performed by the method of active experiment, when statistical methods are used in all stages of experimental research:

- before carrying out the experiment, by establishing the number of experiences and the conditions for their realization;
- during the development of experiments by processing the obtained results;
- after the end of the experiment through conclusions regarding the realization of future experiences. The programming of the experiment involves:
- establishing the necessary and sufficient number of experiences and the conditions for their realization;
- determining by statistical methods the regression equation, which represents with a certain degree of approximation, calculable, the process model;
- determining the conditions for achieving the optimal value of the process performance (parameter to be optimized).

3. Experimental results

In this paper we have made the mathematical model (regression equation) of the hot rolling process for steel slabs brand DD11, by statistical methods, namely regression analysis by active experiment. The equations of the elaborated mathematical model are of the form: $Y = f(x_1, x_2, x_3)$. We considered as main influencing factors (independent variables of the process of making hot rolled strips) the following technological processing parameters:

x_1 - carbon equivalent - C_E, [%];

x_2 - rolling end temperature - T_f, [ºC];

x_3 - winding temperature - T_w, [ºC].

Dependent variables (parameters to be optimized):

Y_1 - breaking strength, R_m, [MPa];

Y_2 - flow limit, R_{p02} [MPa];

Y_3 - specific elongation at break, A_5, [%];

In order to code the experiment, the following notations and symbols were used: x_1, x_2, x_3 - the independent variables (process parameters) and Y_1, Y_2, Y_3 - the dependent variables of the process.

There are the following links between natural and coded values of factors x_i:

$$x_1 = \frac{C_E - C_{E0}}{\Delta C_E}, x_2 = \frac{T_f - T_{f0}}{\Delta T_f}, x_3 = \frac{T_{\hat{i}} - T_{\hat{i}0}}{\Delta T_w} \quad (1)$$

where: C_E-carbon equivalent, %; C_{E0}-carbon equivalent, base value, %; ΔC_E-variation of C_E between upper and lower level and between basic and lower level; T_f - end rolling temperature, ºC; T_{f0} - end rolling temperature at the base level, ºC; ΔT_f - variation of T_{sf} between the upper level and the basic level and between the basic level and the lower level, ºC; T - temperature end of rolling, ºC; T_{w0} - end rolling temperature at the base level, ºC; ΔT_w - variation of $T_{\hat{i}}$ between the upper level and the basic level and between the basic level and the lower level, ºC; Y_i values are expressed in natural units.

Since the influence of the three factors on the performance of the process (Y) is studied, a complete factorial experiment of the type 2^3 has been achieved [2].

Extended matrix of the complete factorial experiment 2^3

Nr. exp.	X_0	X_1	X_2	X_3	X_1X_2	X_1X_3	X_2X_3	Y_1	Y_2	Y_3
1	+1	+1	+1	+1	+1	+1	+1	382	306	29
2	+1	-1	+1	+1	-1	-1	+1	380	304	30
3	+1	+1	-1	+1	-1	+1	-1	420	336	28
4	+1	-1	-1	+1	+1	-1	-1	395	316	27
5	+1	+1	+1	-1	+1	-1	-1	393	314	29
6	+1	-1	+1	-1	-1	+1	-1	383	306	29
7	+1	+1	-1	-1	-1	-1	+1	428	340	24
8	+1	-1	-1	-1	+1	+1	+1	320	320	26

THE ANNALS OF "DUNAREA DE JOS" UNIVERSITY OF GALATI
FASCICLE IX. METALLURGY AND MATERIALS SCIENCE
Nº. 2 - 2021, ISSN 2668-4748; e-ISSN 2668-4756
Article DOI: https://doi.org/10.35219/mms.2021.2.01

Based on the matrix of the complete factorial experiment, the coefficients of the regression equation are calculated (mathematical model). Considering the function Y_i as the analytical expression of the first order model, it is of the form:

$$Y = c_0x_0 + c_1x_1 + c_2x_2 + c_3x_3 + c_{12}x_1x_2 + c_{13}x_1x_3 + c_{23}x_2x_3 \quad (2)$$

$$Y_1 = 397.2 + 8.125 \cdot x_1 - 13.125 \cdot x_2 - 3.375 \cdot x_3 - 5.125 \cdot x_1 \cdot x_2 - 1.375 \cdot x_1 \cdot x_3 - 0.125 \cdot x_2 \cdot x_3$$

$$Y_2 = 317.5 + 6.25 \cdot x_1 - 10.25 \cdot x_2 - 2.25 \cdot x_3 - 3.75 \cdot x_1 \cdot x_2 - 0.75 \cdot x_1 \cdot x_3 - 0.25 \cdot x_2 \cdot x_3$$

$$Y_3 = 27.5 - 0.25 \cdot x_1 + 1.5 \cdot x_2 + 0.75 \cdot x_3 + 0 \cdot x_1 \cdot x_2 + 0.25 \cdot x_1 \cdot x_3 - 0.5 \cdot x_2 \cdot x_3$$

By replacing the coded variables xi with the relations (1) in the above equations and performing the related calculations, the following equations in natural quantities are obtained, equations that represent the mathematical model:

$$Y_1(C_E, T_f, T_w) = -1748.456 + 2799.3 \cdot C_E + 1.515 \cdot T_f + 2.102 \cdot T_i - 17.08 \cdot C_E \cdot T_f - 22.916 \cdot C_E \cdot T_i - 0.000694 \cdot T_f \cdot T_w \quad (3)$$

$$Y_2(C_E, T_f, T_w) = -1595 + 19000 \cdot C_E + 1{,}614 \cdot T_f + 1.958 \cdot T_w - 12.5 \cdot C_E \cdot T_f - 12.5 \cdot C_E T_i - 0.00138 \cdot T_f \cdot T_i \quad (4)$$

$$Y_3(C_E, T_f, T_w) = -1272.9 - 2525 \cdot C_E + 1.67 \cdot T_f + 2.099 \cdot T_w + 4.16 \cdot C_E \cdot T_w - 0.0027 \cdot T_f \cdot T_w \quad (5)$$

The equations: (3), (4), (5) make up the mathematical model of the studied process valid for: C_E = 0.08-0.1%, T_f = 840…900 ºC and T_w = 594…606 ºC.

Tables 1-3 show the measured values, those calculated using the mathematical model and the difference between the measured values and those calculated for the 3 mechanical properties studied.

Table 1. *Measured, calculated and the difference between measured and calculated values for R_m*

Nr. crt.	$Y_{1\ measured}$ R_m [MPa]	$Y_{1calculated}$ R_m [MPa]	$Y_{1meas} - Y_{1calc}$ [MPa]
1	382	384.098	-2.098
2	380	383.348	-3.348
3	420	410.93	9.07
4	395	403.68	-8.68
5	393	383.869	9.131
6	383	387.348	-4.348
7	428	419.201	8.799
8	400	406.451	-6.451

Table 2. *Measured, calculated and the difference between measured and calculated values for $R_{p0,2}$*

Nr. crt.	$Y_{2measured}$ $R_{p0,2}$ [MPa]	$Y_{2calculated}$ $R_{p0,2}$[MPa]	$Y_{2meas} - Y_{2calc}$ $R_{p0,2}$ [MPa]
1	306	308.996	-2.996
2	304	305.496	-1.496
3	336	337.332	-1.332
4	316	318.832	-2.832
5	314	315.404	-1.404
6	306	308.904	-2.904
7	340	342.747	-2.747
8	320	321.247	-1.247

THE ANNALS OF "DUNAREA DE JOS" UNIVERSITY OF GALATI
FASCICLE IX. METALLURGY AND MATERIALS SCIENCE
N°. 2 - 2021, ISSN 2668-4748; e-ISSN 2668-4756
Article DOI: https://doi.org/10.35219/mms.2021.2.01

Table 3. *Measured, calculated and the difference between measured and calculated values for A_5*

Nr. crt.	$Y_{3measured}$ A_5 [%]	$Y_{3calculated}$ A_5 [%]	$Y_{3meas} - Y_{3calc}$ A_5 [%]
1	29	29.11	-0.11
2	30	29.190	0.81
3	28	27.082	0.918
4	27	27.162	-0.162
5	29	28.09	0.91
6	29	29.169	-0.169
7	24	24.118	-0.118
8	26	25.197	0.803

Figures 1-6 show the variation of mechanical properties calculated with equations (3), (4), (5) depending on the values of the analysed factors, giving different values to the parameters of the studied process (C_E, T_f, T_w).

Figure 1 shows the variation of the mechanical properties R_m and $R_{p0.2}$, for different values of the C_E parameter, keeping constant, at the basic level, the values T_f and T_w.

Figure 2 shows the variation of elongation at break A_5, for different values of the C_E parameter, keeping constant, at the basic level, the values T_f and T_w.

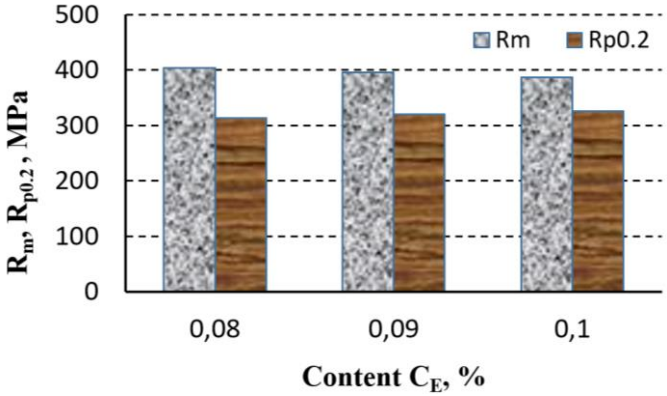

Fig. 1. *$R_m = f(C_E)$ and $R_{p0.2} = f(CE)$ for T_f = ct. and T_w = ct.*

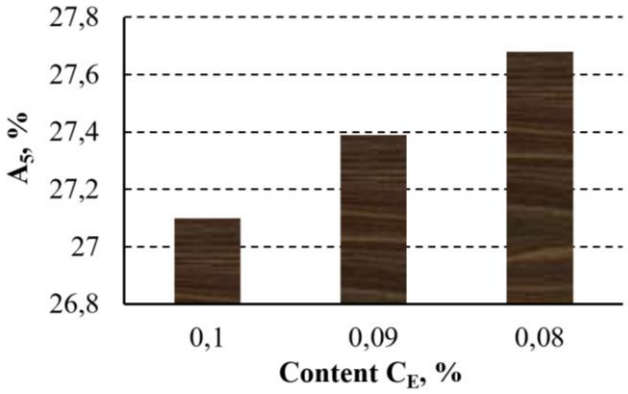

Fig. 2. *$A_5 = f(C_E)$ for T_f = ct. and T_w = ct.*

Figure 3 shows the variation of the mechanical properties R_m and $R_{p0.2}$, for different values of the parameter T_f, keeping constant, at the basic level, the values C_E and T_w.

THE ANNALS OF "DUNAREA DE JOS" UNIVERSITY OF GALATI
FASCICLE IX. METALLURGY AND MATERIALS SCIENCE
No. 2 - 2021, ISSN 2668-4748; e-ISSN 2668-4756
Article DOI: https://doi.org/10.35219/mms.2021.2.01

Figure 4 shows the variation of elongation at break A_5, for different values of the parameter T_f, keeping constant, at the basic level, the values C_E and T_w.

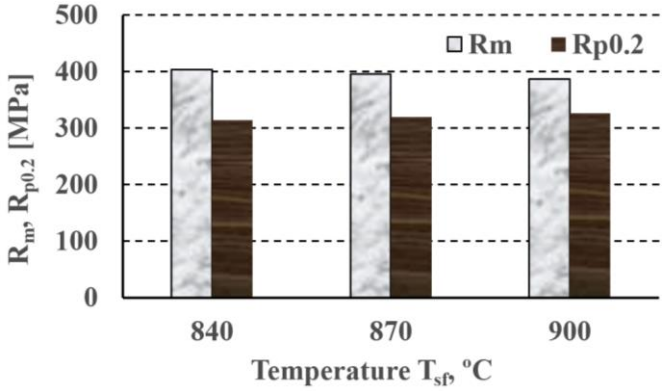

Fig. 3. *$R_m = f(T_f)$ and $R_{p0.2} = f(T_f)$ for C_E = ct. and T_w = ct.*

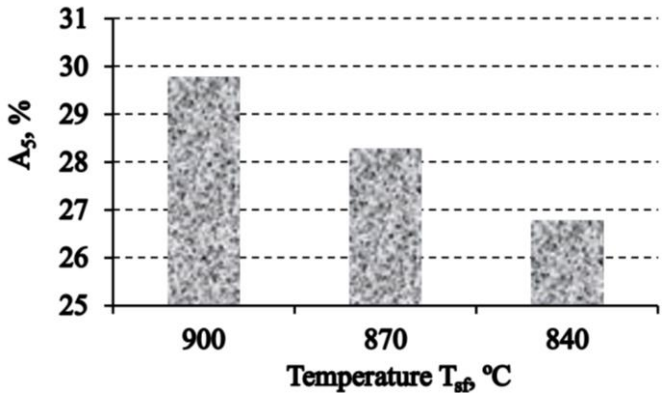

Fig. 4. *$A_5 = f(T_f)$ for C_E = ct. and T_w = ct.*

Figure 5 shows the variation of the mechanical properties R_m and $R_{p0.2}$, for different values of the parameter T_w, keeping constant, at the basic level, the values C_E and T_f.

Figure 6 shows the variation of elongation at break A_5, for different values of the parameter T_w, keeping constant, at the basic level, the values C_E and T_f.

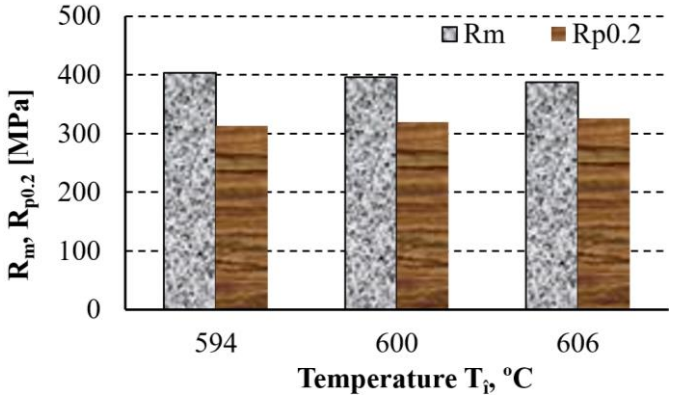

Fig. 5. *$R_m = f(T_w)$ and $R_{p0.2} = f(T_w)$ for C_E = ct. and T_f = ct.*

THE ANNALS OF "DUNAREA DE JOS" UNIVERSITY OF GALATI
FASCICLE IX. METALLURGY AND MATERIALS SCIENCE
Nº. 2 - 2021, ISSN 2668-4748; e-ISSN 2668-4756
Article DOI: https://doi.org/10.35219/mms.2021.2.01

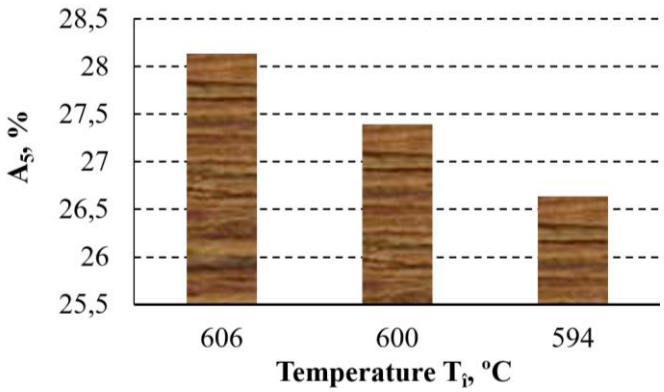

Fig. 6. *$A_5 = f(T_f)$ for C_E = ct. and T_w = ct.*

As it can be seen, the calculated values, using the mathematical model, for the parameter to be optimized Y_i (i = 1…3) are very close to the measured values. Therefore, the mathematical model presented in the set of equations (3), (4), (5) allows the prediction of the properties for DD11 steel laminated to LBC from the Liberty Steel Galati plant. The prediction of the properties is achieved by varying the values of the technological parameters, within the experienced limits.

4. Conclusions

The elaborated mathematical model can be described as a function with three parameters, each studied mechanical property (output quantity) depends on:

- C_E - carbon equivalent,
- T_f - end rolling temperature,
- T_w - temperature of the winding of the roller;

The differences between the values recorded when measuring the mechanical properties and those obtained by calculation based on the mathematical model developed, are small or very small.

The equations of the mathematical model, for the 3 studied mechanical properties, allow the prediction of the values of these properties by calculation, without the need of performing specific mechanical tests.

By using this mathematical model, time and money can be saved by those who apply it.

The elaborated mathematical model is in close accordance with the process of rolling hot strips.

References

[1]. Taloi D. Bratu C., Florian E., Berceanu E., *Optimizarea proceselor metalurgice*, E.D.P., Bucureşti 1983.
[2]. Taloi D., *Optimizarea proceselor tehnologice-aplicaţii în metalurgie*, Editura Academiei, Bucureşti, 1987.
[3]. Popescu D., Ionescu F., Dobrescu R., Stefanoiu D., *Modelare in ingineria proceselor industriale*, Editura AGIR Bucuresti, 2011.
[4]. Ciuca I., Dumitriu S., *Modelarea si Optimizarea proceselor metalurgice de deformare plastica si tratamente termice*, Ed. Didactica si Pedagogica, Bucuresti, 1998.
[5]. Baron T., *et al.*, *Statistică teoretică şi economică*, Editura Didactică şi Pedagogică, Bucureşti, 1995.
[6]. Cazimirovici E., *Bazele teoretice ale deformării plastice*, Ed. Bren Bucureşti, 1999.

THE ANNALS OF "DUNAREA DE JOS" UNIVERSITY OF GALATI
FASCICLE IX. METALLURGY AND MATERIALS SCIENCE
No. 2 - 2021, ISSN 2668-4748; e-ISSN 2668-4756
Article DOI: https://doi.org/10.35219/mms.2021.2.02

RESEARCH ON CONSTRUCTION AND SIZING OF THE METAL STRUCTURE OF A WINDING INSTALLATION

Marin-Silviu NAN[1], Dorina BĂDIȚĂ (POPESCU)[2], Danut GRECEA[3]
Cosmin VITAN[1], Bogdan BRĂNIȘTEANU[3]
[1]University of Petrosani, Romania
[2]Colegiu Tehnic "Constantin Brancus" Petrila, Romania
[3]National Institute for Research and Development in Mine Safety and Protection to Explosion - INSEMEX, Petrosani, Romania
e-mail: vitan.daniel.cosmin@gmail.com

ABSTRACT

The paper focuses on the design of the metal tower for the sinking of Netiș de-ventilating shaft in Râul Mare Retezat hydro-energetic setup. The analytical calculation of sizing and verification of the metal structure is doubled by the graphic simulation with speciality software, in view of obtaining results as close as possible to the real exploitation conditions of the tower. The tower of the de-ventilating shaft is considered to be a temporary construction, and its component parts will be decommissioned once the sinking is finalized. The tower is made up of metal structures in four transoms, 3 being mounted with junction plates and screws, the fourth being the roof.

KEYWORDS: winging installation, metal structures, design and simulation, de-ventilating shaft

1. Introduction

To improve the present utilization and exploitation conditions in Râul Mare Retezat hydro-energetic setup, it is necessary to sink a de-ventilating shaft; this is the object of the present paper. The de-ventilating shaft is a classical mining working, similar to those generally used for the extraction of useful mineral substances; what is particular in this case is the position conditions in a mountain area of the winding machine.

De-ventilating shafts are hydro technical workings intended to remove air from underground galleries, in order to increase and make even the flow of the handled water. This phenomenon is translated in supplementing the electricity production, determined by the reduction of the air resistance in case of water flow in the head race [1].

2. Establishing the load forces

The winding tower is stressed in time due to the hoisting of the sterile extracted during the sinking of the de-ventilation shaft. In the following, the conditions for the analytical calculation will be defined and materialized [1].

Thus, in Fig. 1 the calculation model is presented with the geometric dimensions of the tower to determine its state of load.

Determination of the position of the weight centre of the tower on the three geometric axes is calculated according to the weights of the transoms, the positions of the weight centres of each transom, the weight of the pulleys and their weight centres. The total weight of the tower in N is:

$$G = G_{ti} + G_m + G_{ts} + G_a + G_{ps} + 2 \cdot G_{ts} + G_{pd} + G_{mm} + 4 \cdot G_{m6} = 2.347 \text{ x } 10^5 \quad (1)$$

where: G_{ti} - lower transom weight, in N; G_m - intermediary transom weight of the tower, in N; G_{ts} - upper transom weight, in N; G_{ps} - weight of the upper platform of the tower, in N; G_a - tower roof weight, in N; G_{ts} - weight of the stair's transom of the tower, in N; G_{pd} - weight of the tower's discharge platform, in N; G_{mm} - weight of the 2000 pulley with support, in N; G_{m6} - weight of the 600 pulley, in N.

THE ANNALS OF "DUNAREA DE JOS" UNIVERSITY OF GALATI
FASCICLE IX. METALLURGY AND MATERIALS SCIENCE
N°. 2 - 2021, ISSN 2668-4748; e-ISSN 2668-4756
Article DOI: https://doi.org/10.35219/mms.2021.2.02

Position of the tower's weight centre, in mm:

$$z_G = \frac{K+G_{ts}\cdot z_{tsi}+G_{ts}\cdot z_{tss}+G_{pd}\cdot z_{pd}+G_{mm}\cdot z_{mm}+4\cdot G_{mб}\cdot z_{mбe}}{G} = 1.058 \text{ x } 10^4 \quad (2)$$

$$x_G = \frac{G_{ts}\cdot x_{tsi}+G_{ts}\cdot x_{tss}+G_{pd}\cdot x_{pd}+G_{mm}\cdot x_{mm}+2\cdot G_{mб}\cdot x_{mбe}+2\cdot G_{mб}\cdot x_{mбi}}{G} = 29.745 \quad (3)$$

$$y_G = \frac{G_{ts}\cdot y_{tsi}+G_{ts}\cdot y_{tss}+G_{pd}\cdot y_{pd}+G_{mm}\cdot y_{mm}+2\cdot G_{mб}\cdot y_{mбe}+2\cdot G_{mб}\cdot y_{mбi}}{G} = -54.334 \quad (4)$$

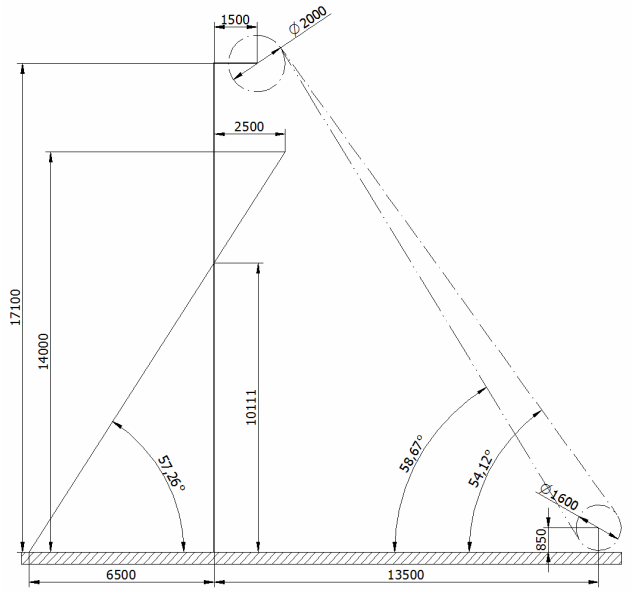

Fig. 1. *Calculation model*

In order to establish the maximum charging load of the tower, the inclination angle of the cable and anchor will be used, the height up to the pulley axis, the distance from the pulley axis to the tower axis, the weighs of the mobile bridge, the gripper trolley, the gripper, the useful load, weight of the cylinder, of the cable, together with the minimum and maximum length of the cable.[5]

Determination of the maximum load at the launching of the mobile bridge is determined with the formula:

$$S = G_{pm} + G_{tg} + G_g + G_{iu} + G_c + g_{cab} \cdot l_c = 5.568 \text{ x } 10^4 \quad (5)$$

where: G_{pm} - weight of the mobile bridge, in N; G_{tg} - weight of the gripper trolley, in N; G_g - weight of the gripper, in N; G_{iu} - weight of the useful load, in N; G_c - weight of the cylinder, in N; g_{cab} - specific weight of the Φ25 mm cable, in N/ml; l_c - minimum length of the cable, from the pulley to the bridge, in m.

Determination of the load vertically of the rocks taken out with the skip, is defined by the weight of the skip, transport of the materials taken out by skips, the weight of the skip, the weight of the safety hook, the weight of e-169 device, the weight of the slide carriage and of the skip load, all in N.

$$S_t = G_{ch} + G_{cr} + G_E + G_{sg} + G_{ic} + g_{cab} \cdot l_{cm} = 2.07 \text{ x } 10^4 \quad (6)$$

where: G_{ch} – 0.75 m^3 skip weight, in N; G_{cr} - safety hook weight, in N; G_E - E-169 device weight, in N; G_{sg} - slide carriage weight, in N; G_{ic} - skip load weight, in N; l_{cm} - maximum cable length, from the pulley to E-169, in m.

Determination of the tower strain vertically and horizontally, statically and dynamically, in N, is influenced by the dynamic coefficient of the winding installation, which is equal to 1.6.

THE ANNALS OF "DUNAREA DE JOS" UNIVERSITY OF GALATI
FASCICLE IX. METALLURGY AND MATERIALS SCIENCE
No. 2 - 2021, ISSN 2668-4748; e-ISSN 2668-4756
Article DOI: https://doi.org/10.35219/mms.2021.2.02

Case I: Determination of the stresses in the case of launching the mobile bridge:

$$H_1 = S \cdot \cos(\alpha) = 3.264 \text{ x } 10^4 \quad (7)$$

$$H_{1d} = H_1 \cdot C_d = 5.222 \text{ x } 10^4 \quad (8)$$

$$V_1 = S \cdot (1 + \sin(\alpha)) = 1.008 \text{ x } 10^5 \quad (9)$$

$$V_{1d} = V_1 \cdot C_d = 1.613 \text{ x } 10^5 \quad (10)$$

Case II: Determination of the stresses in the case of vertical transport of material:

$$H_2 = S_t \cdot \cos(\alpha) = 1.213 \text{ x } 10^4 \quad (11)$$

$$H_{2d} = H_2 \cdot C_d = 1.941 \text{ x } 10^4 \quad (12)$$

$$V_2 = S_t \cdot (1 + \sin(\alpha)) = 3.747 \text{ x } 10^4 \quad (13)$$

$$V_{2d} = V_2 \cdot C_d = 5.996 \text{ x } 10^4 \quad (14)$$

3. Verification of the tower

For the winding installation equipped with skip, the height of the winding tower, H_T, in *m*, from the ground to the upper platform on which the winding pulley is extracted, is calculated by the formula:

$$H_t = h_r + h_c + h_s + \frac{D_m}{2}, \text{ in m} \quad (15)$$

where: h_r represents the positioning height of the skip discharge ramp and material loading, in m. The material is loaded in vehicles by means of a loading chute, so that h_r = 8 m is adopted [3]; h_c - skip height together with the safety hook, the cable connecting device (to the upper clamp) and the skip guiding device, in m. Summing up the dimensions of the elements mentioned, h_c = 5.550 m results [4]; h_s - safety space in case the skip is over lifted, as a result of a handling error, in m, which is adopted at the value h_s = 1.45 m, imposed by the labour safety regulations, specific to small speed values; D_M - diameter of the winding pulley, in m, D_M = 2000 mm.

Fig. 2 shows the constructive dimensions and critical sections of the tower [2].

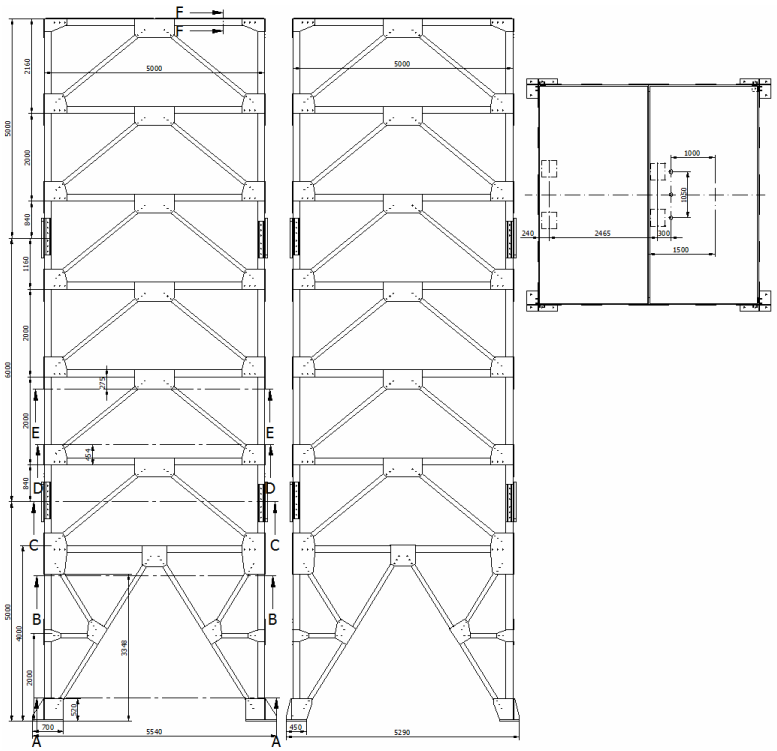

Fig. 2. *Constructive dimensions of the tower*

Establishing the geometrical characteristics of the critical transoms of the tower and the results of the modelling and simulation in specialised software are succinctly presented in Fig. 3-7.

THE ANNALS OF "DUNAREA DE JOS" UNIVERSITY OF GALATI
FASCICLE IX. METALLURGY AND MATERIALS SCIENCE
Nº. 2 - 2021, ISSN 2668-4748; e-ISSN 2668-4756
Article DOI: https://doi.org/10.35219/mms.2021.2.02

Thus in Fig. 3 section A-A through the lower transom of the tower is presented, for which the following geometrical characteristics have been established:

- Inertia moment for axis X-X, in mm^4 is 213611970443.74;
- Inertia moment for axis Y-Y, in mm^4 is 213531375516.67;
- Section area, in mm^2 is 37800.35;
- Maximum distance, in mm is 2500;
- Resistance module, in mm^3 $W_{xA} = 8.544 \times 10^7$ and $W_{yA} = 8.541 \times 10^7$.

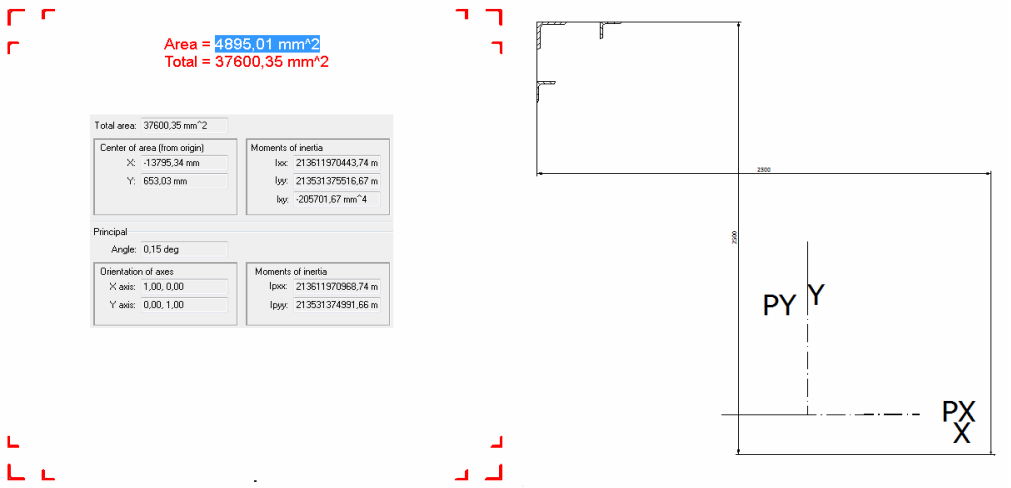

Fig. 3. *Geometrical characteristics of section A-A through the lower transom of the tower*

Fig. 4 shows section B-B through the lower transom of the tower.

In Fig. 4 A-A through the lower transom of the tower, for which the following geometric characteristics have been established:

- Inertia moment for axis X-X, in mm^4 equal to 267807002222.8;
- Inertia moment for axis Y-Y, in mm^4 equal to 267674515148.12;
- Section area, in mm^2 equal to 55610.95;
- Maximum, in mm equal to 2500;
- Resistance module, in mm^3 $W_{xB} = 1.071 \times 10^8$ and $W_{yB} = 1.071 \times 10^8$.

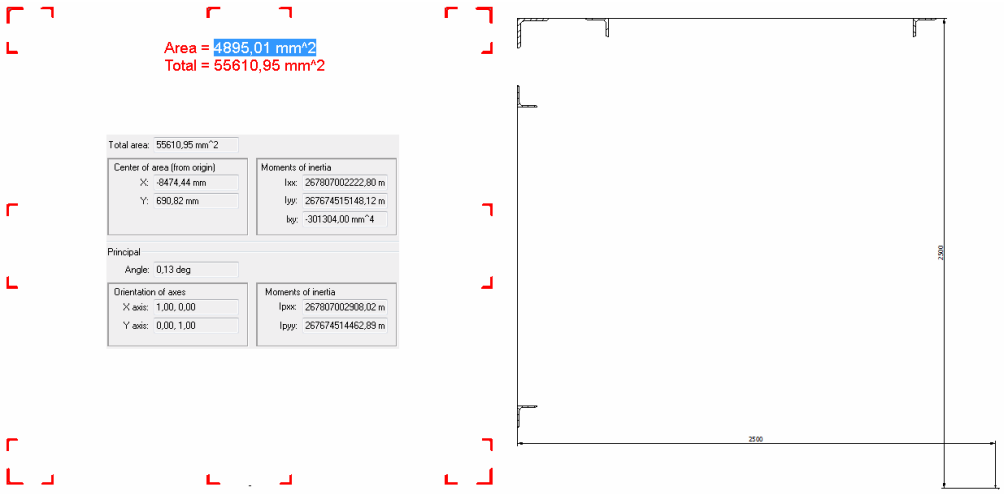

Fig. 4. *Geometrical characteristics of section B-B through the lower transom of the tower*

In Fig. 5 section C-C is presented through the joining area of the lower transom with the intermediary transom of the tower, for which the following geometric characteristics have been established:

- Inertia moment for axis X-X, in mm^4 equal to 310565505011.8;

THE ANNALS OF "DUNAREA DE JOS" UNIVERSITY OF GALATI
FASCICLE IX. METALLURGY AND MATERIALS SCIENCE
N°. 2 - 2021, ISSN 2668-4748; e-ISSN 2668-4756
Article DOI: https://doi.org/10.35219/mms.2021.2.02

- Inertia moment for axis Y-Y, in mm^4 equal to 310565310834.47;
- Section area, in mm^2 equal to 60352.53;
- Maximum distance, in mm equal to 2566;
- Resistance module, in mm^3 $W_{xC} = 1.21 \times 10^8$ and $W_{yC} = 1.21 \times 10^8$.

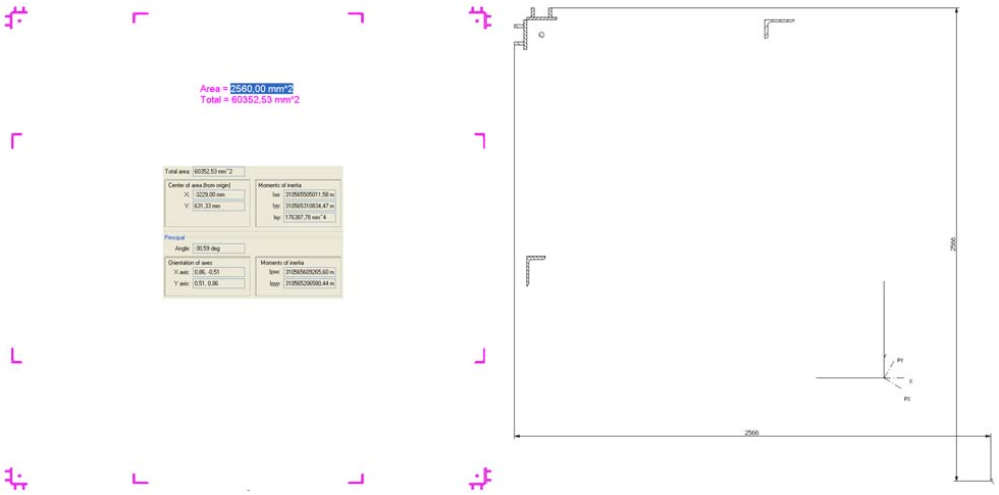

Fig. 5. *Characteristics of section C-C by joining lower and intermediate transoms of the tower*

Fig. 6 shows sections D-D and E-E by the intermediary transom of the tower, for which the following geometric characteristics have been established:

Geometric characteristics at section D-D:

- Inertia moment for axis X-X, in mm^4 equal to 241920563998.18;
- Inertia moment for axis Y-Y, in mm^4 equal to 241921289707.71;
- Section area, in mm^2 equal to 43825.13;
- Maximum distance, in mm equal to 2500;
- Resistance module in mm^3 $W_{xD} = 9.677 \times 10^7$ and $W_{yD} = 9.677 \times 10^7$.

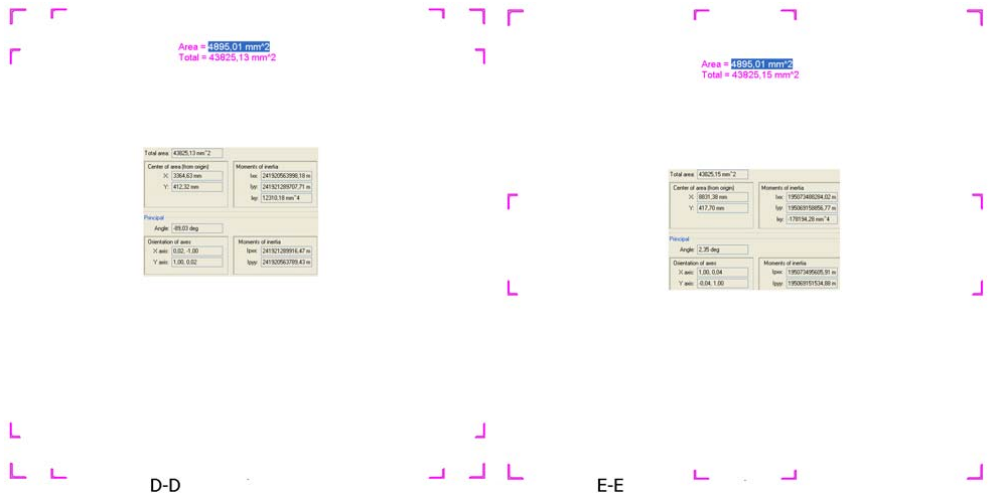

Fig. 6. *Geometric characteristics of sections D-D and E-E through intermediary transom of the tower*

Geometric characteristics at section E-E:

- Inertia moment for axis X-X, in mm^4 equal to 195073488284.02;
- Inertia moment for axis Y-Y, in mm^4 equal to 195069158856.77;
- Section area, in mm^2 equal to 43825.15;
- Maximum distance, in mm equal to 2500;
- Resistance module, in mm^3 $W_{xE} = 7.803 \times 10^7$ and $W_{yE} = 7.803 \times 10^7$.

Fig. 7 presents section F-F through the upper platform of the tower, for which the following geometric characteristics have been established:

THE ANNALS OF "DUNAREA DE JOS" UNIVERSITY OF GALATI
FASCICLE IX. METALLURGY AND MATERIALS SCIENCE
No. 2 - 2021, ISSN 2668-4748; e-ISSN 2668-4756
Article DOI: https://doi.org/10.35219/mms.2021.2.02

- Inertia moment for axis X-X, in mm^4 equl to 139159414.63;
- Inertia moment for axis Y-Y,in mm^4 equal to 120254491995.14;
- Section area, in mm^2 equal to 50707.8;
- Maximum distance, in mm equal to 128.39;
- Resistance module, in mm^3 $W_{xF} = 4.81 \times 10^6$ and $W_{yF} = 1.084 \times 10^7$.

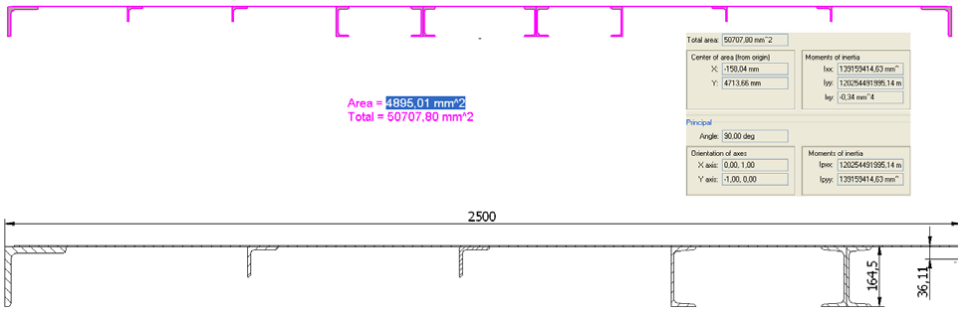

Fig. 7. *Geometric characteristics of section F-F through the upper platform of the tower*

By all the simulations and from the above mentioned succinctly presented facts, it was pointed out that the maximum values calculated and those resulted from simulations fall into the value range prescribed by the standards and norms in force in the moment of construction and exploitation of the winding machines.

4. Conclusions

The metal structure of the winding tower is modelled as a plane framework, which represent a simple undetermined static system, loaded with technological forces that occur in the winding cable and with mass forces given by the weight of the tower.

Maximum technological forces, applied in the symmetry centre of the winding pulley are calculated for two situations, a first case, for the rock transport by skip, and the second, to launch the mobile working bridge or take it out. Considering the importance of the installation, the safety norms impose a safety coefficient of more than 3, especially that people are also transported, so that the calculations adopt a dynamic coefficient of 1,6 by which the module of the technological forces used in the calculation of the metal structure is multiplied.

Thus, for the verification calculation of the winding tower, the components of the technological forces applied in the centre of the pulley are Fx = 19410 N and Fz = 59960 N, for the case of the transport of the material by skip and Fx = 52220 N and Fz = 161300 N, for the launching of the mobile working bridge or taking it out.

The tower weight is defined by the vector oriented according to axis z, having the module as sum of component elements weights, and the point of application calculated function of the weight centres of the component's elements.

Maximum tensions in the resistance structure of the tower occur in the area of the upper platform, this being demonstrated by the application of the methods of study of the stresses and deformations with the help of finite elements as well as, by using Cosmos Design Star and Abaqus utilities.

References

[1]. Adam C. D., *Instalaţii de extracţie miniere*, Partea I-a, II-a, Editura Universitas, Petroşani, 2008.
[2]. Băduţ M., Iosip M., *Bazele proiectării cu Solid Edge*, Editura Albastră, Cluj-Napoca, 2003.
[3]. Buzdugan Gh., *Rezistenţa materialelor*, Editura Didactică şi Pedagogică, Bucureşti, 1986.
[4]. Itu V., Dumitrescu I., Ridzi M. C., Magyari A., *Solicitări mecanice tehnologice ale turnurilor de extracţie miniere*, Editura Edyro Press, Petroşani, 2008.
[5]. Magyari A., Achim M. I., *Culegere de caracteristici tehnice pentru alegerea şi proiectarea instalaţiilor de extracţie miniere*, Litografia Institutului de Mine Petroşani, 1988.
[6]. ***, *COSMOS Design STAR Basic User's Guide*.
[7]. ***, *Solid Edge Software v.19. Academic license ADA Computers.*

THE ANNALS OF "DUNAREA DE JOS" UNIVERSITY OF GALATI
FASCICLE IX. METALLURGY AND MATERIALS SCIENCE
No. 2 - 2021, ISSN 2668-4748; e-ISSN 2668-4756
Article DOI: https://doi.org/10.35219/mms.2021.2.03

DETERMINING THE MAINTAINABILITY OF BURNING OVENS FROM CEMENT FACTORY

Teodor VASIU, Adina BUDIUL BERGHIAN, Corneliu BIRTOK BANEASA
University POLITEHNICA Timişoara, Engineering faculty of HUNEDOARA, Romania
e-mail: teodor.vasiu@fih.upt.ro

ABSTRACT

For any industrial entity put into operation, it is of interest to its ability to fulfil its mission under certain conditions, at a given time or during a given period of time, assuming that the means of maintenance are provided. This represents availability and is a complex form of system / product quality, as it includes both reliability and maintainability. Availability can be increased by: maximum reliability, maintenance, respectively by maximum maintainability, correct use of equipment / machines, renewal, optimization of reliability and maintainability characteristics, but provided that such balancing does not lead to contradictory solutions. The availability of a product will be higher the more reliable it is and requires less maintenance. It should be borne in mind that in order to ensure a certain level of reliability, maintenance costs must not exceed 10...20% of the purchase price of the product each year [1]. Restoration of reliability to a normal level is achieved through corrective or preventive maintenance. In practice, a compromise is sought between the purchase price, the service imposed and the accepted risk, as in order to achieve availability through reliability, very reliable parts must be used, which cost 5-10 times more than usual [2]. Maintenance-based availability results from the consideration that reliability is a probability of trouble-free operation over a period of time. Reliability is technically and financially limited. Defects in the initial period of operation of the product, as well as those in the final period derive from inevitable physical phenomena, and defects in the maturity period have a normal accidental character. In addition, the reliability can deteriorate over time even during storage, thus causing additional damage. Reliability is restored to its normal level through corrective or preventive maintenance, as failures are foreseeable or unpredictable. Product availability is the result of a combination of reliability and maintainability and they support each other. Increasing the maintainability of products leads to increased availability. In this case, the real maintainability of a burning oven of a cement factory was studied, with the aim of finding practical solutions to increase the service life. Achieving the proposed objective required monitoring the operation / failure of such equipment for nine months and statistical processing of the information obtained.

KEYWORDS: cement factory, burning oven, maintainability

1. Introduction

This introduction has the role of showing the place and importance of burning ovens in the technological flow of obtaining cement. Cement is a fine, grey powder, obtained by grinding clinker, gypsum, as well as additives (slag, limestone, etc.), judiciously dosed. Mixed with a limited amount of water, the cement sets and hardens, giving durability to the concrete or mortar in which it is incorporated. The manufacturing industry has a major role, being inconceivable the development and modernization of human society without the widespread use of cement. Cement production begins in quarries, with the excavation of limestone and clay. They are crushed and then transported to the factory, by conveyor belt systems and/or by rail. Limestone and clay are finely ground together with other materials that bring iron and/or silicon, each of the components being carefully

THE ANNALS OF "DUNAREA DE JOS" UNIVERSITY OF GALATI
FASCICLE IX. METALLURGY AND MATERIALS SCIENCE
No. 2 - 2021, ISSN 2668-4748; e-ISSN 2668-4756
Article DOI: https://doi.org/10.35219/mms.2021.2.03

dosed and analysed to comply with the flour preparation recipe, which is placed in the oven to obtain the clinker. Raw flour, heated in a rotary kiln to a temperature of up to 1,450 °C [3], is transformed by sudden cooling into a new, crystalline, granular-looking material called clinker, which is an intermediate - but essential - product in the manufacture of cement. After grinding the clinker, together with well-controlled dosages of gypsum and manufacturing additives (slag, limestone, etc.) at a particularly high fineness, the final product is obtained – cement. On the other hand, the appreciation of the production of cement factories is made according to the capacity offered by the burning oven (clinker). Therefore, any research on them is adequate.

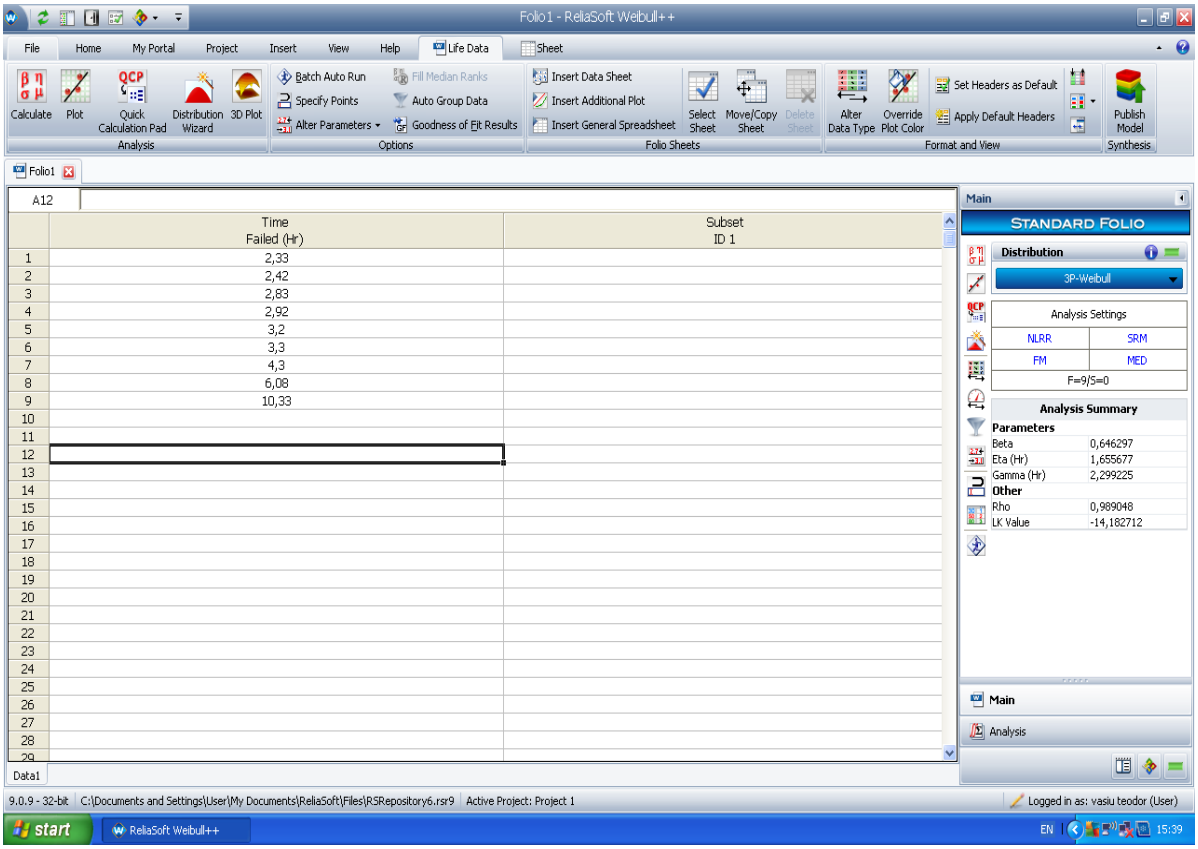

Fig. 1. *Maintenance times*

2. Recording and processing of experimental data

Determining the maintainability of burning ovens requires monitoring the operation of these equipment for as long as possible and recording the downtime due only to the repair of defects. Logistic delay times and administrative delay times are taken into account in the calculation of maintainability, because the real determination of maintainability was wanted. In this case, the follow-up was done daily for nine months, according to the recommendations from [1]. The purpose of this action is to determine the mathematical expression of the maintainability of the oven so that at any time of the repair - other than the recorded values - the probability of restoring the machine is known. This requires the use of laws and techniques for processing mathematical statistics. Following the application of statistical knowledge, the law of distribution of maintainability is determined, with a certain probability.

The processing of the experimental data was done with the Weibull ++ 9 software of the Reliasoft company [4]. The

maintenance times, introduced in the program, are shown in figure 1. The software used shows that the distribution law of maintenance times M(t) is Weibull (Figure 2), whose mathematical expression is [5]:

$$\mathbf{M(t) = 1 - e^{-\left(\frac{t-\gamma}{\eta}\right)^{\beta}}} \quad (1)$$

in which t[Hr] is the repair time.

THE ANNALS OF "DUNAREA DE JOS" UNIVERSITY OF GALATI
FASCICLE IX. METALLURGY AND MATERIALS SCIENCE
N°. 2 - 2021, ISSN 2668-4748; e-ISSN 2668-4756
Article DOI: https://doi.org/10.35219/mms.2021.2.03

Starting from the idea that the rate of falls is time-dependent (which largely agrees with the development of a wide range of phenomena), Weibull proposes for this indicator the following function:

$$z(t)=\frac{\beta}{\eta}\left(\frac{t-\gamma}{\eta}\right)^{\beta-1} \quad (2)$$

The three parameters of the Weibull distribution, results from Figure 1 are: the shape parameter (dispersion, slope) β = 0.646; the scale parameter η = 1,655 hours and the position parameter (initialization) γ = 2,299 hours.

In the case of the Weibull distribution, the average repair time of the MTR has the expression:

$$\mathbf{MTR}=\eta\Gamma\left(\frac{1}{\beta}+1\right) \quad (3)$$

in which Γ is the Eulerian integral (Gamma function) which has the expression:

$$\Gamma(p)=\int_0^{\infty} t^{p-1}e^{-t}dt \quad (4)$$

where p > 0 is a real parameter. In this case MTR ≈ η = 1,655 hours.

The Allan Plait diagram (Figure 2), whose coordinate axes are double - logarithmic, is used to certify the Weibull distribution law and to determine the parameters of this law.

The concavity to the right of the initial curve shows that the studied equipment is repaired most often after accidental falls, a fact that will be seen from Figure 3.

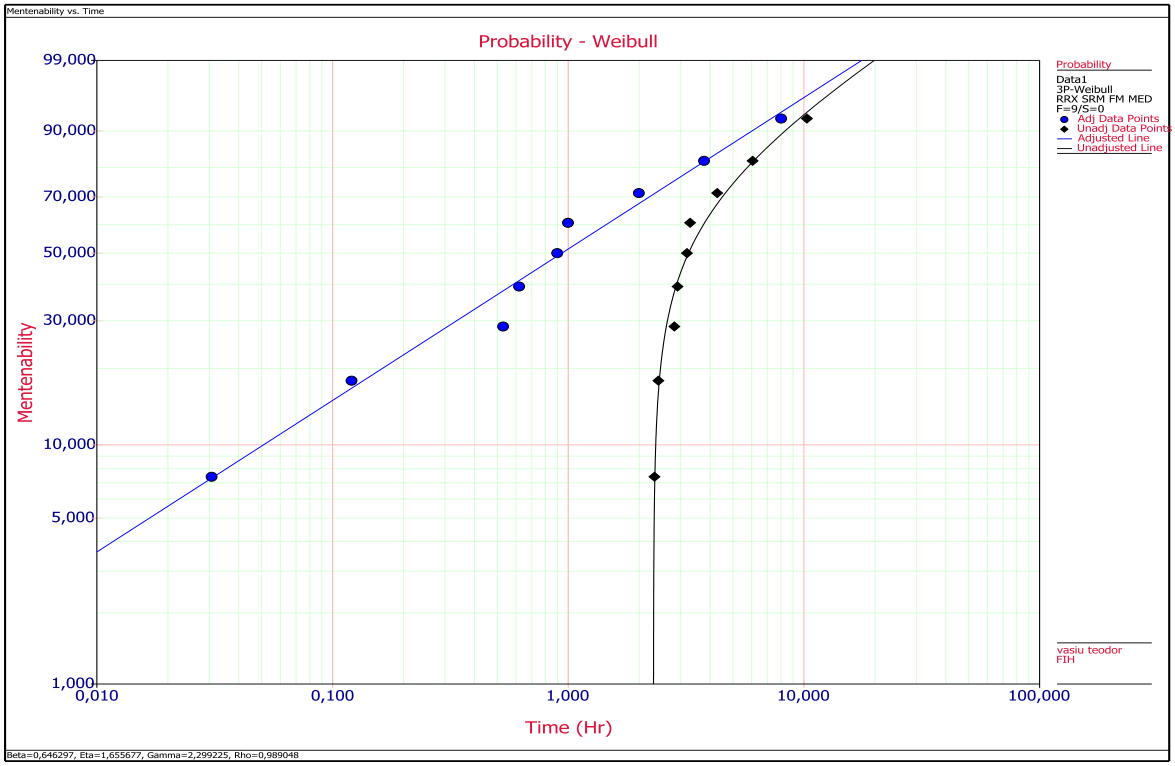

Fig. 2. *Allan Plait diagram*

3. Interpretation of the obtained results

The specialized literature offers few rules for interpreting the values of the statistical parameters of the distribution laws; that is why experience in the field has a major role [6-8].

The graphical representation, in cartesian coordinates, of the expression (1) is shown in Figure 3.

Figure 3 shows that from the moment t = 0 of the fall to t = γ = 2,299 hours the maintainability is zero i.e., in this time the probability of restoring the defective oven is zero. The reasons for the delay are related to the fact that the stops are usually accidental,

THE ANNALS OF "DUNAREA DE JOS" UNIVERSITY OF GALATI
FASCICLE IX. METALLURGY AND MATERIALS SCIENCE
No. 2 - 2021, ISSN 2668-4748; e-ISSN 2668-4756
Article DOI: https://doi.org/10.35219/mms.2021.2.03

in which case it is not possible to anticipate the necessary personnel for the intervention, the volume of materials, spare parts and the duration of the repair. Only after 2,299 hours the chances of repair begin to increase, reaching after about 16 hours that the probability of repairing the furnaces (maintainability) becomes maximum i.e., 1.

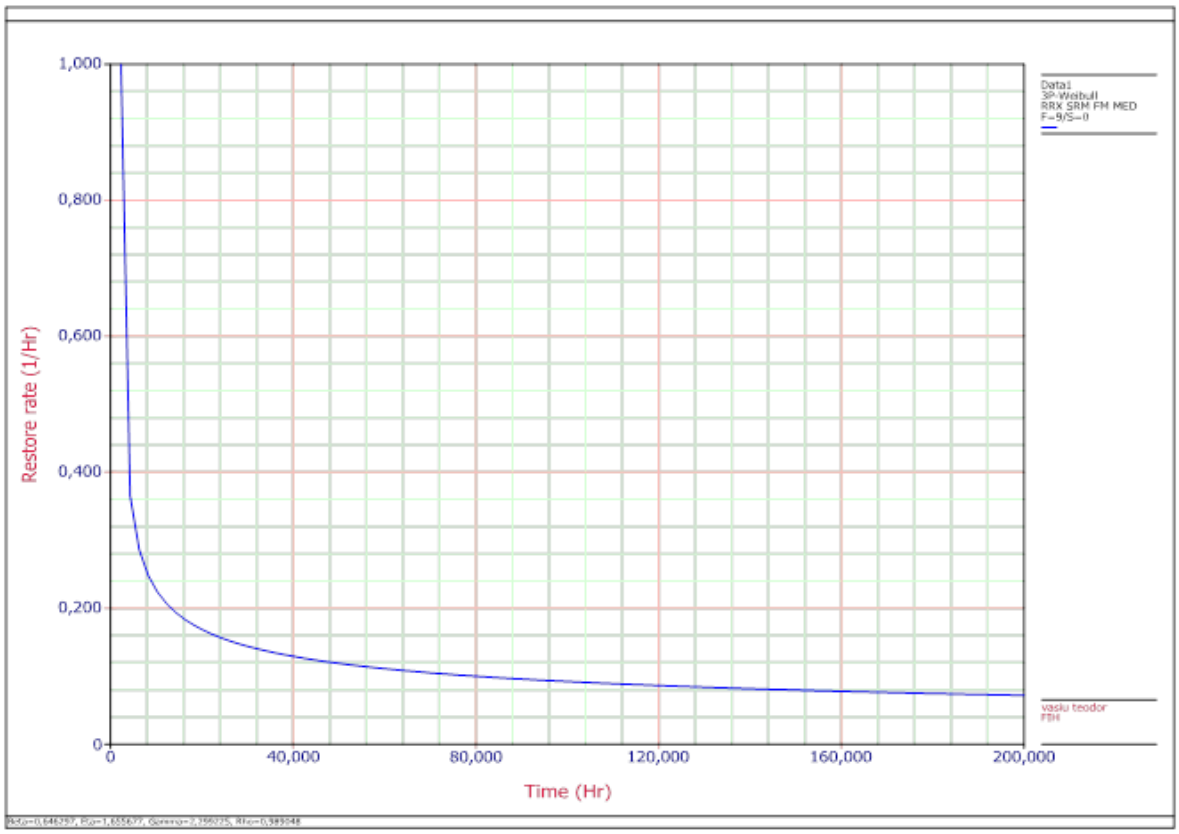

Fig. 3. *Maintainability versus time*

Although after 16 hours the probability of recovery is maximum, that time should not be considered as a minimum that can be exceeded no matter how much that in any case the maintainability does not decrease. Looking at figure 4 of the variation of the restoration rate over time, it is found that it decreases suddenly at a certain moment, which shows that although the possibility of repair is maximum, it is not done for various reasons that involve some very serious analyses.

The parameter $\beta = 0.646 < 1$, shows that the oven faults start before it is put into operation, which shows that its repairs are done improperly, which must also be analysed very well.

In statistics, the maximum verisimilitude function or the Likelihood function is used to determine the parameters of distribution laws. The method of maximum verisimilitude [5] proposes, for the case studied in the paper, the consideration of a sample that contains the values $t_1, t_2, \ldots, t_9$ of the random variable "repair time". The probability density $f(t_i, \beta, \eta, \gamma)$, $i = 1,2, \ldots, 9$ is known, of the variable "repair time", in which β, η and γ are the parameters of the Weibull distribution law:

$$\mathbf{f(t)} = \begin{cases} \dfrac{\boldsymbol{\beta}}{\boldsymbol{\eta}}\left(\dfrac{\mathbf{t}-\boldsymbol{\gamma}}{\boldsymbol{\eta}}\right)^{\boldsymbol{\beta}-1} \mathbf{e}^{-\left(\frac{\mathbf{t}-\boldsymbol{\gamma}}{\boldsymbol{\eta}}\right)^{\boldsymbol{\beta}}} & \mathbf{;\ if\ t} \geq \boldsymbol{\gamma} \\ \mathbf{0} & \mathbf{;\ if\ t} < \boldsymbol{\gamma} \end{cases} \quad (5)$$

The Likelihood function is:

$$\mathbf{Lk} = \prod_{\mathbf{i}=1}^{9} \mathbf{f}(\mathbf{t_i}, \boldsymbol{\beta}, \boldsymbol{\eta}, \boldsymbol{\gamma}) \quad (6)$$

The values of the parameters β, η and γ are determined from the condition that the probability function Lk has the maximum value i.e., the point estimators of the parameters β, η and γ are obtained from the solutions of the equations:

THE ANNALS OF "DUNAREA DE JOS" UNIVERSITY OF GALATI
FASCICLE IX. METALLURGY AND MATERIALS SCIENCE
Nº. 2 - 2021, ISSN 2668-4748; e-ISSN 2668-4756
Article DOI: https://doi.org/10.35219/mms.2021.2.03

$$\left[\frac{\partial Lk}{\partial \beta}\right]_{\hat{\beta}} = \left[\frac{\partial Lk}{\partial \eta}\right]_{\hat{\eta}} = \left[\frac{\partial Lk}{\partial \gamma}\right]_{\hat{\gamma}} = 0 \quad (7)$$

However, since the maximum of Lk occurs together with the maximum of the function lnLk, the values of the parameters β, η and γ are more easily determined from the equations:

$$\left[\frac{\partial \ln Lk}{\partial \beta}\right]_{\hat{\beta}} = \left[\frac{\partial \ln Lk}{\partial \eta}\right]_{\hat{\eta}} = \left[\frac{\partial \ln Lk}{\partial \gamma}\right]_{\hat{\gamma}} = 0 \quad (8)$$

Equations (8) are called Likelihood equations, and the solutions of the system of equations (8) are called maximum Likelihood estimates or maximum probability indicators.

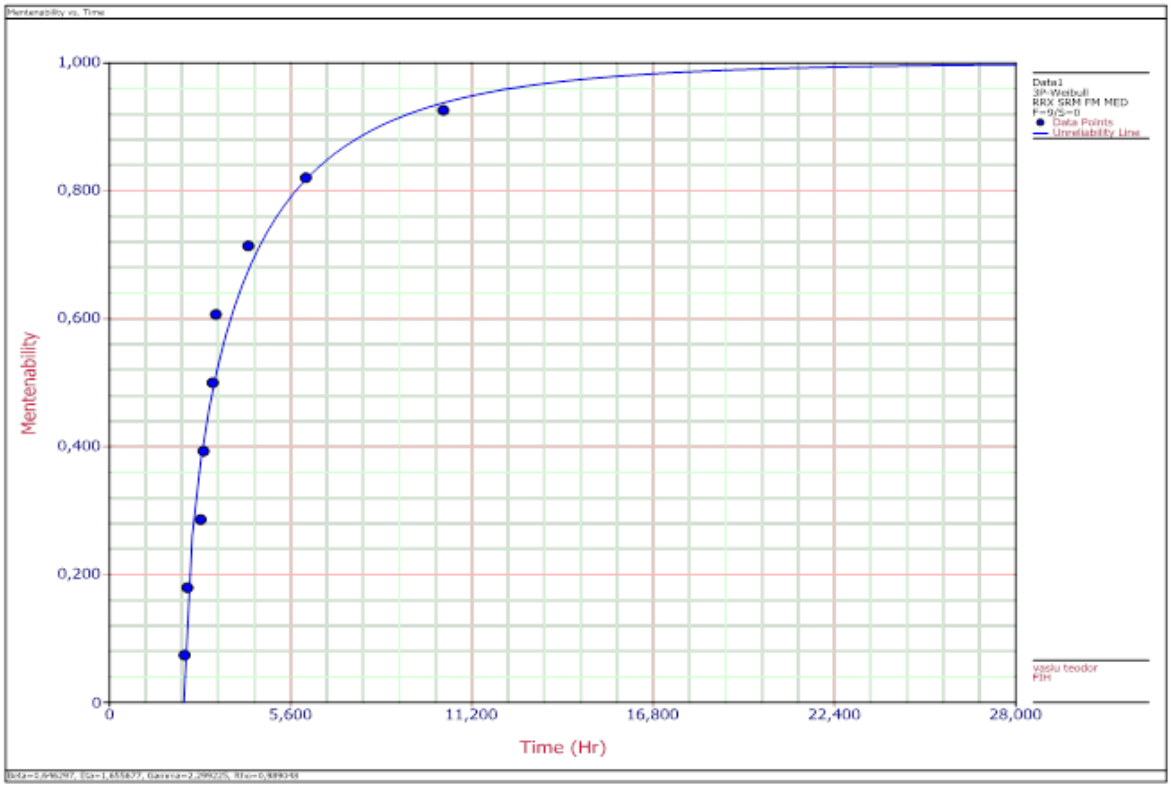

Fig. 4. *Restoration rate versus time*

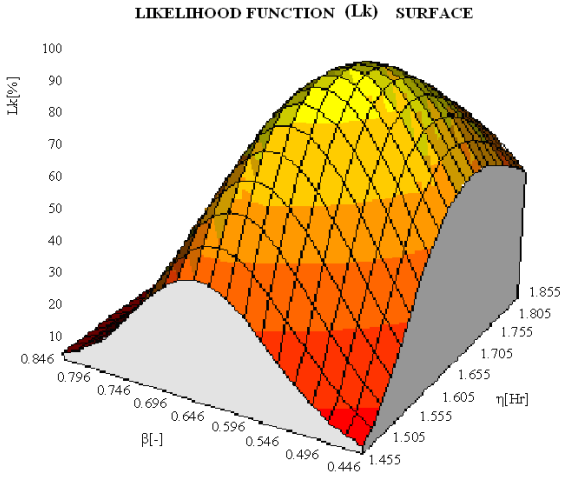

Fig. 5. *Likelihood function of maximum verisimilitude*

The problem can be asked the other way around: having the parameters β, η and γ you can calculate the Likelihood function and see if it is maximum (100%) or not. Figure 5 shows that the values β = 0.646 and η = 1,655 hours for γ = 2,299 hours, are the most likely.

4. Conclusion and proposals to reduce maintenance demands

In conclusion, drastic measures are required to reduce downtime for maintenance, especially those where maintenance is zero. From a mathematical point of view, it is necessary that the position parameter γ be as small as possible, if possible zero. This means knowing very well the defects that may occur, own maintenance personnel (not works in the company) who immediately notice the defect and start repairing it with logistical means prepared in advance. Ideally, $\gamma < 0$ i.e., the defect should be found

THE ANNALS OF "DUNAREA DE JOS" UNIVERSITY OF GALATI
FASCICLE IX. METALLURGY AND MATERIALS SCIENCE
N°. 2 - 2021, ISSN 2668-4748; e-ISSN 2668-4756
Article DOI: https://doi.org/10.35219/mms.2021.2.03

before it occurs. This is possible if a coherent system of predictive maintenance i.e., technical diagnosis, is adopted. The introduction of predictive maintenance involves funds allocated for the purchase of specific equipment and last but not least the training of maintenance personnel.

The mean time to repair is MTR = 1,655 hours, lower than any of the values of the parking times shown in Figure 1. This means that the analysed equipment stops for corrective maintenance, a situation in which the logistic support and the qualified personnel for repair are obtained relatively slowly, not being able to anticipate their size. Here is another reason to introduce predictive maintenance.

Another superior solution for reducing falls is the introduction of a proactive maintenance system. Proactive maintenance is aimed at reducing maintenance demands and maximizing equipment life by systematically eliminating the causes of failures [9].

Within the strategy, several priority objectives can be identified for furnace manufacturers and their users:

- Increasing production capacity by eliminating oven falls; permanent knowledge of the condition of the equipment so as to realistically evaluate the production capacity of the installation;
- Significant reduction of maintenance costs; anticipating and planning maintenance needs;
- Increasing the quality of production and reducing scrap;
- Reducing energy consumption through efficient operation of ovens;
- Reducing the need for spare parts;
- Increasing the safety of the ovens, which leads to the elimination of human accidents and material damage;
- Improving environmental conditions;
- Extending the life cycle of the ovens by eliminating the causes that generated the failure mode;
- Creating a maintenance-production-design team to ensure maximum capacity;
- Improving profit.

Within these objectives, preventive, predictive and proactive technologies act both independently and in conjunction.

Proactive maintenance or maintenance based on determining the root causes of failures uses advanced technologies to prevent the recurrence of failures. Repetitive faults are identified and eliminated by changing the designed parameters and operating conditions.

Valorisation of performance is used to ensure that the new or repaired oven will operate without malfunctions. It is based on the acceptability standards imposed by the equipment suppliers and on the verification of the fulfilment of the requirements of these standards.

The installation and operation of the ovens must be carried out in accordance with the accuracy required by the standards (especially for alignments, balancing), which leads to the extension of the life of the equipment.

Factors that shorten the life of furnaces are identified and significantly reduced by analysing the root causes of failures. If certain machine parts break down with a certain regularity, this fact, although it is accepted as a normality, constitutes the symptoms of much more serious problems. Traditional maintenance solves only the symptoms of problems and accepts frequent repairs as normal.

Root cause analysis is based on a set of analytical and engineering procedures for identifying and correcting developmental problems. The application of such a program leads to remarkable savings and a significant reduction in the failure of the burning ovens of cement plants. As a result of various technologies, it is necessary to redesign, modify and improve existing components or to provide new components. The proactive maintenance aims to determine and analyse the failure rate of the critical components of the furnace and on this basis the adaptation of components with better reliability or redundant elements. Industrial practice shows that elements with high reliability are the best solution.

The implementation of the program requires a balanced strategy between preventive, predictive and proactive maintenance. Within this strategy, predictive maintenance is the point of equilibrium. Knowing the condition of the equipment offered by preventive maintenance, the components are selected that are treated preventively and proactively, respectively, taking into account technical and economic criteria. Usually, the programs start on a small scale, and after the first successes, after 6-12 months the program is extended.

The program will include three stages of implementation:

- initiation, training, primary results;
- extension of preventive maintenance and introduction of proactive maintenance;
- mature proactive maintenance program.

Usually, the first stage the program is considered as an attempt to introduce new concepts. This stage is recommended primarily for equipment that benefits from corrective maintenance (as is the case of the studied oven) or where preventive maintenance is incipient. At this stage, the organizational structure of the maintenance department changes by the emergence of two new groups: the planning team and the reliability improvement team. The duties of the first group must

include: coordination of all preventive activities, including technical diagnosis actions; coordination of maintenance activities with production, in order to obtain the least possible impact on availability; coordination of predictive and proactive activities; planning of maintenance works including procedures, tools, spare parts, inspections, calibrations; tracking work orders and costs; updating the equipment history files; evaluation of the trend of the life cycle of the equipment that need improvements; spare parts inventory.

The team of improving the reliability is initially oriented towards the implementation of the preventive maintenance of the furnace and the guidance towards the proactive maintenance. The team consists of one or two specialists in vibration analysis, a specialist in thermography and a specialist in lubricant analysis. The group's responsibilities include: involvement in the direct operation of the furnace and the application of predictive maintenance technologies; providing data on the condition of the furnace to the planning team in order to eliminate unplanned shutdowns; implementation of proactive technologies and respective methods, with identification of repetitive problems; performance monitoring, availability analysis, maintenance costs, quality; identification of schooling needs; identification of parts that need redesign in order to improve reliability.

In the second stage of implementation i.e., the second and third year of the program, several maintenance technologies are added. These technologies include precision alignment, balancing and analysis of the causes of failures. At this stage the attitude of production towards maintenance will change. Management will eliminate production interruptions, and the attitude of employees will be oriented towards preventing and eliminating the causes of failures.

The last stage of program implementation is materialized in the total change of attitude towards the maintenance department. The stage is materialized by an aggressive strategy of eliminating production interruptions and increasing the quality of the product (clinker) by maintaining the performance of the oven in the parameters.

This concept of maintenance based on reliability represents a progress in the development of the maintenance activity, of tightening the links between maintenance and production, the latter being interested in improving the quality and increasing the productivity.

References

[1]. Baron T., Isac Maniu A., Tovissi L., Niculescu D., Baron C., Antonescu V., Roman I., *Calitate şi fiabilitate - manual practic*, vol. 1 şi 2 (Quality and reliability - practical manual, vol. 1 and 2), Editura Tehnică, Bucureşti, 1988.
[2]. ***, https://ro.wikipedia.org/wiki/Ciment.
[3]. Cadar I., Clipii T., Tudor A., *Beton armat (Reinforced concrete)*, ediția a 2-a, Editura Orizonturi Universitare, Timișoara, 2004.
[4]. ***, www.reliasoft.com.
[5]. Mihoc Gh., Muja A., Diatcu E., *Bazele matematice ale teoriei fiabilităţii (The mathematical foundations of reliability theory)*, Editura Dacia, Cluj-Napoca, 1976.
[6]. Vasiu T., *Fiabilitatea sistemelor electromecanice (Reliability of electromechanical systems)*, Editura Bibliofor, Deva, 2000.
[7]. Vasiu T., Budiul Berghian A., *Reliability of clincher burners from cement industry*, Annals of Faculty of Engineering Hunedoara – International Journal of Engineering, Tom XVI, Iss. 3 August 2018.
[8]. Vasiu T., Budiul Berghian A., *Determining the reliability of clincher coolers*, The Annals of the University of Dunarea de Jos of Galati, Fascicle IX. Metallurgy and Materials Science, no. 3, p. 51-56, 2018.
[9]. Banescu A., *Menetenanţa bazată pe fiabilitate – noua viziune pentru îmbunătăţirea calitii şi productivităţii (Reliability-based maintenance - the new vision for improving quality and productivity)*, Asigurarea Calităţii – Quality Assurance, Anul I, Numărul 1, Ianuarie-Martie, 1995.

THE ANNALS OF "DUNAREA DE JOS" UNIVERSITY OF GALATI
FASCICLE IX. METALLURGY AND MATERIALS SCIENCE
N°. 4 - 2021, ISSN 2668-4748; e-ISSN 2668-4756
Article DOI: https://doi.org/10.35219/mms.2021.2.04

ASSESSMENT OF $PM_{2.5}$ AND PM_{10} EMISSIONS IN THE METALLURGICAL INDUSTRY FROM ROMANIA

Carmelia Mariana DRAGOMIR BĂLĂNICĂ, Daniela Ecaterina ZECA, Vasile BAȘLIU*, Ștefan PINTILIE
"Dunarea de Jos" University of Galati, Romania
e-mail: vasile.basliu@ugal.ro

ABSTRACT

The article focuses on the evaluation of $PM_{2.5}$ and PM_{10}, pollutants resulting from the metallurgical industry in Romania. The analysed period is 2008-2018 and the dataset was provided by the National Institute of Statistics. The purpose of this paper is to examine the impact of final energy consumption in the metallurgical industry on PM_{10} and $PM_{2.5}$ emissions. We included in the study three fundamental factors: the final energy consumption in the metallurgical industry and the particulate matter (PM_{10} and $PM_{2.5}$). The average of PM_{10} for reference period is 4026 Tone (Mg) while for the $PM_{2.5}$ the average is 3645 Tone (Mg). The trend of final energy consumption in the metallurgical industry is identical to the trend of $PM_{2.5}$ and PM_{10}, which indicates that this factor has a major influence on the amount of $PM_{2.5}$ and PM_{10} emissions. $PM_{2.5}$ and PM_{10} emission factors represent primary emissions from the metallurgical industry activities and do not consider the formation of secondary aerosol from chemical reaction in the environment afterwards the discharge.

KEYWORDS: PM_{10}, $PM_{2.5}$, energy consumption, metallurgical industry

1. Introduction

Air pollution is presently the most critical environmental threat to human health, and it is considered as the second major environmental concern for Europe, following climate change [1]. More than that the air quality has an essential impact on human health and aquatic and terrestrial ecosystems.

In the last decades constant concentrations of dust particles with aerodynamic diameters ≥ 10 μm (PM_{10}) and fine particulate matter < 2.5μm ($PM_{2.5}$) have been an important issue for air in terms of achieving the limits of pollution and the relevant related health hazards. According to European Environment Agency (EEA) among 2006 and 2016, the exposure of citizens to concentrations of $PM_{2.5}$ above the EU limit was diminished from 16% to 5%, while the PM_{10} concentrations has decreased from 32% to 13% over the period 2000-2016 [2].

Efficient measures to decrease air pollution and its effects demand a proper comprehension of its sources, transport and circumstances of different transformation in the atmosphere, the chemical composition alterations during a certain period and the effect of pollutants on population, flora and fauna and afterwards the impact on community and on economy [3, 4].

Low incomes population is living in major area of Europe, more frequently those who reside close to busy streets or industrial zones consequently confront larger vulnerability to air pollution. Energy neediness is further predominant in southern and central-eastern Europe and it is a major factor of the burning of low-quality solid fuels, such as charcoal and wood, in low-efficiency furnaces for domestic heating [5]. This causes significant vulnerability of the poor inhabitants to particulate matter (PM) and polycyclic aromatic hydrocarbons (PAHs), either inside and outside [6].

As stated by EEA the dominant sectors contributing to pollution of atmosphere in Europe are: transport (road and non-road); housing, commercial and institutional; energy providers; production and mining industry; agriculture; and waste management [7, 8].

The metallurgical operations require melting techniques, improvement of alloys and casting in various forms contingent on the demand. Fundamentally, extraction of the metal and

THE ANNALS OF "DUNAREA DE JOS" UNIVERSITY OF GALATI
FASCICLE IX. METALLURGY AND MATERIALS SCIENCE
Nº. 4 - 2021, ISSN 2668-4748; e-ISSN 2668-4756
Article DOI: https://doi.org/10.35219/mms.2021.2.04

subsequent operations generates a contamination of the natural environment especially alterations in ecosystems [9, 10].

Starting with 1992, it was introduced the European Monitoring and Evaluation Programme EMEP/EEA air pollutant emission inventory guidebook, with the purpose to monitor and assess the long-range transportation of air pollutants. Air Emission Accounts (AEA) are secondary accounts in the European System of Accounts (ESA) providing information on the link between the environment and the economy. The National Institute of Statistics of Romania has applied the procedure of Air Emission Accounts (AEA) developed by Eurostat and data have been stated starting with 2008, in compliance with the demands and the reporting pattern - split by section of economic activities and households [11].

The aim of this paper was to analyse the impact of $PM_{2.5}$ and PM_{10} resulted from metallurgical industry between 2008 and 2018 in Romania and also to observe the trend of pollution depending on final energy consumption and final heat consumption. This analysis is useful over a decade, especially as $PM_{2.5}$ and PM_{10} have a significant share in pollution at the national level.

2. Materials and methods

The database used in this paper assesses the period 2008-2018 and it was collected by Romanian National Institute of Statistics according to the methodology of Air Emission Accounts (AEA) developed by Eurostat. National inventories include calculations for the calendar year within which the emissions to the atmosphere are generated. If suitable data are absent, emissions may be approximate using data from other years and applying adequate methods in particular averaging, interpolation and extrapolation.

According to European methodology air emissions at the level of national economies are estimated. The main idea is to assess air emissions, applying distinct emission factors technology, which are increased by a certain variable activity (e.g., use of a type of fuel). A general emission model can be expressed as:

$$E\ pollutant = AD\ production \times EF\ pollutant \quad (1)$$

where: E = Emissions; AD = Activity Data; EF = Emission Factor.

The air emissions included in the analysis refer to those physical flows of gaseous materials or suspended particles that originate in the economic system (production or consumption processes) and that are released into the atmosphere and remain suspended in the air for a substantial period of time. Most of these residues are in the gaseous state, others in a solid state remain effectively suspended in the atmosphere for a long time, respectively the suspended particles ($PM_{2.5}$ and PM_{10}) and heavy metals.

Air emissions accounts provide a close framework for national accounts and a general image of air emissions of the national economy and household consumption. In accordance with the data collected, diverse technical measures can be adopted to protect the environment, prevent, reduce and eliminate emissions of air pollutants, that directly damage health of citizen and the environment.

Industrial operations are commonly facile to identify considering the fact that the company frequently must report these data to pollution control authorities. The industry classification is connected with the reporting company within a business register number.

Evaluations of emissions of particulate matter from metallurgical industry may use techniques that provide filterable, condensable or total particulate matter (PM). Several factors bias the measurement and calculation of primary PM emissions from activities like iron and steel manufacture. The amount of PM obtained in an emission measuring relates to a substantial proportion on the measurement regime. This is especially true for activities including upper temperature and semi-volatile emission elements – therefore the PM emission may be divided amongst a solid/aerosol stage and material that is gaseous at the analysing area, but that may condense in the atmosphere. The percentage of filterable and condensable element will change, determined by the temperature of the flue gases and in sampling device. A mixture of filterable PM determination techniques is used generally with 70-160 °C filter temperatures.

Condensable portions can be obtained outright by recovering condensed constituent from chilled impinger schemes downstream of a filter. A regular method for total PM includes dilution where sampled flue or exhaust gases are combined with ambient air (likewise using a dilution sampling procedure) which accumulates the filterable and condensable constituents on a filter at low temperatures (15-52 °C) [12].

Emissions used in this paper consist in PM2.5 and PM_{10} dataset collected for a period of 11 years. To these emissions were added final energy consumption, final electricity consumption and final heat consumption for the same reporting period 2008-2018.

3. Results and discussions

In order to evaluate the percentage wherewith the $PM_{2.5}$ and PM_{10} is accountable for metallurgical

THE ANNALS OF "DUNAREA DE JOS" UNIVERSITY OF GALATI
FASCICLE IX. METALLURGY AND MATERIALS SCIENCE
No. 4 - 2021, ISSN 2668-4748; e-ISSN 2668-4756
Article DOI: https://doi.org/10.35219/mms.2021.2.04

industry from national emissions we calculated the percentage for each pollutant. In Figure 1 we compared the percentage of $PM_{2.5}$ and PM_{10} between 2008-2018. It is obvious that these pollutants make a significant contribution to the total amount of emissions into the atmosphere.

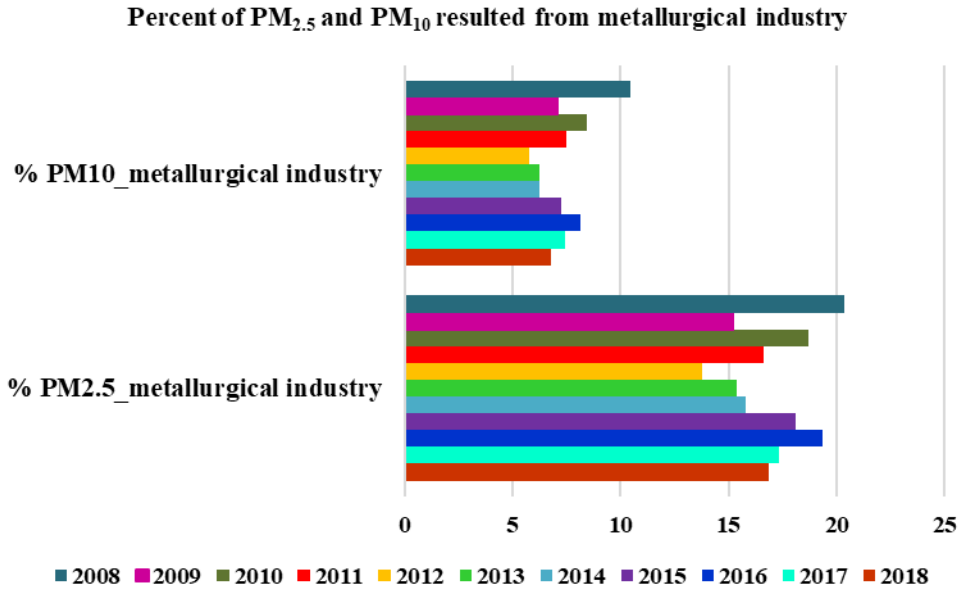

Fig. 1. *Percentage of $PM_{2.5}$ and PM_{10} resulted from metallurgical industry*

According to the analysed data, it cannot be stated that there is a clear, increasing or decreasing trend of pollutants. From the PM_{10} analysis it is obvious that the percentage with which it contributes to the pollution in the metallurgical industry varies from 5.74% in 2012 to 10.44% in 2008. In the case of $PM_{2.5}$ the percentages are much higher, starting from 20.35% in 2008 and the lowest being 13.78 in 2012. For both PM_{10} and $PM_{2.5}$ it can be affirmed that 2008 is the year in which the highest percentage of contribution of pollutants in the metallurgical industry was obtained, and 2012 is the year with the lowest percentage.

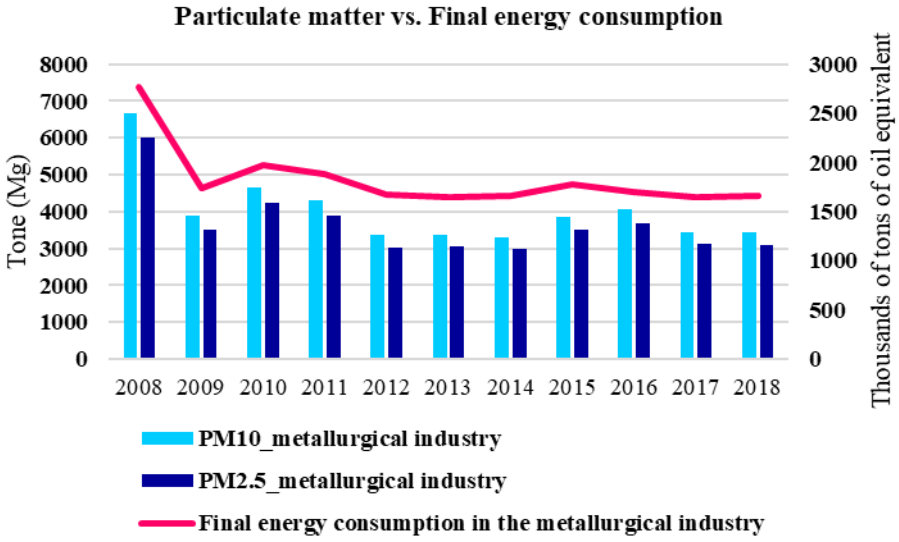

Fig. 2. *Particulate matter vs. Final energy consumption in metallurgical industry between 2000 – 2018 in Romania*

In most EU countries the metallurgical industry and industry of supplying electricity is among the largest contributors of greenhouse gas emissions. It is extremely interesting to identify which pollutant or

THE ANNALS OF "DUNAREA DE JOS" UNIVERSITY OF GALATI
FASCICLE IX. METALLURGY AND MATERIALS SCIENCE
N°. 4 - 2021, ISSN 2668-4748; e-ISSN 2668-4756
Article DOI: https://doi.org/10.35219/mms.2021.2.04

industry is contributing greater proportion to national totals and when. The energy consumption is a significant parameter that indicates the amount of fuel/energy, implicitly the intensity of the production process in the metallurgical industry.

By overlapping the final energy consumption in the metallurgical industry over the PM_{10} and $PM_{2.5}$ it is clear that the three elements analysed have the same trend, which leads to the conclusion that there is a significant correlation between these factors.

Between 2008-2009 there is an obvious decrease in both final energy consumption in the metallurgical industry and PM_{10} and $PM_{2.5}$, and in the following years the trend remains relatively constant with small increases between 2010-2011 and 2015-2016.

The final energy consumption in the metallurgical industry has two major components: final electricity consumption and final heat consumption. The final electricity consumption varies from 7826 million of kilowatt- hours in 2008 to 5899 million of kilowatt- hours in 2018. The differences between final energy consumption from the analysed period are not too large, the trend remaining more or less constant in the 11 years.

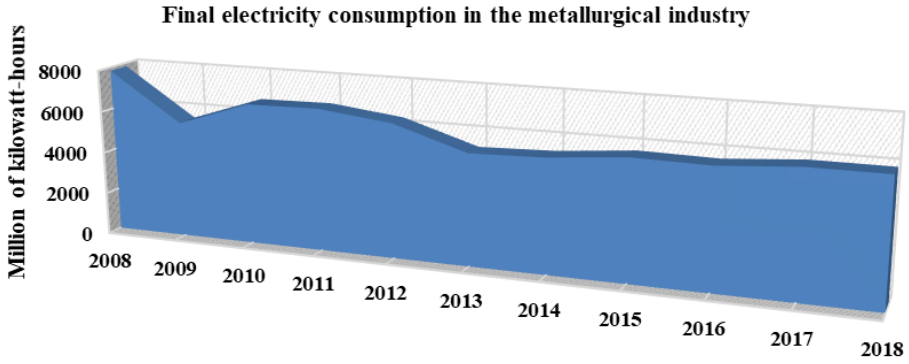

Fig. 3. *The final electricity consumption in metallurgical industry between 2000-2018 in Romania*

The final heat consumption is the second type of energy analysed. The quantities of final heat consumption in the metallurgical industry in the 11 years analysed vary from 6 thousand of giga calories in 2008 to 10 thousand of giga calories in 2018.

In contrast to the final electricity consumption the trend is not a constant one but there is a sudden increase up to 131 thousand of giga calories in 2011 the trend is not a constant one but there is an unexpected increase up to 131 and a significant decrease from 59 to 15 thousand of giga calories in the period 2014-2015.

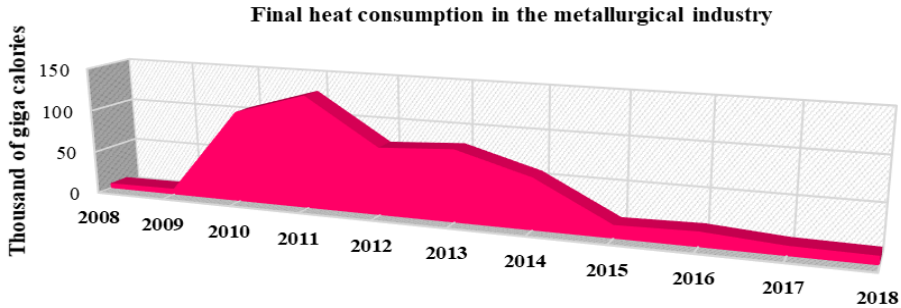

Fig. 4. *The final heat consumption in metallurgical industry between 2000 – 2018 in Romania*

4. Conclusions

The metallurgical industry is a considerably material and energy - intensive sector. Exceeding half of the mass input turns into outputs through released gases and solid wastes or derivates. The emissions of PM_{10} and $PM_{2.5}$ dominate the general emissions for most of the sectors. The role of this sector to the total emissions to air in Romania is significant for a considerable number of pollutants.

In the present paper we calculated the percentage of $PM_{2.5}$ and PM_{10} resulted from metallurgical industry for period 2008-2018 from Romania. For $PM_{2.5}$ these percentages vary approximative 15-20%, while the percentages for PM_{10} ranged between 5-10%. The final energy consumption in metallurgical industry was analysed

together with $PM_{2.5}$ and PM_{10} and it is obvious that in the analysed period these factors are very well connected.

The contribution of this article to the specialized literature consists in the analysis for a period of eleven years at national level of particulate matter emissions as well as of final energy consumption.

The periodical pollution assessment is crucial for establishing environmental priorities and determining the activities accountable for the various issues, the estimation of the environmental costs and benefits of distinct strategies and more than that to monitor the status of the environment conditions and to check if objectives are being accomplished.

References

[1]. European Commission, 2017, Special Eurobarometer 468: Attitudes of European citizens towards the environment (http://data.europa.eu/euodp/en/data/dataset/S2156_88_1_468_ENG).

[2]. EEA, Report No 9/2020 ISBN 978-92-9480-292-7, ISSN 1977-8449, doi:10.2800/786656, 2020.

[3]. Maxim A., *et al.*, *European Journal of Sustainable Development*, 6(1), p. 247-260, doi.org/10.14207/ejsd.2017.v6n1p247, 2017.

[4]. Sehic-Music N., Goletic S., Pihura D., Music L., Hasanovic K., Metalurgija 52, 4, p. 533-536, 2013.

[5]. ***, *Report on the energy poverty and air quality status in the eastern European countries*, InventAir project, Energy Agency of Plovdiv, https://www.inventair-project.eu/images/IA-Status-report.pdf, 2018.

[6]. ***, *IPCC Guidelines for National Greenhouse Gas Inventories*, Prepared by the National Greenhouse Gas Inventories Programme, Eggleston H. S., Buendia L., Miwa K., Ngara T., Tanabe K. (eds). I GES, Japan, 2006.

[7]. ***, EEA Report No 13/2019, https://www.eea.europa.eu/publications/emep-eea-guidebook-2019.

[8]. ***, *Iron and steel production EMEP/EEA air pollutant emission inventory guidebook*, 2019.

[9]. Habashi F., Journal of Mining and Environment, 2(1), 17-26. doi: 10.22044/jme.2012.16, 2012.

[10]. Visschedijk A. J. H., Pacyna J., Pulles T., Zandveld P., Denier van der Gon H., *Proceedings of the PM emission inventories scientific workshop*, Lago Maggiore, Italy, 18 October 2004. EUR 21302 EN, JRC, p. 163-174, 2004.

[11]. ***, *Best Available Techniques (BAT) Reference Document for Iron and Steel Production*, European Commission, Available at: http://eippcb.jrc.es, March 2012.

[12]. ***, *Manual for air emissions accounts*, Eurostat, ISSN 2315-0815, doi: 10.2785/527552, 2015.

THE ANNALS OF "DUNAREA DE JOS" UNIVERSITY OF GALATI
FASCICLE IX. METALLURGY AND MATERIALS SCIENCE
N°. 2 - 2021, ISSN 2668-4748; e-ISSN 2668-4756
Article DOI: https://doi.org/10.35219/mms.2021.2.05

COMPARISON OF TECHNOLOGIES FOR METAL RADIOACTIVE WASTE DECONTAMINATION

Yavor LUKARSKI, Hristo ARGIROV, Ilian ATANASOV
Institute of Metal Science, Equipment and Technologies with a Centre for Hydro-and Aerodynamics "Acad. A. Balevski", Sofia, Bulgaria
e-mail: yasu@abv.bg

ABSTRACT

A review is made of the growth dynamics of metal radioactive waste on a world scale. The most commonly applied technologies (hydro- and pyrometallurgical) for deactivation of this waste are presented.

The implementation of the blocks obtained by remelting for the manufacture of fasteners of nuclear reactors is demonstrated. Based on the conducted experiments and drawn conclusions, the inference is made that the pyrometallurgical methods of processing have greater advantages.

The paper exhibits a convincing motivation for the essential necessity of investigation of the metal radioactive waste processing, following the system D&D (deconstruction + deactivation), using effective and environmentally friendly technology.

KEYWORDS: nuclear reactor, radioactive waste, decontamination technologies, metallurgy under pressure

1. Introduction

Nuclear energy programs are being realized in more than 40 countries worldwide. According to summarized data of the International Atomic Energy Agency (IAEA) the number of the operating power units in 2016 was 443 and other 61 were under construction. There are also others at the "design" stage. The plants under operation with a nuclear-thermal cycle (NTC) are 123, including 56 for uranium ore processing, 17 for uranium isotope separation, 50 for nuclear fuel production and spent nuclear fuel processing. About 30 NTC plants are either under construction or under design. The old installations with exhausted service life are 66 and they have to be decommissioned. In some countries there are reactors for weapon-grade plutonium production (14 such reactors in the USSR in 1987). In addition, 58 countries possess over 320 nuclear research facilities. Taking into account also 458 submarine atomic reactors, 29 reactors of military ships and 16 icebreaker reactors, the number of nuclear power facilities in operation exceeds 1400. World nuclear power generation at the beginning of the XXI century has entered such a phase of its development, when the problems related to the exhausted service life and decommissioning of the nuclear energy facilities built in the 60s, 70s and some in the 80s of the XX century, have become especially topical [1].

It is obviously that the 21st century is characterized by the exhausted resource of a great number of reactors: about 50 in the USA, 14 in Great Britain, over 20 in the Russian Federation. A number of reactors have to be decommissioned in Eastern Europe [2].

Large amounts of metal waste are generated during the process of nuclear installation decommissioning, which have to be treated in an appropriate manner by the D&D (dismantling and decontamination) system. It is estimated that as of the present moment about $15 \cdot 10^6$ t of radioactive waste of different origin are accumulated in the world [3].

The main problem to be solved during utilizing metal wastes from nuclear power plants is to reduce the level of their radioactivity for the purpose of further application. In case this is not possible, the waste should be compacted in order to use less space for its disposal. This is achieved mechanically or by melting the waste and pouring the liquid metal in moulds of suitable volume and shape. In this way the volume of the metal sent for disposal can be reduced up to 20 times [4].

Up to 95% of the radioactivity of metal waste obtained during dismantling NPP equipment is

THE ANNALS OF "DUNAREA DE JOS" UNIVERSITY OF GALATI
FASCICLE IX. METALLURGY AND MATERIALS SCIENCE
N°. 2 - 2021, ISSN 2668-4748; e-ISSN 2668-4756
Article DOI: https://doi.org/10.35219/mms.2021.2.05

determined by the isotopes of Cs^{137} and $cobalt^{60}$ [5]. In the process of metal melting the basic radionuclides with longer half-decay period (cesium, strontium, uranium, plutonium) are transferred in the slag and dust, captured in the filters, while in the metal remains mainly the isotope of $cobalt^{60}$ (with a half-decay period of 5,3 years), which is distributed homogeneously in the ingot. This reduces significantly the storage time.

Depending on the residual contamination of the metal after crystallization, the blocks can be used in industry without restrictions or can be with limited utilization:

- Use for manufacturing facilities in nuclear industry as protective shields, radioactive waste (RAW) containers, parts for reactors and other equipment, etc.
- Storage in special repositories till the final decomposition of the radionuclides contained in them.

The metal blocks intended for unrestricted use in industry are ecologically safe for any kind of further processing. In addition, due to the deep purification of the metal and removal of the heavy nuclides such as cesium, strontium, uranium and plutonium, the necessary time for storage of the heavily contaminated blocks is sharply reduced till the decay of the remaining radionuclides in them (mainly Co^{60}).

The present work considers the research and comparison of the different decontamination technologies and offers the most effective one for metal radioactive waste (MRAW).

2. Technologies for MRAW decontamination

There are different methods for MRAW decontamination – hydrometallurgical, chemical, electrochemical, mechanical, pyrometallurgical, etc.

The following criteria should be taken under consideration when selecting a specific technology:

- Safety: The implementation of the method should not lead to higher radiation;
- Effectiveness: The selected method should be able to remove radioactivity to the level that would allow manual treatment of the products for deactivation without the use of robots or recycling (reuse of materials) or at least their transfer to a lower category of contamination;
- Cost efficiency: Although in the case of deactivation of large amounts of radioactively contaminated metals the price is not of primary importance, the ratio between deactivation costs/revenues from scrap sales should also be taken into account;
- Minimization of wastes: The decontamination method must not result in producing large amounts of secondary radioactive waste.

2.1. Hydrometallurgical technologies

Hydrometallurgical technologies use the regularities of the chemical interactions between MRAW coatings and different types of solutions. In electrochemical processes the chemical interaction is accompanied by the action of an electric field.

The main advantages of chemical and electrochemical decontamination are:

- The processes are relatively elementary and are easy for control and operation;
- With the correct choice of chemicals almost all radionuclides can be removed from the surface of the treated element;
- Radioactivity can be removed from internal and hidden surfaces;
- Compared to the volume of liquids needed for chemical decontamination, the volumes of electrolytes for electrochemical deactivation are relatively low.

The chemical and electrochemical processes of decontamination have also certain disadvantages:

- Generation of relatively large amounts of liquid secondary waste (spent solutions), which have to be annihilated or deposited;
- Chemical decontamination is usually inefficient for treatment of porous surfaces;
- These methods are restricted in operation by the bath size and the geometry of treated surfaces.

A team with the participation of scientists and specialists from the Institute of Metal Science, Equipment and Technologies with a Center for Hydro- and Aerodynamics "Acad. A. Balevski" (IMSETCHA) of the Bulgarian Academy of Sciences has developed a project of an installation for surface decontamination of MRAW using hydrometallurgical methods;

The applied technology is a combination of physical, chemical and electrochemical decontamination methods. The deactivation is carried out in different modules – baths for alkaline, acidic and electrochemical decontamination. The spent solutions are neutralized, the radioactive sludge is compacted and the water is sent for treatment as low-level radioactive waste.

The main facilities used for implementing the technology are "Module for jet alkaline degreasing", "Module for jet chemical decontamination" and "Module for electrochemical decontamination".

It is envisaged that surface polluted MRAW will be subjected to decontamination in the installation, which according to the classification of Ordinance No

THE ANNALS OF "DUNAREA DE JOS" UNIVERSITY OF GALATI
FASCICLE IX. METALLURGY AND MATERIALS SCIENCE
No. 2 - 2021, ISSN 2668-4748; e-ISSN 2668-4756
Article DOI: https://doi.org/10.35219/mms.2021.2.05

7 of the Commission on the Use of Atomic Energy for Peaceful Purposes (CUAEPP) [6] fall into:

• I category (generated power of the equivalent dose at 0.1 m from the surface of $1 \cdot 10^{-3}$ to $3 \cdot 10^{-1}$ mSv/h);

• II category (generated power of the equivalent dose at 0.1 m from the surface of $3 \cdot 10^{-1}$ to 10 mSv/h).

• At the stage of trial operation of the installation no treatment of metal RAW of the II category is envisaged, which generates power of the equivalent dose at 0.1 m from the surface exceeding 2 mSv/h.

The expected surface β + γ contamination is from 2 Bq/cm^2 to 50 Bq/cm^2, the expected equivalent dose rate of gamma radiation Pγ is from 0.1 mSv/h to about 5 μSv/h.

2.2. Pyrometallurgical technology

Most of the technologies developed by leading companies for the utilization of radioactively contaminated metals include several basic stages: sorting of metals according to the level of radioactive contamination; cutting; preliminary deactivation to remove fission and activation products, contained in coatings, depositions, oxide layers and dust in the facility; remelting of the metal waste.

The principles of metallurgical thermodynamics are in the basis of the processes of transferring heavy nuclides to the slag. The effect of enthalpy and entropy on the direction and degree of a chemical reaction is given by the equation of Gibbs [7]:

$$\Delta G = \Delta H - T \cdot \Delta S \qquad (1)$$

Here T is the absolute temperature, K.

The stability of the single oxides can be seen in the diagram of Ellingham [8]. It shows the dependence of the free energy ΔG on temperature for the individual oxides. The more negative the ΔG value, the more stable the oxide.

In general, the metals with lines below the line of iron can be oxidized and transferred from the molten steel into slag. The metals with lines above the line of iron cannot be oxidized. Cobalt will remain in the melt because the line of cobalt oxide is above that of iron. Uranium will pass into the slag because the position of the line of uranium oxide is below that of iron oxide.

After analysing the processes of MRAW melting, the decision was made to propose two melting technologies, one of them being with two options for realization [9].

2.2.1. Processing of metal RAW using fluxes

The scrap, cut and cleaned of organic and other contaminants, is fed into an induction furnace – Fig. 1 [9].

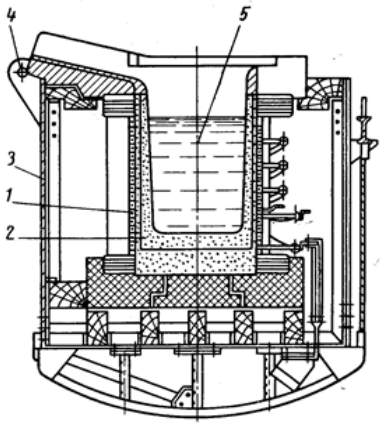

Fig. 1. *Crucible induction furnace: 1 – inductor; 2 – crucible; 3 – supporting structure; 4 – furnace inclination mechanism; 5 – molten metal* [9]

After reaching the specified temperature, special refining fluxes are introduced into the liquid metal in the amount of 2-3% of its mass but up to 10% of the melt mass can be reached. Flux composition depends on the radioactive element content in the scrap and on slag alkalinity. Usually the fluxes contain quartz sand, lime, dolomite, magnesium and additives regulating slag viscosity (for example CaF_2). The liquid metal is stirred due to the magnetic field generated by the inductor and the temperature gradient along the height of the induction furnace crucible. After a delay of 15-20 min allowing the completion of the refining processes, the furnace power is reduced, and the slag is scraped off. The metal is cast in molds.

This technological solution may also have another option of performance, which is more expensive, but more efficient, namely MRAW processing with additional metal treatment in a foundry ladle. In this case scrap is fed into the furnace, melted and overheated by about 50-100 °C above the specified temperature in order to prevent overcooling of the melt when poured in the ladle. In addition, it is necessary that the ladle should be heated too. The metal melted in the induction furnace is poured into the ladle, which has a porous plug at the bottom. An inert gas (nitrogen, argon) is blown through it. The refining fluxes are fed in the specified quantity and the metal is intensively stirred. After 10-15 min the gas flow is stopped, the slag is scraped off and the metal is poured in moulds.

THE ANNALS OF "DUNAREA DE JOS" UNIVERSITY OF GALATI
FASCICLE IX. METALLURGY AND MATERIALS SCIENCE
Nº. 2 - 2021, ISSN 2668-4748; e-ISSN 2668-4756
Article DOI: https://doi.org/10.35219/mms.2021.2.05

2.2.2. Processing of MRAW without using fluxes

No refining fluxes are introduced in this technological solution. On the other hand, after overheating of the metal it is maintained at the given temperature twice as long, so that the light isotopes are transferred to the gas phase and then to the gas-cleaning facilities. With this process it is practically impossible to obtain metal ready for unrestricted use and therefore it is recommendable to apply it for melting of relatively pure scrap with respect to radioactive contamination.

2.2.3. Comparison of the three technological processes

In terms of technological complexity, the most easily implemented process is that of MRAW treatment without using fluxes. Its main shortcoming was mentioned above. The most complicated technological method is the processing of MRAW with an additional treatment of the metal in a foundry ladle. The problem with this technological process is to maintain a specified temperature of the liquid metal in the ladle during the refining processes. The temperature has to be constantly monitored in order to avoid a situation when the metal cools down and the refining processes stop. The most frequently used method is to heat the ladle through its lid.

In terms of overall productivity, the technological processes for MRAW treatment, with or without using fluxes, are comparable because the time for refining the melt with fluxes is comparable to the additional heating in the flux-free option. In the case of MRAW treatment with additional processing of the metal in a foundry ladle, the productivity is lower due to the more complicated technology and the additional time for pouring the metal into the ladle and its refining under conditions of gas blowing. This process is most effective in terms of the production of metal intended for unrestricted use, also reducing the relative share of the other two groups of treated metal – for restricted use and for disposal.

The technological process for MRAW treatment without using fluxes can be most easily implemented because no additional devices for flux feeding and slag scraping are necessary. The method of MRAW processing with additional treatment of the metal in a foundry ladle is most complicated.

After analysing the results from the comparison of the single technological solutions, the authors consider that the most advantageous option is to melt MRAW in an induction furnace with introduction of a certain amount of refining fluxes without additional heating.

3. Application of the decontaminated scrap

A method is shown of implementing the already decontaminated by melting metal scrap, unconditionally released from control based on low residual radioactivity [10]. This metal can be implemented as a raw material in the production of fasteners for nuclear reactors. In this case these are studs for the outer contour with sizes: length of 2000 mm, diameter of 120 mm and mass of 180 kg each.

The steel 32NiCrMo of type (DIN 1.6745), used as a basis, is of the type of the constructional complexly alloyed medium-carbon steels, intended for the manufacture of fasteners for nuclear reactors. A new steel brand of the type 30Cr2NiMoVN with higher nitrogen content has been developed by mathematical modeling using artificial neural networks of the dependence "steel properties/chemical composition". It is produced using the methods of the metallurgy under pressure. The method is applied to produce new steels and alloys under higher pressure compared to the atmospheric one. The theoretical grounds of the alloying with super-equilibrium nitrogen concentrations were developed in IMSETCHA-BAS. The main advantages of this type of metallurgy are: replacement of expensive alloying elements (nickel) by nitrogen, which is distributed homogeneously in the bulk of the metal; smooth and homogeneous filling of the crucible with metal; improved structure and high density of castings.

The conducted investigations on both steels prove that the new one has a fine-grained structure of the strengthening phase, which ensures 30-50% higher strength and plastic properties as well as impact toughness. Therefore, it can be operated without problems up to T = 350 ºC, for fasteners of nuclear reactors in particular.

The next step in stud production is to obtain the intermediate blanks in a ВП-0,5 induction furnace, where the scrap is calculated so as to use the contaminated and remelted blocks yielded by metal utilization from decommissioned plants. Even if minimal residual radiation is present in them, when dissolved in the liquid bath, the residual nuclide values are negligibly small. Further on the metal rods of the new steel are subjected to Electroslag Remelting under nitrogen pressure and blanks of the 30Cr2NiMoVN steel are obtained. Then the studs are forged and finally mechanically treated. The finished studs are shown in Fig. 2 [10]. The PWR reactor in operating position with the mounted stubs is seen in Fig. 3 [10].

THE ANNALS OF "DUNAREA DE JOS" UNIVERSITY OF GALATI
FASCICLE IX. METALLURGY AND MATERIALS SCIENCE
No. 2 - 2021, ISSN 2668-4748; e-ISSN 2668-4756
Article DOI: https://doi.org/10.35219/mms.2021.2.05

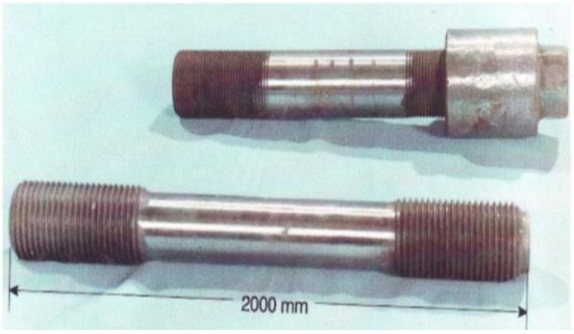

Fig. 2. *Fasteners of steel 30Cr2NiMoVN. Length 2000 mm, diameter 120 mm* [10]

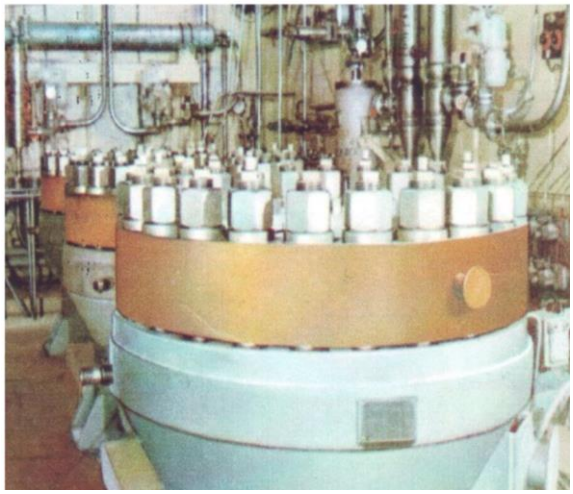

Fig. 3. *Outer contour of PWR reactor with mounted studs [10]*

4. Comparison of the two types of MRAW decontamination technologies

When analysing the specifics of both technologies, several things have to be pointed out:

First, hydrometallurgical methods are more complex and require higher efforts from the service personnel in contrast to the pyrometallurgical ones, which are simpler in terms of operation and maintenance. The fact that in the case of the "wet" methods the staff works under conditions of evaporating chemical substances should not be ignored too. Additional, significant amounts of secondary RAW are generated, which require special attention, it becomes clear that the hydrometallurgical methods are lagging behind the development of the pyrometallurgical ones.

The main advantage of the latter is the possibility of multifold reduction of the volume of melted materials with all ensuing beneficial consequences. This is not relevant to the hydrometallurgical processes, where the shape and volume of scrap are not changed during treatment. The more salubrious work environment in the pyrometallurgical technologies, as well as the possibilities for automation of a great part of the processes have to be also taken into account [11].

The decontamination of MRAW by melting and processing with refining fluxes has also the advantage that redistribution of radioactive nuclides occurs between the metal block, slag and dust in the purification filters, thus achieving additional deactivation of the primary material. Moreover, uniform distribution of residual radioactivity is obtained in the volume of the ingot.

5. Conclusion

Based on the conducted research and pilot trials the team determines that the most prospective method for MRAW processing is by melting the metals in an induction furnace. Refining fluxes are introduced during melting, which reduce the number of radioactive nuclides, and the produced metal is subjected to unconditional release from control. The ideal option would be to cut and preliminary treat the dismantled elements applying some of the hydrometallurgical or mechanical methods and then to melt them in an induction furnace. However, this will make the decontamination technology rather expensive.

References

[1]. ***, *Communication of the Ural Electrochemical Plant*, Out. No 16-30/659 from 13.05.99, (in Russian).

[2]. Slaveykova M. E., Demireva G. Simova. *Estimate of the streams of dismantled materials from EE of Units 1 and 2 of "Kozloduy" Nuclear Power Plant*, Conf. of the Bulgarian Nuclear Society, 10-13 Oct., 2012, Hisarya, Bulgaria, (in Bulgarian).

[3]. Quade U., Kluth T., Kreh R., *Melting of Low-Level Radioactive Non-Ferrous Metal for Release*, Proc. ICEM '07, Paper 7036, Brügge, Sept., 2007.

[4]. Quade U., Kluth T., *German Experience in Recycling of Ferrous Metallic Residues from Nuclear Decommissioning by Melting*, Proc. SFEN, Decommissioning Challenges: An Industrial Reality, Avignon, Sept., 2008.

[5]. Andreev D. E., Gelbutovski A. B., *Existing Practices and Economic Aspects of the Problem of the Treatment of Metal Radioactive Waste*, ZAO „ECOMET-C", Report from 07.10.2005, (in Russian).

[6]. ***, *Regulation No 7 of the Committee on the use of nuclear energy for peaceful purposes for collection, storage, processing, transport and disposal of radioactive waste on the territory of the Republic of Bulgaria*, State Gazette, No 8/1992, https://www.bcci.bg/bulgarian/eurozone/negotiations. (in Bulgarian).

[7]. Cotton F., Wilkinson G., *Basic Inorganic Chemistry*, New York. John Wiley & Sons, 1979.

[8]. Cotton F. A., Wilkinson G., Gaus P., *Basic Inorganic Chemistry*, 7th edition, J. of Chemical Education, № 77(3), March, 2000.

[9]. Lukarski Y., Argirov Cr., *Possibilities of Optimizing the Processing of Metallic Radioaktive Waste*, NDT Journal, vol. II, Issue 2, p. 125-133, 2019.

[10]. Kortenski G., Argirov H., *Effect of Hydrogen on the Mechanical Properties and Notch Toughness of Hewly Created Steel*, J. of Theoretical and Appl. Mechanics, №1, p. 83-86, 1996.
[11]. Lukarski Y., Atanasov I., Argirov Ch., *Protection of the Personnel from Irradiation during Pyrometallurgical Processing of the Base of Model Calculations*, 27th International Conf. Ecological Truth and Environmental Research "EcoTER", Bor, Serbia, June, p. 404-411, 2019.

THE ANNALS OF "DUNAREA DE JOS" UNIVERSITY OF GALATI
FASCICLE IX. METALLURGY AND MATERIALS SCIENCE
Nº. 6 - 2021, ISSN 2668-4748; e-ISSN 2668-4756
Article DOI: https://doi.org/10.35219/mms.2021.2.06

MATHEMATICAL MODELING OF THE COLD ROLLING PROCESS AND HEAT TREATMENT FOR DC01 STEEL

Marian-Iulian NEACȘU
"Dunărea de Jos" University of Galaţi, Romania
e-mail: uscaeni@yahoo.com

ABSTRACT

The paper presents the elaboration of a mathematical model of the cold strip rolling process combined with the recrystallization annealing after the rolling at LBR Liberty Galati.

The elaborated mathematical model allows the prediction of the mechanical properties of cold rolled strips subsequently subjected to a heat treatment.

The realization of this mathematical model was based on statistical measurements of the mechanical properties Rm, $R_{p0.2}$ (Rc) and A_5 for the rolled steel strip DC01 from Liberty Steel Galati. To achieve this mathematical model, the active experiment method was used.

With the help of this mathematical model, it is possible to optimize the rolling process by significant savings of time and materials in the process of testing the mechanical properties for cold rolled tape, but also by choosing the most appropriate process parameters.

KEYWORDS: mathematical model, mechanical properties, statistical measurements, active experiment, recrystallization annealing

1. Introduction

Process modeling is a useful basic tool both in the design phase and in the analysis of the operation of metallurgical installations. This, together with the use of computers, allows the determination of the optimal regimes of metallurgical processes. The development of the specific mathematical apparatus and of the statistical methods allowed to approach the problem of the optimal decision as a problem of great technical and economic efficiency [1].

Mathematical modeling is a basic tool in the design phase but also in the execution phase as well as in the analysis of the functioning of the processes. With the help of mathematical modeling and computers by using specialized programs, we can determine the optimal conditions for a metallurgical process [2].

The construction of models associated with processes and systems is an essential side of the simulation process, a distinction between the different types of models that can be used by analysts being absolutely necessary [3].

The modeling process can be considered as consisting of two stages:

- one that specifies the form in which the model is to be expressed.

- and the second stage is the one that describes how the mathematical model is used to provide a series of predictions or to offer the optimal solution of the studied problem. The mathematical model of a process, in this case a metallurgical process, is used to determine the best conditions for the process but can also be used to provide information on the optimal management of the process [4].

However, some very important factors should not be neglected in the evaluation of modeling methods, such as: the relative cost of using these models (their efficiency), the ease with which they can be transmitted from those who made them to those who apply them, handling facilities, the degree of accuracy offered, the limits within which the respective models can be applied.

Mathematical modeling is the transposition into a mathematical form of a real physical process.

Statistical mathematical modeling is performed in two stages:

- in the first stage, which is called a preliminary experiment, the problem of choosing the process factors as well as the interactions that may occur are solved;

THE ANNALS OF "DUNAREA DE JOS" UNIVERSITY OF GALATI
FASCICLE IX. METALLURGY AND MATERIALS SCIENCE
N°. 6 - 2021, ISSN 2668-4748; e-ISSN 2668-4756
Article DOI: https://doi.org/10.35219/mms.2021.2.06

- in the second stage, the experiment on which the operator relies to perform the actual modeling and statistical analysis of the model takes place [5].

Operational research, like other research disciplines, has progressed through the use of mathematical models, which concisely use mathematical notations to represent the variable states in the system and to describe how variables change and interact with each other. Predictions regarding the behavior of the system are made with the help of symbolic representations, through mathematical procedures.

2. Experimental conditions

In the paper we realized the mathematical model of the process of cold plastic deformation and heat treatment of recrystallization annealing applied to the studied alloy by statistical methods, namely regression analysis by active experiment.

A number of 25 experiments were performed in a cold rolled strip trial, the brand of the material being DC01, on which degrees of reduction between 61 and 65% were applied with a step of 1%, and in the thermal treatment of recrystallization annealing, times were maintained at 700 °C between 35 and 39 hours as well as a 1-hour step.

The following technological parameters were taken into account as main influencing factors (independent variables) of the process:

- recrystallization annealing heat treatment time - τ, [hours];
- degree of plastic deformation - ε, [%].

To establish the baseline and the range of variation of the influencing factors we used values obtained from mechanical tests on the samples used.

Thus, we established the following experimental conditions:

- for the duration of recrystallization annealing heat treatment:
  - basic level: X_{01} = 37 hours;
  - variation interval: ΔX_1 = 2 hours;
  - upper level: X_{1s} = 39 hours;
  - lower level: X_{1i} = 35 hours.
- for the degree of deformation:
  - basic level: X_{02} = 63%;
  - variation range: Δx_2 = 2%;
  - upper level: X_{2s} = 65%;
  - lower level: X_{2i} = 61%.

In order to represent the coded experiment, the following notations and symbols were used:

Independent variables:

- X_1 - recrystallization annealing heat treatment time, τ [hours];
- X_2 - degree of deformation, ε [%];

Dependent variables (parameters to be optimized):

- Y_1 - breaking strength, Rm [MPa];
- Y_2 - flow limit, $R_{p0.2}$ [MPa];
- Y_3 - specific elongation at break, A_5 [%];

There are the following links between natural and coded values of factors x_i:

$$x_1 = \frac{\tau - \tau_0}{\Delta\tau}, \quad x_2 = \frac{\varepsilon - \varepsilon_0}{\Delta\varepsilon} \tag{1}$$

Yi values are expressed in natural units.

Next, based on the matrix of the complete factorial experiment, the coefficients of the regression equation are calculated (mathematical model). Considering the Yi function as the analytical expression of the first order model, it is of the form:

$$Y_i = c_0 + \sum_{i=1}^{2} c_i \cdot x_i + \sum_{\substack{i=1 \\ j=1 \\ i \neq j}}^{2} c_{ij} x_i x_j \tag{2}$$

Following the specific calculations, the equations of the mathematical model (3), (4), (5) resulted for the three studied mechanical properties:

$$Y_1(\tau,\varepsilon) = 859{,}25 - 6 \cdot \tau - 5{,}25 \cdot \varepsilon \tag{3}$$

$$Y_2(\tau,\varepsilon) = 1004{,}19 - 11{,}31 \cdot \tau - 8{,}44 \cdot \varepsilon + 0{,}06 \cdot \tau \cdot \varepsilon \tag{4}$$

$$Y_3(\tau,\varepsilon) = -163{,}25 + 2{,}5 \cdot \tau + 1{,}75 \cdot \varepsilon \tag{5}$$

3. Experimental results

Following the laboratory tests on the specimens taken from the rolls caught in the experimental program, the values of the studied mechanical properties were registered. The variation of these values depending on the two parameters of the process are illustrated in Figures 1, 2, 3.

THE ANNALS OF "DUNAREA DE JOS" UNIVERSITY OF GALATI
FASCICLE IX. METALLURGY AND MATERIALS SCIENCE
Nº. 6 - 2021, ISSN 2668-4748; e-ISSN 2668-4756
Article DOI: https://doi.org/10.35219/mms.2021.2.06

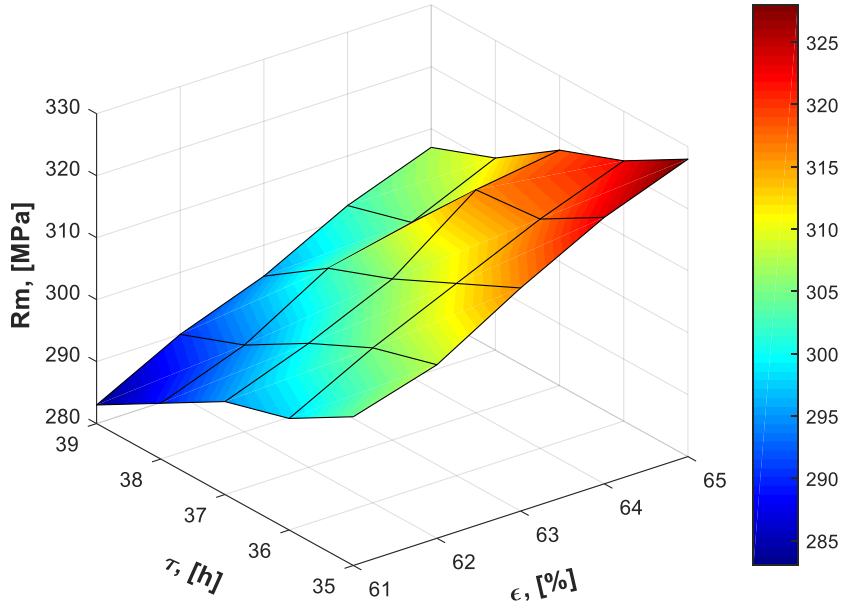

Fig. 1. *Variation of mechanical strength with the degree of cold plastic deformation and with the time of recrystallization annealing*

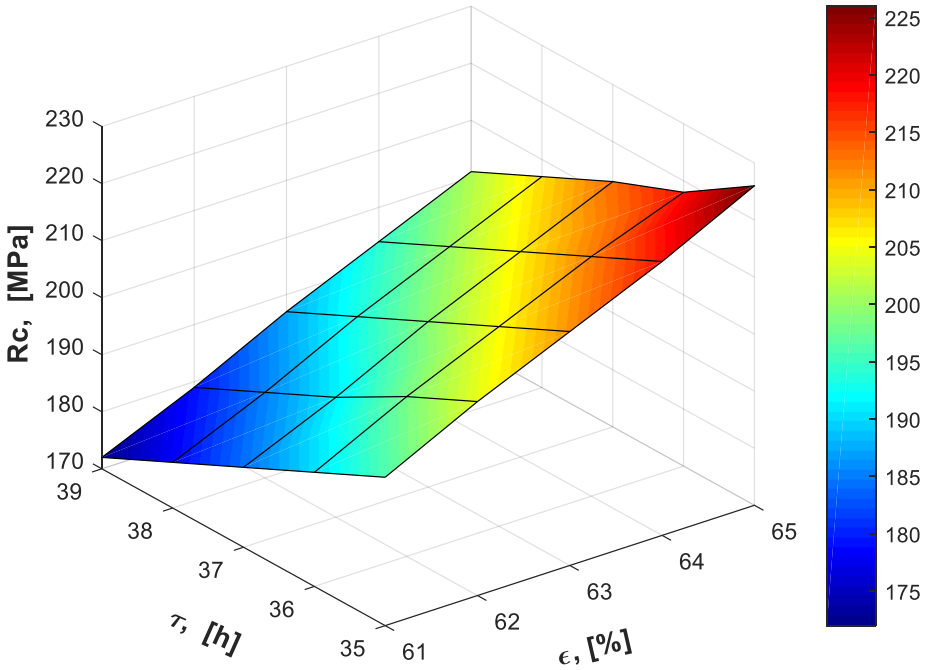

Fig. 2. *Variation of the flow limit with the degree of cold plastic deformation and with the recrystallization annealing time*

THE ANNALS OF "DUNAREA DE JOS" UNIVERSITY OF GALATI
FASCICLE IX. METALLURGY AND MATERIALS SCIENCE
Nº. 6 - 2021, ISSN 2668-4748; e-ISSN 2668-4756
Article DOI: https://doi.org/10.35219/mms.2021.2.06

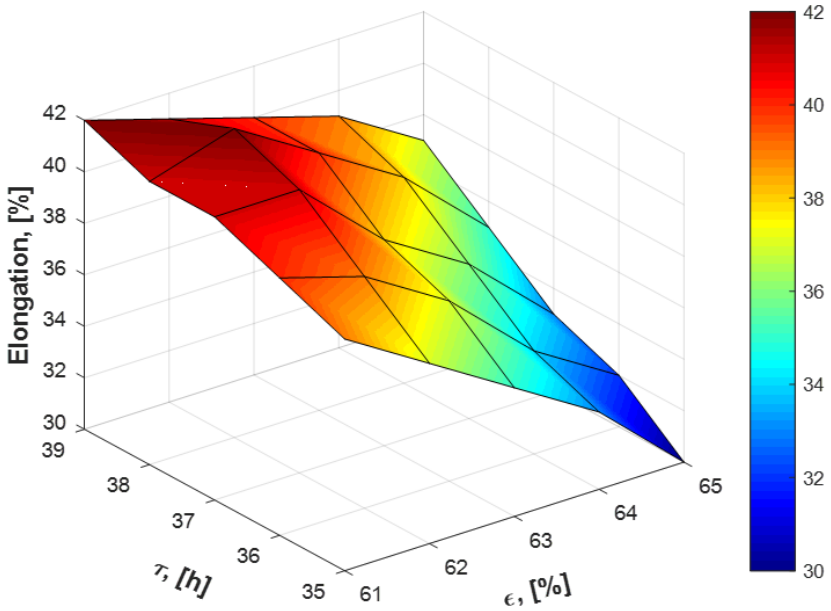

Fig. 3. *Variation of elongation at break with the degree of cold plastic deformation and with the time of recrystallization annealing*

4. Conclusions

During this research work, several technological variants for obtaining cold rolled steel strips of DC01 brand were studied, in the conditions of Liberty Steel Galati.

For all the 25 technological variants studied, the related mechanical properties comply with the norms in force on the Liberty Steel Galati platform (SR EN 10310).

Carrying out the mathematical modeling of the process of obtaining cold-rolled strips led to obtaining mathematical equations of the studied process, valid for a time τ, with values ranging from 35 hours to 39 hours, maintenance to recrystallization annealing and a degree deformation during cold rolling ε, with values between 61-65%.

The equations of the mathematical model obtained are first order equations and were statistically verified using the Fischer criterion.

The mathematical model obtained in this paper can be likened to a function with two variables, each of the three studied mechanical properties (output quantity) depends on:

- recrystallization annealing heat treatment time, τ [hours];
- degree of deformation, ε [%];

In the future, for the three studied mechanical properties, the equations of the mathematical model allow the prediction of the values of these properties by calculation, without the need to perform specific mechanical tests.

Interpreting the equations of the model, it results that the mechanical properties of resistance increase as the value of the degree of deformation increases and decrease as the recrystallization annealing time decreases.

Elongation at break is influenced, according to the mathematical model, primarily by the treatment time in the sense that, as the temperature of the recrystallization annealing heat treatment increases, so does the elongation.

The presented mathematical model allows the calculation of the optimization of the parameters of the process of obtaining cold rolled strips in Liberty Steel Galati, so as to obtain the optimal complex of resistance and plasticity properties, with minimal costs.

References

[1]. Taloi D., Bratu C., Florian E., Berceanu E., *Optimizarea proceselor metalurgice*, E.D.P., Bucureşti, 1983.
[2]. Taloi D., *Optimizarea proceselor tehnologice-aplicaţii în metalurgie*, Editura Academiei, Bucureşti, 1987.
[3]. Popescu D., Ionescu F., Dobrescu R., Stefanoiu D., *Modelare in ingineria proceselor industriale*, Editura AGIR Bucuresti, 2011.
[4]. Ciuca I., Dumitriu S., *Modelarea si Optimizarea proceselor metalurgice de deformare plastica si tratamente termice*, Ed. Didactica si Pedagogica, Bucuresti, 1998.
[5]. Baron T., *et al.*, *Statistică teoretică şi economică*, Editura Didactică şi Pedagogică, Bucureşti, 1995.
[6]. Cazimirovici E., *Bazele teoretice ale deformării plastice*, Ed. Bren Bucureşti, 1999.

THE ANNALS OF "DUNAREA DE JOS" UNIVERSITY OF GALATI
FASCICLE IX. METALLURGY AND MATERIALS SCIENCE
Nº. 2 - 2021, ISSN 2668-4748; e-ISSN 2668-4756
Article DOI: https://doi.org/10.35219/mms.2021.2.07

CORROSION BEHAVIOR OF MATERIALS AL5083 ALLOY, 316L STAINLESS STEEL AND A681 CARBON STEEL IN SEAWATER

Gina Genoveva ISTRATE, Alina Crina MUREȘAN
"Dunărea de Jos" University of Galaţi, Romania
e-mail: gina.istrate@ugal.ro

ABSTRACT

In this paper the corrosion behavior of different materials has been evaluated based on exposure in seawater. The laboratory immersion test technique has been applied to evaluate the effect of seawater on the corrosion behavior of different materials. In three sets of experiments, carbon steels (A681 Type O7), austenitic stainless steels (316L) and aluminium alloys (Al5083) were utilized. The specimens were fixed fully submerged in seawater. The corrosion process was evaluated using weight loss method, open-circuit potential measurements (OCP) and polarization techniques. To determine gravimetric index and the rate of penetration, samples were immersed in corrosive environment for 89 days and weighed periodically. The electrochemical experiments were conducted with a Potentiostat/Galvanostat (PGP 201) analyzer. It was connected to a PC. The Voltamaster software was used for electrochemical data analysis. A three-electrode cell composed of a specimen as a working electrode, Pt as counter electrode, and saturated calomel electrode (SCE) (Hg (l)/ Hg_2Cl_2 (s)) as a reference electrode were used for the tests. The weight loss tests revealed the lowest corrosion rate values for stainless steel and aluminium alloys, indicating a beneficial use for these materials in marine environments. The potentiodynamic method shows that the lowest corrosion rate in seawater (2.8 μm /year) was obtained for the Al5083 alloy, and the highest value of the corrosion rate (41.67 μm/year) for A681 carbon steel.

KEYWORDS: corrosion, weight loss, seawater, corrosion rate

1. Introduction

Corrosion represents the deterioration in time of metals, alloys, and also of materials in general, that are exposed to the action of some factors which are in the surrounding environment by chemical and electrochemical reactions.

The problem of corrosion is very important. In order to control this effect, certain methods of control or reduction of damages are needed, resulted after this process. Simultaneously, these methods are additional reasons for the maintenance of equipment.

Corrosion is a process that cannot be avoided and that causes damages to the industry and implicitly affects the world economy. For this reason, measures for preventing and slowing down the corrosion of equipment and metal parts had to be taken [1].

Seawater is the only electrolyte that contains a relatively high concentration of salts that usually occurs in nature, covering at the same time two-thirds of Earth's surface.

Metallic corrosion in the marine environment has been studied since the beginning of the century. Due to the high dissolved oxygen content in seawater, the corrosion mechanism of different metals is that of oxygen depolarization (except Mg and its alloys). In the Black Sea, the water can have a high content of hydrogen sulphide with the approximately total absence of dissolved oxygen. Due to the increase of acidity, the corrosion effect can take place due to the hydrogen depolarization, the cathodic overvoltage of the hydrogen release decreases, and the anodic depolarization increases due to the formation of sulphides on the metal surface [2-7].

After some studies, Vermeșan discovered that salinity, the biological component, and the seas and oceans' temperature are variables, as well as the corrosion rates are different in these waters. In warm seas, where under normal conditions the corrosion rate increases with the temperature, the deposition reaction of calcareous layers on metal surfaces is accelerated and these layers prevent corrosion. The alloy's nature is very important because it influences

THE ANNALS OF "DUNAREA DE JOS" UNIVERSITY OF GALATI
FASCICLE IX. METALLURGY AND MATERIALS SCIENCE
N°. 2 - 2021, ISSN 2668-4748; e-ISSN 2668-4756
Article DOI: https://doi.org/10.35219/mms.2021.2.07

the corrosion effect. That is why alloys that have high Cu content cannot be covered by marine organisms due to the copper's toxicity [8].

In the naval industry, a series of materials with various characteristics necessary to develop a quality product is used to manufacture ships.

Different destructive attack forms can appear in structures, ships, and equipment that are exploited. Marine corrosion describes most of the problems that appear in contact with seawater. But not only, it also contains the way how corrosion evolves as a result of metal exposure to the atmospheric action or to salt corrosion in naval engines that operate with open cooling systems [9-11].

In this paper, the corrosion behaviour of some materials i.e., the Al5083 alloy, 316L stainless steel, and A681 (type O7) carbon steel, was studied in seawater (Black Sea), and also their level of resistance to factors met in the corrosive environment.

2. Materials and methods

The tested samples were purchased from the DAMEN Shipyards Galati, one of the 32 biggest shipyards of the Damen Shipyards Group, repair sites and related companies around the world.

These materials, the Al5083 alloy, the 316L stainless steel, and the A681 (type O7) carbon steel are used to manufacture various products: coastal ships, patrol ships, cargo ships, and logistic support ships, ferries, and barges.

The Al5083 alloy, the 316L stainless steel, and the A681 (type O7) carbon steel were selected for constructing products for the naval industry, and not only, due to certain characteristics that make them resistant to corrosion up to a certain level.

The applied methods in studying the corrosion of metals must fulfil the conditions of detailed control of the factors that characterize the corrosion effect. Choosing the study methods firstly depends on the type of corrosion process which must be assessed, the purpose pursued, and the place where it is determined. Most of the time, more methods, quantitative and qualitative, are used simultaneously.

In this case, for the study of corrosion behaviour of the Al5083 alloy, 316L stainless steel, and O7 carbon steel materials quantitative study methods were used. The quantitative methods of corrosion assessment are classified as follows:

- gravimetric methods;
- electrochemical methods.

The gravimetric methods are the most used in studying general corrosion (uniform or non-uniform) of metals, applying for electrolyte solutions and for non-polar organic substances.

These methods also have disadvantages which consist of high consumption of metal, errors after weighing, and the pickling that is done on the metal, long period of determination, and the fact that it is not applied to the forms of localized corrosion (pitting, intergrain) where the metal loss and the consumed oxygen quantity are very low [12, 13].

The gravimetric index or the corrosion rate (V_{cor}), indicated by $g/m^2 \cdot h$ or by $mg/dm^2 \cdot day$ represent the weight variation of the metal sample (Δm) as a result of corrosion, in the time unit (t) and on the surface unit (S), being demonstrated by the ratio:

$$V_{cor} = \frac{\Delta m}{S \cdot t} \quad [g/m^2 \cdot h] \quad (1)$$

The penetration index (P) indicates the average depth of the penetration of the corrosive environment in the metal mass. In other words, the average decreases in the thickness of the exposed sample (d) in the unit of time (t), being defined by the ratio:

$$P = \frac{d}{t} \quad [mm/year] \quad (2)$$

The penetration index can be measured with a corrosion resistance conventional scale for materials (Table 1) which provides indicative information on the opportunity to use an alloy or metal as construction material for a corrosive environment.

Table 1. *Corrosion resistance conventional scale for materials* [14]

Corrosion resistance group	The penetration index [mm/year]	Stability coefficient
Perfectly stable	<0.001	1
Very stable	0.001-0.005	2
	0.005-0.01	3
Stable	0.01-0.05	4
	0.05-0.1	5
Relatively stable	0.1-0.5	6
	0.5-1.0	7
Less stable	1.0-5.0	8
	5.0-10	9
Unstable	>10	10

THE ANNALS OF "DUNAREA DE JOS" UNIVERSITY OF GALATI
FASCICLE IX. METALLURGY AND MATERIALS SCIENCE
Nº. 2 - 2021, ISSN 2668-4748; e-ISSN 2668-4756
Article DOI: https://doi.org/10.35219/mms.2021.2.07

For determining the corrosion rate by gravimetric method, the seawater (Black Sea) was chosen as testing environments.

The tested materials were the Al5083 aluminium alloy, the O7 carbon steel, and the 316L stainless steel.

Before determining the corrosion rate of the materials, the samples were measured, cleaned, and prepared with metallographic paper, weighted with the help of an electronic balance, and then submerged in solution (seawater).

The most frequent polarization methods used in the laboratory for corrosion tests are: potentiodynamic polarization, potentiostatic polarization, and cyclic voltammetry. These techniques can provide important data regarding the corrosion mechanism, corrosion rate, and susceptibility to corrosion of specific materials in the environment. The polarization methods imply changing the working electrode potential and monitoring the current obtained as a function of time or potential.

The potentiodynamic method consists of varying the electrode potential at a determined speed by applying a direct current to the electrode. It is one of the most used polarization methods for determining corrosion resistance and is used for a wide range of analyses.

The corrosion current in the potentiodynamic charts can be calculated with the Stern-Geary formula which expresses the dependence between the polarization resistance and the corrosion current:

The value of the corrosion rate was calculated with the relation:

$$V_{cor} = \frac{i_{cor} \cdot A \cdot 10}{D \cdot v \cdot 96500} \quad (3)$$

where:

i_{cor} - the density of the corrosion current calculated with the Stern-Geary formula;

A - atomic mass of the metal;

D - metal density;

v - valence of the metal.

The specialized literature presents references to the behaviour of metallic materials used in the naval industry in seawater (natural or artificial) [15-17].

The corrosion tests were done using VOLTAMASTER 4 (PGP 201) connected to the electrochemical cell with three electrodes: the working electrode (W.E.), the tested sample on whose surface the measurement was done, the counter electrode (C.E.), the platinum electrode and calomel electrode SCE (Hg (l)/ Hg_2Cl_2 (s), KCl, sol sat) as the reference electrode (R.E.; E Hg/Hg_2Cl_2 = +0.2444 V at 25 ºC/ESH). The system was connected to a computer with data analysis software. The analysed samples (the working electrode) have been isolated on one side before being immersed in the seawater testing solution.

The corrosion tests of each sample began with the monitoring of the open circuit potential – OCP, after submerging the samples in the testing solution until it reached the stationary value.

For the potentiodynamic polarization tests, the following parameters were used: initial potential (I.P.) -1.0V (SCE), final potential (F.P.) +300 mV (SCE), scanning speed 2 mV/s.

3. Results and discussions

3.1. Results obtained by gravimetric methods

Determining the corrosion rate after 7 days since immersion: After a 7-day period from immersion of the samples in the seawater, they were cleaned, weighted, and submerged again. The masses of the samples both initial and at 7 days are shown in Table 2.

Table 2. *Weight variation at 7 days*

Materials	Initial weight (g)	Weight after 7 days (g)
Al5083 aluminium alloy	7.4395	7.4299
316L stainless steel	19.6243	19.6187
A681 carbon steel	20.1641	20.1429

The values of the corrosion rate were calculated with the ratio (1), after submerging the samples in seawater for 7 days.

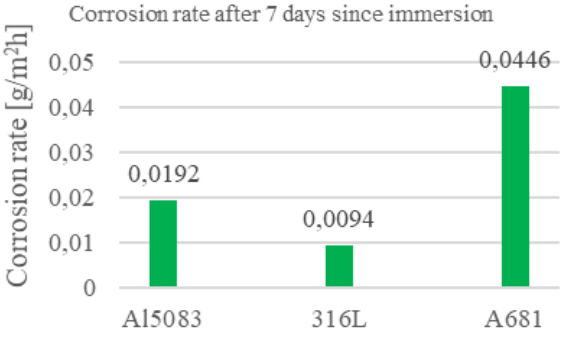

Fig. 1. *The corrosion rate after submerging in seawater for 7 days*

THE ANNALS OF "DUNAREA DE JOS" UNIVERSITY OF GALATI
FASCICLE IX. METALLURGY AND MATERIALS SCIENCE
N°. 2 - 2021, ISSN 2668-4748; e-ISSN 2668-4756
Article DOI: https://doi.org/10.35219/mms.2021.2.07

According to the data from Figure 1, it can be seen that after 7 days of immersion in seawater, the corrosion rate has the highest value in the case of the O7 carbon steel, 0.0446 g/m^{2}h. Lower values were obtained for the other materials, such as a value of 2.3 times lower was calculated in the case of the Al 5038 aluminium alloy i.e., 0.0192 g/m^{2}h. The lowest value for the corrosion rate at 7 days of immersion was calculated for the 316L stainless steel (0.0094 g/m^{2}h), a value 4.7 times lower than that calculated for the A681 (type O7) carbon steel.

Determining the corrosion rate after 28 days since immersion: The variation of the masses of the samples tested in seawater after 28 days of immersion is presented in Table 3 and the corrosion rate for each tested material is presented in Figure 2.

Table 3. *Weight variation at 28 days*

Materials	Initial weight (g)	Weight after 28 days (g)
Al5083 aluminium alloy	7.4395	7.4216
316L stainless steel	19.6243	19.6106
A681 (O7) carbon steel	20.1641	20.1165

The corrosion rate for the three tested materials Al5038, 316L, and A681 (O7) have the same rate in the chart comparatively presented with that from the 7 and 14 days since immersion.

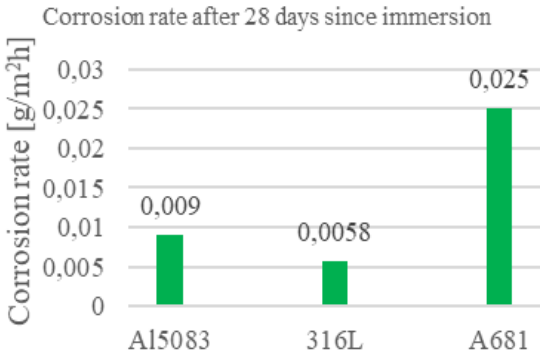

Fig. 2. *The corrosion rate after submerging in seawater for 28 days*

According to the data from Figure 2, it can be observed that after 28 days of immersion in seawater the corrosion rate has the highest value in the case of the O7 carbon steel (0.025 g/m^{2}h). Lower values were obtained for the other materials, like a value of 2.7 times lower for the Al 5038 aluminium alloy i.e., 0.009 g/m^{2}h. The lowest value for the corrosion rate after 7 days of immersion was calculated for the 316L stainless steel (0.0058 g/m^{2}h), a value 4.3 times lower than that calculated for the carbon steel.

Determining the corrosion rate after 89 days since immersion: The variation of the masses of the samples tested in seawater after 89 days of immersion is presented in Table 4. and the corrosion rate for each tested material is presented in Figure 3.

Table 4. *Weight variation at 89 days*

Materials	Initial weight (g)	Weight after 89 days (g)
Al5083 aluminium alloy	7.4395	7.4216
316L stainless steel	19.6243	19.6106
A681 (O7) carbon steel	20.1641	20.1165

The corrosion rate for the three tested materials Al5038, 316L, and A681 (O7) have the same rate in the chart comparatively presented with that from the 7 and 28 days since immersion.

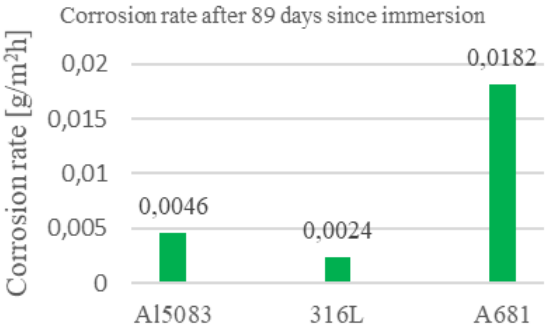

Fig. 3. *The corrosion rate after submerging in seawater for 89 days*

According to the data from figure 3, it can be observed that after 89 days of immersion in seawater the corrosion rate has the highest value in the case of the O7 carbon steel (0.0182 g/m^{2}h). Lower values were obtained for the other materials, like a value of 3.9 times lower for the Al5038 aluminium alloy i.e., 0.0046 g/m^{2}h. The lowest value for the corrosion rate after 7 days of immersion was calculated for the 316L stainless steel (0.0024 g/m^{2}h) a value 7.5 times lower than that calculated for the O7 carbon steel.

THE ANNALS OF "DUNAREA DE JOS" UNIVERSITY OF GALATI
FASCICLE IX. METALLURGY AND MATERIALS SCIENCE
Nº. 2 - 2021, ISSN 2668-4748; e-ISSN 2668-4756
Article DOI: https://doi.org/10.35219/mms.2021.2.07

Micrographs were done with the help of an optical microscope to which a USB digital microscopy camera type OPTIKAM 4083.B1 was attached.

In Figures 4-6, micrographs for the Al5038, 316L, and A681 (O7) materials are presented, before and after immersion for 89 days in seawater.

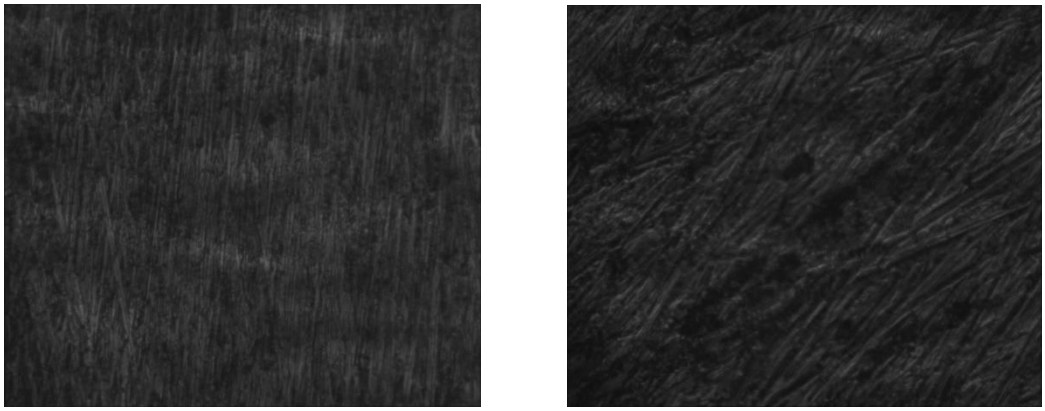

a b

Fig. 4. *Micrographs of Al 5083 alloy in the initial phase (a) and 89 days after immersion (b)*

a b

Fig. 5. *Micrographs of 316L stainless steel in the initial phase (a) and 89 days after immersion (b)*

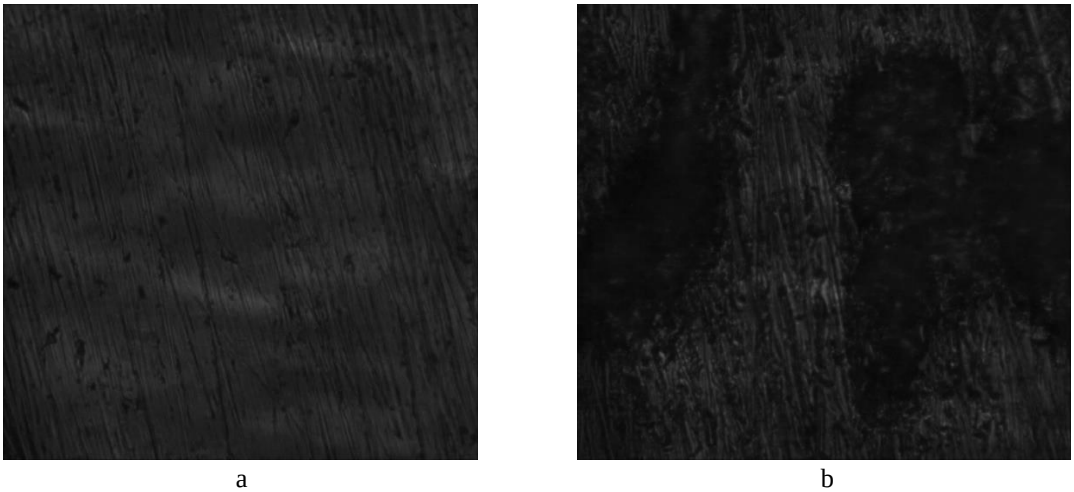

a b

Fig. 6. *Micrographs of A681 type O7 carbon steel in initial phase (a) and 89 days after immersion (b)*

THE ANNALS OF "DUNAREA DE JOS" UNIVERSITY OF GALATI
FASCICLE IX. METALLURGY AND MATERIALS SCIENCE
Nº. 2 - 2021, ISSN 2668-4748; e-ISSN 2668-4756
Article DOI: https://doi.org/10.35219/mms.2021.2.07

It can be observed that a degradation process of the initial surface after the interaction with the seawater appears.

The corrosion that was gravimetrically discovered in the seawater was highlighted by metallographic analyses on the surfaces of the Al5083, 316L, and A681 (O7) materials subjected to corrosion for 89 days. The induced modifications by various corrosion mechanisms to the corrosion material/environment interface were studied by relating to the witness samples (before corrosion). After the 89 days of immersion, the morphology of the samples' surfaces is deeply modified. It is found that the degradation mechanisms of materials due to corrosion are complex. Thus, it can be noticed that the localized corrosion highlighted by corrosion spots – relatively big and small depth portions in the case of the stainless steel, corrosion plates – relatively small but deep surfaces in the case of the carbon steel, and pitting concentrated on small surfaces (with diameters to 100 µm) in the case of aluminium alloy.

Determining the penetration index after 7 days since immersion: Figure 7. represents the penetration index P for the tested materials after being immersed in seawater for 7 days.

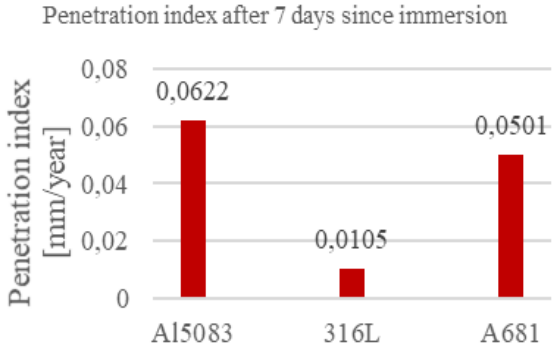

Fig. 7. *Penetration index calculated after 7 days since immersion*

After 7 days of immersion in seawater and after the calculations were done, the highest penetration index was obtained for the Al 5038 aluminium alloy with a value of 0.0622 mm/year. According to Table 1, the Al5038 alloy presents the stability ratio of 5 in the marine environment, which is group III of resistance i.e., stable.

The lowest penetration index was obtained by the 316L stainless steel with a value of 0.0105 mm/year which is also in group III of resistance, meaning that is stable, well usable.

The O7 carbon steel had a close value of the penetration index to that of the aluminium alloy i.e., 0.0501 mm/year, thus proving that the carbon steel also presents the stability ratio of 5 in the marine environment, which is group III of resistance i.e., stable.

Determining the penetration index after 89 days since immersion: Figure 8. represents the penetration index P for the tested materials after being immersed in seawater for 89 days.

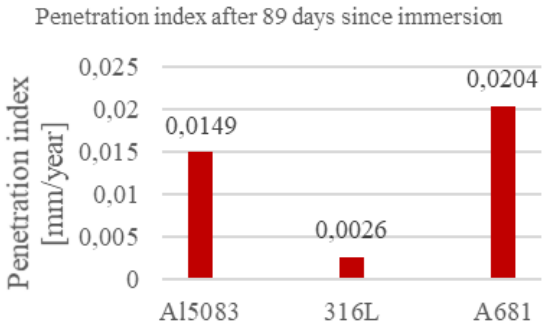

Fig. 8. *Penetration index calculated after 89 days since immersion*

After 89 days of immersion in seawater and after the calculations were done, the highest penetration index was obtained for the O7 carbon steel with a value of 0.0204 mm/year. According to Table 1, the O7 carbon steel presents the stability ratio of 4 in the marine environment, which is group III of resistance that is stable after 89 days since immersion.

The lowest penetration index was obtained by the 316L stainless steel with a value of 0.0026 mm/year, resulting in a stability ratio of 2, which is group II of resistance, that is very stable.

The Al5038 aluminium alloy had a penetration index value of 0.0149 mm/year, this demonstrating that the carbon steel presents the stability ratio of 4 in the marine environment, which is group III of resistance, that is stable.

3.2. Results obtained by the electrochemical method

Tracing and interpreting the Tafel curves give information about the corrosion current's intensity, polarization resistance, and the corrosion rate for the tested systems. The corrosion rate values were calculated with the ratio (3).

The open circuit potential of the 316L stainless steel inclines towards more positive values, suggesting a better corrosion behaviour in the seawater. The open circuit potential for the Al5038 alloy starts from the most negative potential (-670) and increases linear, passing the open circuit potential for the carbon steel.

The potentiodynamic charts for the Al5038 alloy, O7 steel, and 316L steel in the seawater are

THE ANNALS OF "DUNAREA DE JOS" UNIVERSITY OF GALATI
FASCICLE IX. METALLURGY AND MATERIALS SCIENCE
N°. 2 - 2021, ISSN 2668-4748; e-ISSN 2668-4756
Article DOI: https://doi.org/10.35219/mms.2021.2.07

presented in figure 10 and the corresponding values of the corrosion current, polarization resistance, and the calculated Tafel parameters are presented in Table 5.

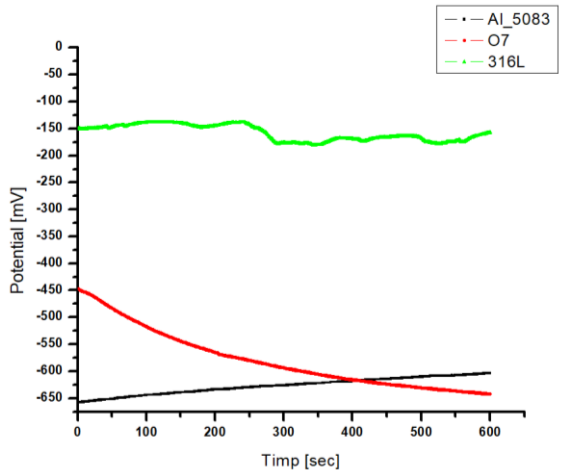

Fig. 9. *Evolution of open circuit potential in the seawater testing solution*

From the presented data, it can be observed that the corrosion potential inclines towards negative values for the O7 carbon steel.

For the tested materials, the lowest corrosion rate in seawater (2.8 μm/year) was obtained for the Al5038 alloy and the highest value of the corrosion rate (41.67 μm/year) for the O7 carbon steel. For the stainless steel, a corrosion rate close to that of the aluminium alloy has been calculated i.e., 4.2 μm/year.

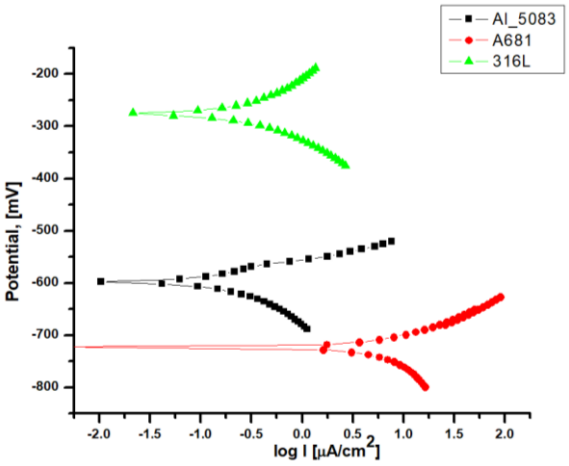

Fig. 10. *Comparative potentiodynamic curves for Al5083 alloy, A681 type O7 carbon steel and 316L stainless steel in seawater*

Table 5. *Corrosion parameters determined from Tafel curves*

Materials	Potential [mV]	Rp [kohm cm^2]	i cor [μA/cm^2]	βa [mV/decade]	βc [mV/decade]	V cor [μm/year]
Al 5083 aluminium alloy	-598.2	76.70	0.2573	48.8	137.9	2.801
A681 carbon steel	-724.0	3.36	3.8484	60.4	107.2	41.670
316L stainless steel	-275.6	61.97	0.3522	124.4	110.5	4.214

4. Conclusions

On the entire research period of 89 days, it was observed how each material, the Al5083 alloy, the 316L stainless steel, and the O7 carbon steel suffered modifications in terms of material density, but also at the materials' surface, these cracking at the surface.

After the studies were finished, which consisted of measuring the corrosion rate, the penetration index of the metals, and the corrosion potential, it was observed that of all materials the least resistant to seawater corrosion is the A681 (type O7) carbon steel, and the most resistant were the Al5038 alloy and the 316L stainless steel.

Marine corrosion can be prevented and the most important factors in preventing marine corrosion are: the project, material selection, cost criteria, manufacturing factors, purchasing criteria, elements of influence due to the construction system, and the mode of operation and maintenance.

References

[1]. Zaki Ahmad, *Principles of Corrosion Engineering and Corrosion Control*, ISBN: 0750659246, Elsevier Science & Technology Books, 2006.
[2]. Féron D., *Corrosion Behaviour and Protection of Copper and Aluminium Alloys in Seawater*, Imprint Woodhead Publishing, ISBN 978-1-84569-241-4, 2017.
[3]. Abdolreza Mostafanejad, Mehdi Iranmanesh, Arman Zarebidaki, *An experimental study on stress corrosion behavior of A131/A and A131/AH32 low carbon steels in simulated seawater*, Ocean Engineering, vol. 188, 106204, 15 September 2019.
[4]. Xiang Wang, Robert E. Melchers, *Corrosion of carbon steel in presence of mixed deposits under stagnant seawater conditions*, Journal of Loss Prevention in the Process Industries, vol. 45, Pages 29-42, January 2017.
[5]. Takumi Kosaba, Izumi Muto, Yu Sugawara, *Effect of anodizing on galvanic corrosion resistance of Al coupled to Fe or type 430 stainless steel in diluted synthetic seawater*, Corrosion Science, vol. 179, 109145, February 2021.

[6]. Yuanyuan Shen, Yaohua Dong, Yi Yang, Qinghong Li, Hongling Zhu, Wenting Zhang, Lihua Dong, Yansheng Yin, *Study of pitting corrosion inhibition effect on aluminium alloy in seawater by biomineralized film*, Bioelectrochemistry, vol. 132, 107408, April 2020.

[7]. Hosni Ezuber, El-Houd A., El-Shawesh F., *A study on the corrosion behavior of aluminium alloys in seawater*, Materials & Design, vol. 29, iss. 4, Pages 801-805, 2008.

[8]. Horațiu Vermeșan, *Coroziune și protecție anticorozivă*, Editura Risoprint, Cluj-Napoca, 2005.

[9]. Shiqiang Chen, Dun Zhang, *Corrosion behavior of Q235 carbon steel in air-saturated seawater containing Thalassospira sp.*, Corrosion Science, vol. 148, p. 71-82, 2019.

[10]. Baoping Cai, Yonghong Liu, Xiaojie Tian, Fei Wang, Hang Li, Renjie Ji, *An experimental study of crevice corrosion behaviour of 316L stainless steel in artificial seawater*, Corrosion Science, vol. 52, iss. 10, p. 3235-3242, October 2010.

[11]. Kemal Nişancioğlu, *Corrosion Behaviour and Protection of Copper and Aluminium Alloys in Seawater*, European Federation of Corrosion (EFC) Series, p. 145-155, 2007.

[12]. Jeenat Aslam, Ruby Aslam, Salhah Hamed Alrefaee, Mohammad Mobin, Afroz Aslam, Mehtab Parveen, Chaudhery Mustansar Hussain, *Gravimetric, electrochemical, and morphological studies of an isoxazole derivative as corrosion inhibitor for mild steel in 1M HCl*, Arabian Journal of Chemistry, vol. 13, iss. 11, p. 7744-7758, November 2020.

[13]. Kuangtsan Chiang, Todd Mintz, *Gravimetric techniques, Techniques for Corrosion Monitoring* (Second Edition), Woodhead Publishing Series in Metals and Surface Engineering, p. 239-254, 2021.

[14]. Teodora Badea, Mihai V. Popa, Maria Nicola, *Știința și ingineria coroziunii*, Editura Academiei Române, ISBN 973-27-0856-5, București, 2002.

[15]. Loto C. A., Fayomi O. S. I., Loto R. T., Popoola A. P. I., *Potentiodynamic Polarization and Gravimetric Evaluation of Corrosion of Copper in 2M H_2SO_4 and its inhibition with Ammonium Dichromate*, Procedia Manufacturing, vol. 35, p. 413-418, 2019.

[16]. Wei Wang, Peter E. Jenkins, Zhiyong Ren, *Electrochemical corrosion of carbon steel exposed to biodiesel/simulated seawater mixture*, Corrosion Science, vol. 57, p. 215-219, April 2012.

[17]. Xin S. S., Li M. C., *Electrochemical corrosion characteristics of type 316L stainless steel in hot concentrated seawater*, Corrosion Science, vol. 81, p. 96-101, April 2014.

THE ANNALS OF "DUNAREA DE JOS" UNIVERSITY OF GALATI
FASCICLE IX. METALLURGY AND MATERIALS SCIENCE
N°. 2 - 2021, ISSN 2668-4748; e-ISSN 2668-4756
Article DOI: https://doi.org/10.35219/mms.2021.2.08

WASTEWATER TREATMENT FOR HEAVY METALS AND DYES USING LOW-COST BIOSORBENTS: A REVIEW

Andreea BONDAREV
Petroleum-Gas University of Ploiesti, Romania
e-mail: andreeabondarev@yahoo.com

ABSTRACT

The pollution of industrial wastewater with heavy metals and dyes is a highly important environmental problem, because of the propagation of the pollution and because of its unfavourable consequences. Sustainable wastewater treatment is one of the foremost challenges of this century. Various waste materials characterized by lignocellulose composition are low cost, non-conventional adsorbent for biosorptive removal of heavy metal ions from aqueous solutions. Recent studies point to the potential of use of low-cost materials (zeolites, carrot residue and green tea waste) as effective sorbents for the removal of Cd^{2+} from aqueous solution. The use of bentonite to the treatment of wastewater containing reactive dyes in aqueous solutions requires the modification of the hydrophilic surface by inorganic cations with organic cations exchange. The use of bentonite as an inexpensive sorbent for the removal of Remazol Brilliant Blue R (RBBR) from synthetic aqueous solutions has been also presented in recent studies. The influence of some parameters such as: pH, initial dye concentration, sorbent dose on sorption kinetics for dye removal has been reviewed in this paper.

KEYWORDS: adsorption, heavy metals, dyes, waste materials, removal

1. Introduction

Wastewater treatment for organic and inorganic pollutants is one of the foremost areas of scientific research involving many fields of science and engineering. According to WHO and UNICEF, 2000 report approximately 70–80% of total illnesses in developing countries are caused by different water contaminants. With the increasing levels of industrial toxic sludge disposal to water bodies, finding environment friendly and affordable treatment methods is a priority. Adsorption is one of the most researched and used wastewater treatment methods for removing heavy metals and dyes. The need for alternative treatment techniques with wide scale applicability led to a new area: the green chemistry or green technology, which dealt with technological interventions for environmental sustainability by focussing on minimizing pollution and use of non-renewable resources [1].

Various waste materials characterized by lignocellulose composition are low cost, non-conventional adsorbent for biosorptive removal of heavy metal ions from aqueous solutions. The sorption of synthetic dyes on solid materials based on wood wastes have been intensively studied. For example, wood sawdust is a promising natural low-cost material for the treatment of polluted wastewater [1, 2].

Efficient removal of heavy metal ions from wastewater has become an important issue in many countries. Conventional methods have been widely used to remove heavy metals from water: chemical precipitation, chemical oxidation, chemical reduction, ion exchange, filtration, electrochemical treatment and evaporation. All of these procedures have some disadvantages, such as high energy requirements, incomplete disposal and the production of toxic sludge or waste that also requires additional treatment [2-8].

Adsorption is an effective method for removing trace pollutants from water. Activated carbon is widely used as an adsorbent support of different metal ions. Activated carbon requires complexing agents to improve its removal performance for inorganic contaminants. These procedures have an important disadvantage: the high cost of the activation process limits the use of activated carbon sorbent in wastewater treatment [4, 8].

Different types of functionalized materials have been developed for the removal of heavy metals ions

THE ANNALS OF "DUNAREA DE JOS" UNIVERSITY OF GALATI
FASCICLE IX. METALLURGY AND MATERIALS SCIENCE
N°. 2 - 2021, ISSN 2668-4748; e-ISSN 2668-4756
Article DOI: https://doi.org/10.35219/mms.2021.2.08

from wastewater: mesoporous and microporous silica, clays or organic polymers [5, 6]. Clinoptilolite occurring in the zeolitic volcanic tuffs is a hydrated alumina–silicate member of the heulandite group. It is widespread in our country and in the whole world. Clinoptilolite incorporation in different biopolymers membranes is an effective method to control the diffusion outside the zeolite crystals and designed composite systems have many opportunities for applications in wastewater treatment [6].

A low-cost adsorbent is defined as a material that is abundant in nature or is a by-product or residual material from an industry domain. Biomass waste, industrial waste and mineral waste have been researched in many studies and biomass has presented better adsorption capacity [2, 7-10]. Plants possess a special cellular mechanism that may be involved in the removal of heavy metals. These include the capacity for metal binding to cell walls and extracellular exudates for chelation of metals by peptides, such as phytochelatins and by metalothioneins [3].

Adsorbents of agricultural origin have polymeric groups like cellulose, hemi-cellulose, pectin, lignin and proteins as active centers for metal uptake. Various waste materials: almond shell residues, date stones, coffee ground, black tea leaves, olive leaves, carrot residue are low cost and non-conventional adsorbent for biosorptive removal of heavy metal ions from aqueous solutions [5, 11-14].

The adsorption of heavy metal ions is as a result of physico-chemical interaction, ion exchange or complex formation between metal ions and functional groups which are present on the cell surface [2]. Different functional groups are involved, such as carboxyl, amine and amides. The ion exchange mechanism takes into account the metal binding pattern and the proton release reaction [2, 15-19]. The absorption of metals and the efficiency of biosorption by the residual biomass depend on the physical and surface properties of the adsorbent, the properties of metal ions and the operating conditions [9-12, 20, 21].

Adsorption is an efficient method for removing reactive dyes. One of this method advantages is the possibility to use a wide variety of synthetic and natural materials at a reduced price [3]. In recent decades, general attention has been paid to unconventional and low-cost materials that include agricultural and industrial by-products and waste [1-3]. Studies in the literature have reported that biosorption could reduce by 20-36% of capital, operating and total cost compared to conventional systems [4-10].

The detection of reactive dyes in the environment can cause serious problems due to their possible toxicity, due to their aromatic structures. These compounds are stable, not biodegradable and they are difficult to remove from industrial effluents before discharging them into emissaries [1]. Different technologies have been developed for the removal of dyes from wastewater: chemical precipitation, adsorption, membrane filtration, coagulation, ion exchange, oxidation process, reverse osmosis, solvent extraction [1-3]. Physical and chemical characteristics of biosorbents are very important to understand potential application of these materials and adsorption mechanism [13, 14]. For example, wooden materials, coconut shell, pineapple leaves, sugar cane bagasse, coffee waste have the highest cellulose contents (>40%) [16-20].

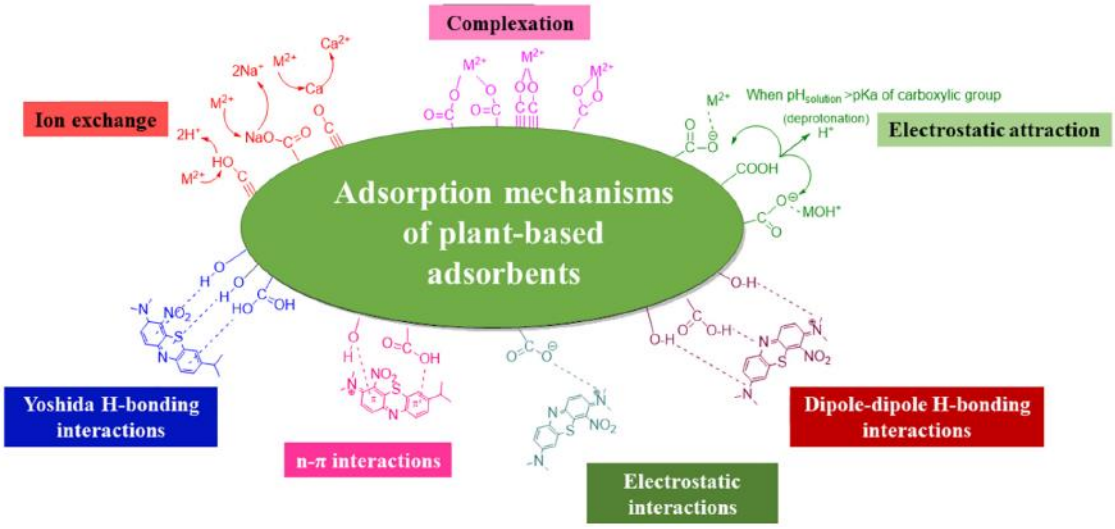

Fig. 1. *Adsorption mechanism of heavy metals and dyes using plant-based adsorbents* [7]

THE ANNALS OF "DUNAREA DE JOS" UNIVERSITY OF GALATI
FASCICLE IX. METALLURGY AND MATERIALS SCIENCE
N°. 2 - 2021, ISSN 2668-4748; e-ISSN 2668-4756
Article DOI: https://doi.org/10.35219/mms.2021.2.08

Researchers have tried to remove heavy metals by using biosorbents; for example, the adsorption process of Cd^{2+} on some adsorbents was studied: clinoptillolite tuff, carrot residue and green tea waste. Carrot residues and tea waste were investigated as unconventional low-cost adsorbent materials for the absorption of Cd^{2+} from contaminated water under different experimental conditions: pH, amount of adsorbent and initial concentration of metal. Equilibrium data were examined using the Langmuir, Freundlich and Temkin isotherm models [21, 22].

Use of bentonite to the treatment of wastewater containing anionic dyes, particularly reactive dyes in aqueous solutions, requires the modification of the hydrophilic surface by inorganic cations with organic cations exchange. The use of bentonite as an inexpensive sorbent for the removal of Remazol Brilliant Blue R (RBBR) from synthetic aqueous solutions has been studied in batch conditions. The influence of some parameters such as: pH, initial dye concentration, sorbent dose on sorption kinetics for dye removal were investigated [21, 22].

2. Biosorptive removal of heavy metals and dyes

2.1. Preparation of the adsorbent supports

Recent research studies presented that clinoptillolite (CLP) and some waste materials: carrot residues (CR) and green tea waste (TW) were used as adsorbents for the removal of cadmium from synthetic wastewater.

Zeolites are crystalline microporous aluminosilicates with ion exchange properties, suitable for a wide range of applications: in catalysis, separation of liquid and gaseous mixtures and in wastewater treatment [6, 22, 23]. The natural CLP sample has the following ideal composition: $[Ca_{1.24}Na_{1.84}K_{1.76}Mg_{0.2}Al_{16}Si_{30}O_{72}(H_2O)_{21.32}]$. Only a selected fraction of clinoptilolite (for example 0.05 mm) was used for the adsorption studies [6].

The cation exchange and/or adsorptive properties of tea and carrot residue can be attributed to the presence of carboxylic, phenolic and other functional groups, which exist in caffein either the cellulosic matrix or in the materials associated with cellulose such as hemicellulose, lignin, peptides [3, 8].

To study the morphology of the clinoptillolite surface, its structure was observed using scanning electron microscopy (SEM). Figure 2 shows SEM image of a clinoptillolite sample and indicates that it has a large distribution of particle size. The presence of nanoparticles and submicron size particles can also be observed from Figure 2.

The carrot residues were dried at 80 °C for 24 hours, grounded to powder and sieved to obtain a homogeneous particle size adsorbent material. To remove soluble components such as tannin or coloring matters, the carrot residue was washed with 0.5 M HCl and deionized distilled water until a constant pH value.

Surface impurities, soluble and coloured ingredients of green tea waste were removed by washing with boiling distilled water. This action was repeated until the solution was colourless. The tea residues were then washed with distilled water and dried in the oven for 12 hours at 105 °C. The dried tea residues were ground and sieved and the fine powder was then used for sorption studies [22].

Data regarding the chemical composition and the content of montmorillonite corresponding to sodium bentonite used in the laboratory experiments for some dyes removals were obtained from the supplier. The ion exchange capacity evaluated from these data was 0.75 g mechiv / 100 g. The laboratory experiments were performed with a grain size fraction of sodium bentonite, with particle sizes less than 200 μm, as it was obtained from the supplier [23].

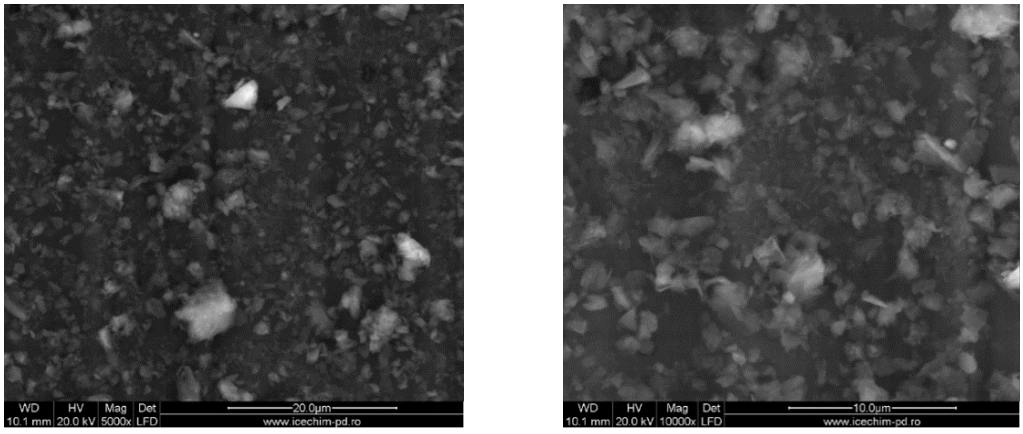

Fig. 2. *SEM micrograph of clinoptillolite (CPL)* [22]

THE ANNALS OF "DUNAREA DE JOS" UNIVERSITY OF GALATI
FASCICLE IX. METALLURGY AND MATERIALS SCIENCE
Nº. 2 - 2021, ISSN 2668-4748; e-ISSN 2668-4756
Article DOI: https://doi.org/10.35219/mms.2021.2.08

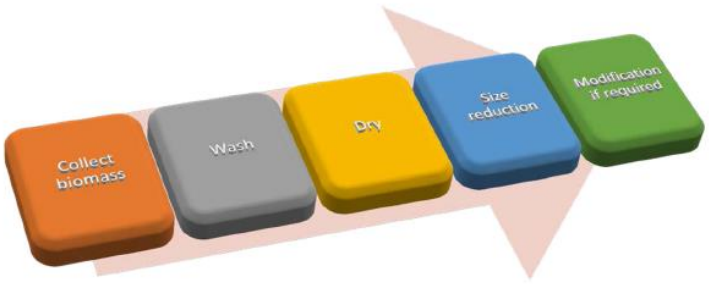

Fig. 3. *General protocol for biosorbent preparation* [8]

2.2. Sorption equilibrium

Analysis of sorption equilibrium data through isotherm models is of paramount importance for designing a biosorption system. Adsorption equilibrium data are important to optimize the parameters which characterize an adsorption system. These data are also useful to provide physico-chemical information to explain the mechanism of adsorption. The absorption capacity of an adsorbent can also be described by the equilibrium sorption isotherm, which is characterized by specific constants, whose values express the surface properties and affinity of an adsorbent [12].

The adsorption capacity q_e (mg/g) after equilibrium was calculated by mass balance relationship equation as follows [4]:

$$q_e = (C_0 - C_e)\, V / W \quad (1)$$

In the relationship equation (1): C_0 (mg/L) is the initial concentration of solute, C_e (mg/L) is the equilibrium metal ion concentration, V is the volume of the aqueous solution (L) and W is the mass of the sorbent used (g).

The percent removal of heavy metal from solution (R%) was calculated by the following equation [4]:

$$\%R = (C_0 - C_e) / C_0 \cdot 100 \quad (2)$$

where C_0 (mg/L) is the initial concentration of metal ion, C_e (mg/L) is the equilibrium metal ion concentration.

The equilibrium between the liquid phase and the solid phase (adsorbent-attached solute) was described in this study by Freundlich, Langmuir and Temkin mathematical models [4, 12].

Freundlich isotherm model can be applied for non-ideal adsorption on heterogeneous surfaces or for multilayer sorption and it is represented by the following equations (Freundlich, 1906) [12-14]:

$$q_e = K_F \cdot C_e^{\,1/n} \quad (2) \text{ original form}$$

$$\lg q_e = \lg K_F + 1/n \lg C_e \quad (3) \text{ linear equation form}$$

where: K_F (mg g^{-1}) and n are Freundlich constants; $1/n$ represents an empirical parameter, which is related to the adsorption intensity; q_e (mg g^{-1}) is the equilibrium sorption concentration of pollutant per gram of adsorbent; C_e (mg L^{-1}) represents the concentration of the solute in solution at equilibrium.

Langmuir isotherm model assumes that the adsorption process occurs at specific homogeneous sites on the adsorbent and it is described by the following equations (Langmuir, 1918) [12, 14].

$$q_e = q_m \cdot K_L \cdot C_e / 1 + K_L \cdot C \quad (4) \text{ original form}$$

$$c/q_e = 1/K_L \cdot q_m + c / q_m \quad (5) \text{ linear equation form}$$

where: q_e (mg g^{-1}) represents the amount of solute adsorbed per amount of adsorbent; C_e (mg L^{-1} or mmol L^{-1}) is the pollutant equilibrium concentration; qm (mg g^{-1}) represents the sorption capacity; K_L (L/mg) is the Langmuir constant related to the adsorption energy (L mg^{-1} or L $mmol^{-1}$).

Temkin isotherm model is represented by the following equation [14]:

$$q = R \cdot T / b_T \cdot \ln (K_T \cdot C_e) \quad (6) \text{ original form}$$

$$q = R \cdot T / b_T \cdot \ln K_T + R \cdot T / b_T \ln C_e \quad (7) \text{ linear equation form}$$

where: K_T (L mg^{-1}) and b_T (KJ/mole) represent Temkin isotherm constants; C_e (mg L^{-1} or mmol L^{-1}) is the pollutant equilibrium concentration.

2.3. Effect of water properties on adsorption of heavy metals and dyes

2.3.1. The adsorption of Cd^{2+}. Effect of initial concentration

The initial concentration is one of the parameters that have an important effect on the

THE ANNALS OF "DUNAREA DE JOS" UNIVERSITY OF GALATI
FASCICLE IX. METALLURGY AND MATERIALS SCIENCE
Nº. 2 - 2021, ISSN 2668-4748; e-ISSN 2668-4756
Article DOI: https://doi.org/10.35219/mms.2021.2.08

removal of adsorbate species from an aqueous solution. (Figure 4).

The effect of the initial concentration of Cd^{2+} on the adsorption rate was investigated for the values of 20, 40, 60 and 80 mg/L. All experiments were performed at room temperature i.e., 22 ± 2 ºC; the amount of adsorbent support was 0.5 g and contact time 24 h [22]

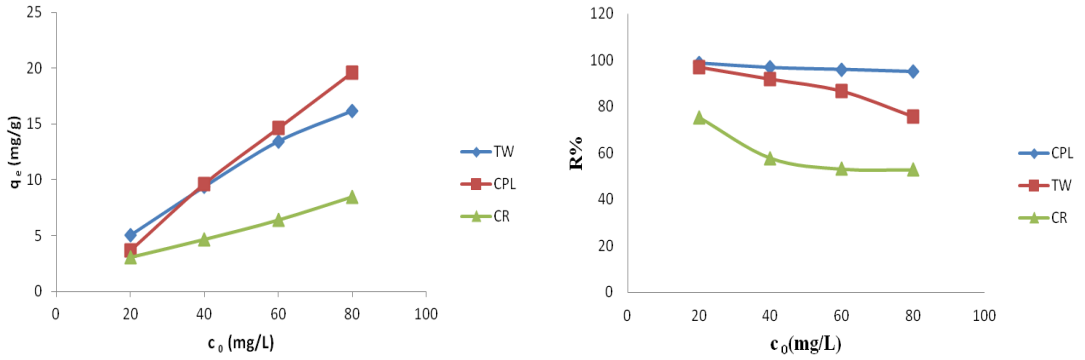

Fig. 4. *Effect of initial concentration of Cd^{2+} on the adsorbent materials (clinoptillolite tuff CPL, carrot residue CR and green tea waste TW)* [22]

The mechanism of metal absorption is especially dependent on the initial concentration of heavy metals: at low concentrations, the metal ions are adsorbed by specific sites; increasing concentration values, specific sites will be saturated and exchange sites will be filled [4].

As the initial cadmium concentrations increase, the percentage of metal removal (R%) decreases. Figure 3 also indicates that CPL and TW had a better percentage elimination than CR.

2.3.2. The adsorption of Cd^{2+}. Effect of adsorbent mass

The amount of adsorbent is also an important parameter in determining the adsorption capacity. As the adsorbent dosage increases, the adsorbent sites available for metal ions are also increased and therefore better adsorption process takes place [13-16].

In the adsorption studies which are presented, the adsorbent mass varied from 0.10 to 1.00 g in 100 mL and 60 mg/L Cd^{+2} solutions, while all the other variables were kept constant.

It was noted that the percentage of Cd^{2+} removal increases according the amount of sorbent mass (Figure 4), the dosage increase of CPL from 0.10 to 1.00 g enhances Cd^{+2} uptake from 69.9 % to 100 %; in case of TW, the percent of metal removal increased from 42.9% to 92.79% and for CR from 66.1% to 80.45%, in the same adsorbent amount interval. The best percentage removal of Cd^{+2} was at about 100%, using CPL as adsorbent and an adsorbent dosage of 0.75 and 1.00 g, in a solution of concentration 60 mg/L Cd^{+2}.

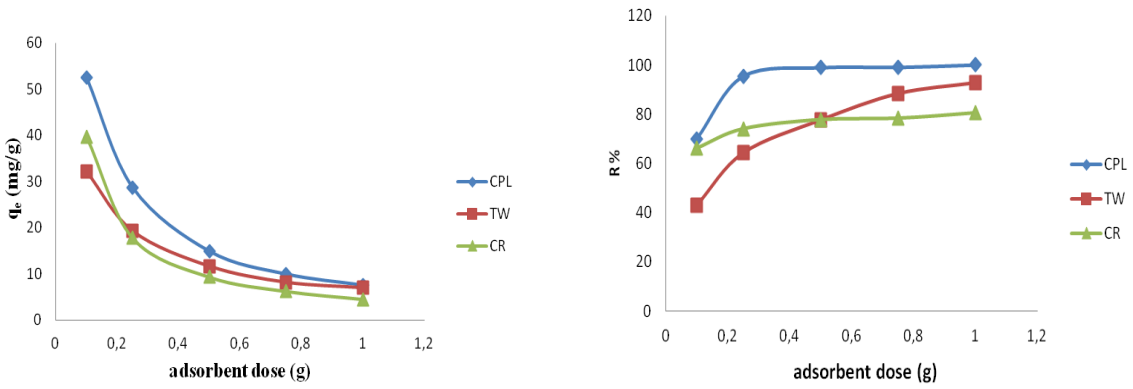

Fig. 5. *Effect of adsorbent mass on the adsorption of Cd^{2+} using different biosorbent materials (clinoptillolite tuff CPL, carrot residue CR and green tea waste TW)* [22]

THE ANNALS OF "DUNAREA DE JOS" UNIVERSITY OF GALATI
FASCICLE IX. METALLURGY AND MATERIALS SCIENCE
Nº. 2 - 2021, ISSN 2668-4748; e-ISSN 2668-4756
Article DOI: https://doi.org/10.35219/mms.2021.2.08

2.3.3. The adsorption of Cd2+. Effect of pH

Solution pH has been reported to be one of the most important variables governing the adsorption of metal ions by an adsorbent. The equilibrium established in solution between metal ions and the sorbent may be described by the following equilibrium [15]:

$$M^{n+} + BH_n \rightleftharpoons BM + n\,H^+ \qquad (8)$$

M represents the metal; n is the metal charge and B is the active sorption sites of the adsorbent [15].

According to equation (8), pH influences metal ion adsorption, due to a competition between the metal ion and H^+ ions for active sorption sites. pH affects the solubility of metal ions and the ionization states of functional groups of the adsorbent material, such as carboxyl and hydroxyl [14, 15].

Equilibrium adsorption experiments at different pH values (3, 6 and 9) were performed to study the effect of pH on Cd^{+2} removal from wastewater. All other variables such as dosage, contact time and temperature were kept constant. The results are illustrated in Figure 5. As it can be observed, Cd^{2+} removal increases with increasing the initial pH of the solution. At lower pH, the concentration of H^+ ion is high, causing a competition for vacant adsorbent site between the H+ ion and heavy metal cations.

From the experiments it was observed that the optimum pH value for the removal of Cd^{+2} was 6, using CPL, TW and CR as adsorbent materials. (Figure 6) The best adsorption results at pH value 6 could be explained because of the cellulose component of the CR adsorbent support, where site binding adsorption might be occurring. From the point of view of an industrial application, this may provide an important advantage, since working at extreme pH would be avoided.

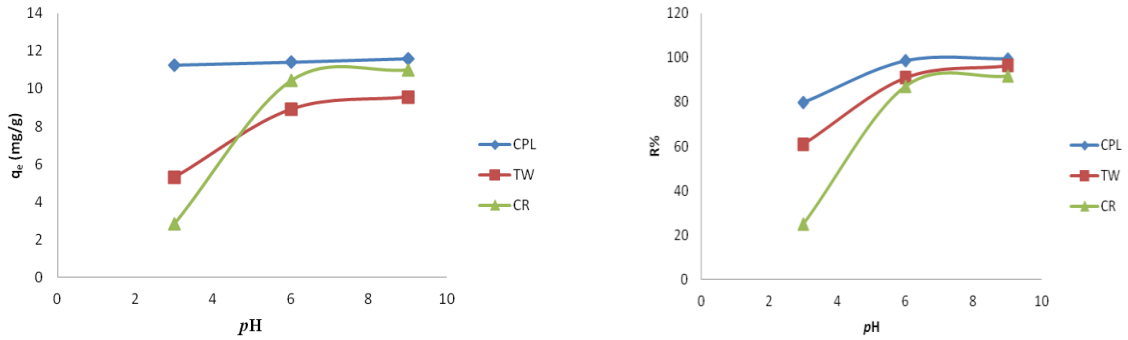

Fig. 6. *Effect of pH on the adsorption of Cd2+ using different materials (clinoptillolite tuff CPL, carrot residue CR and green tea waste TW) [22]*

2.3.4. Adsorption isotherm models for Cd^{2+}

Equilibrium adsorption data are used to determine the maximum capacities of the adsorbents during the experiments of biosorption. The linearized Langmuir, Freundlich and Temkin isotherms of Cd^{2+} are shown in Figures 7-9. The adsorption intensities and adsorption capacities (q_m) were determined from the intercept and slope data, respectively, for each adsorbent.

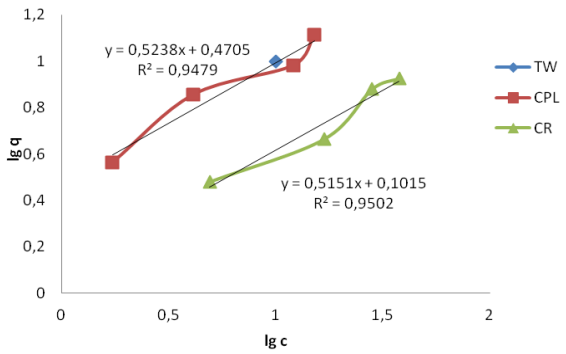

Fig. 7. *Freundlich isotherm of Cd^{2+} removal by different types of adsorbents (clinoptillolite tuff CPL, carrot residue CR and green tea waste TW)* [22]

THE ANNALS OF "DUNAREA DE JOS" UNIVERSITY OF GALATI
FASCICLE IX. METALLURGY AND MATERIALS SCIENCE
Nº. 2 - 2021, ISSN 2668-4748; e-ISSN 2668-4756
Article DOI: https://doi.org/10.35219/mms.2021.2.08

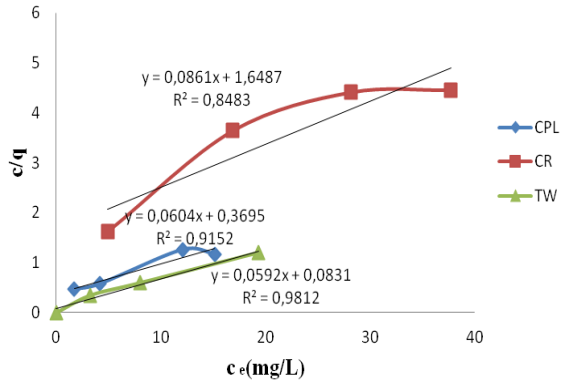

Fig. 8. *Langmuir isotherm of Cd^{2+} removal by different types of adsorbents (clinoptillolite tuff CPL, carrot residue CR and green tea waste TW)* [22]

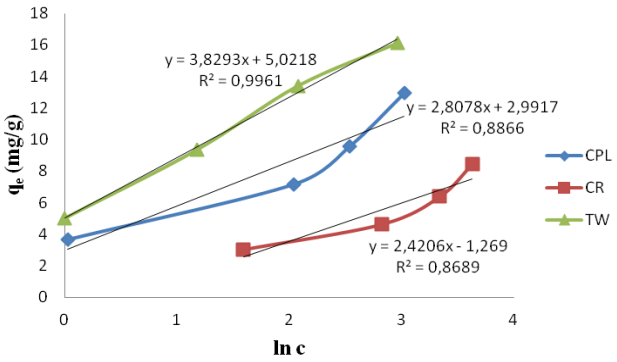

Fig. 9. *Temkin isotherm of Cd^{2+} removal by different types of adsorbents (clinoptillolite tuff CPL, carrot residue CR and green tea waste TW)* [22]

Table 1. *Equilibrium adsorption data for Cd^{2+} sorption on some bio adsorbents* [22-24]

Sorbent	Langmuir Model	Freundlich Model	Temkin Model
Clinoptillolite CPL	R^2 = 0.9152 q_m = 16.55 mg/g K_L = 0.1635 L/mg ΔG = 4.514 KJ/Kmol	R^2 = 0.9479 K_F = 2.95 mg/g n = 2.125	R^2 = 0.8866 K_T = 3.539 L/g b_T = 0.8281 KJ/mol
Carrot residue CR	R^2 = 0.8483 q_m = 11.614 mg/g K_L = 0.0522 L/mg ΔG = 7.357 KJ/Kmol	R^2 = 0.9502 K_F = 1.26 mg/g n = 1.94	R^2 = 0.8689 K_T = 1.688 L/g b_T = 1.006 KJ/mol
Tea waste TW	R^2 = 0.9812 q_m = 16.89 mg/g K_L = 0.7124 L/mg ΔG = 0.848 KJ/Kmol	R^2 = 0.9673 K_F = 6.70 mg/g n = 3.26	R^2 = 0.9961 K_T = 1.57 L/g b_T = 0.6470 KJ/mol
NaOH-modified lemon peel	R^2 = 0.984 q_m = 80.64 mg/g K_L = 0.9910 L/mg ΔG = 0.8 KJ/Kmol	R^2 = 0.917 K_F = 5.58 mg/g n = 6.9	R^2 = 0.8849 K_T = 5.576 L/g b_T = 0.3426 KJ/mol

The results presented in table 1 shows that CPL, NaOH-modified lemon peel and TW exhibited greater adsorption capacities than the values registered for CR adsorbent. It can be observed from the data presented in the Table 1 that the value of 'n' Freundlich specific parameter was greater than 1, which indicates that the adsorption process of Cd(II) on all biosorbents which were tested (CPL, CR and TW) was favourable.

THE ANNALS OF "DUNAREA DE JOS" UNIVERSITY OF GALATI
FASCICLE IX. METALLURGY AND MATERIALS SCIENCE
N°. 2 - 2021, ISSN 2668-4748; e-ISSN 2668-4756
Article DOI: https://doi.org/10.35219/mms.2021.2.08

According to literature studies, the Temkin isotherm considers that the heat of adsorption of molecules would decrease linearly with the coating due to the adsorbed species / adsorbent support interactions [20, 21]. The Temkin b_T (KJ / mol) specific parameter related to the sorption heat is less than 8 for all adsorbents which were tested, indicating a weak interaction between metal and sorbent. [22] The process, as indicated by the Temkin b_T parameter, can be expressed as physiosorption [22-24, 29].

2.4.5. The adsorption of Remazol Brilliant Blue R dye (RBBR). The influence of initial pH

The presence of coloured organic compounds in water causes the decrease in penetration of sun light, that may affect the photosynthetic activity of aquatic plants. Various components of dyes like aromatics, amines are mainly responsible for their toxicity [8].

The use of bentonite as an inexpensive sorbent for the removal of Remazol Brilliant Blue R (RBBR) from synthetic aqueous solutions has been also presented in recent studies. The use of sodium bentonite to the treatment of wastewater containing reactive dyes requires the modification of the hydrophilic surface by inorganic cations with organic cations exchange. The modification of sodium bentonite with organic cations was achieved by ion exchange, according to procedures reported in the literature [23].

The influence of initial pH in the domain 8-11 and the influence of the initial concentration of the reactive dye (concentration domain C_0: 50-100 mg/L) were presented in a research study for the adsorption process of Remazol Brilliant Blue R dye [23].

Figure 10 presents the results of the adsorption tests of RBBR dye at different values of pH. The initial concentration of dye in solution was: C_0 = 50 mg/L and the adsorbent concentration of 10 g/L [23].

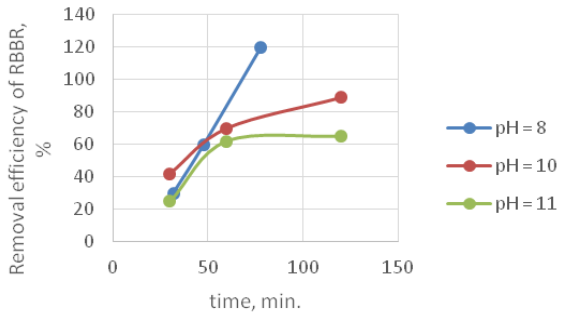

Fig. 10. *The results of the adsorption tests of Remazol Brilliant Blue R (RBBR) dye at different values of pH* [23]

Figure 10 shows that pH of the dye solution is an important factor in the process of adsorption of Remazol Brilliant Blue R (RBBR) anthraquinone dye. In the first part of the process small differences occur in the domain which was studied, but significant differences between the samples can be observed as the contact time increases.

It is obvious that the maximum efficiency was obtained in case of RBBR dye adsorption at pH = 10 (a removal efficiency of 89%, for a contact time of 120 min). This result was taken into consideration for the following experiments of the dye adsorption [23].

2.3.6. The adsorption of Remazol Brilliant Blue R dye (RBBR). The influence of initial concentration of dye solution

Figure 11 presents the data obtained in recent research experiments in which the influence of the initial concentration of dye solution Remazol Brilliant Blue R was studied (for initial dye concentrations of 50 and 100 mg/L at pH 10 and the temperature of 25 °C), on the bentonite sample NaB-S1 (CTAB = 1.3 CEC) [23].

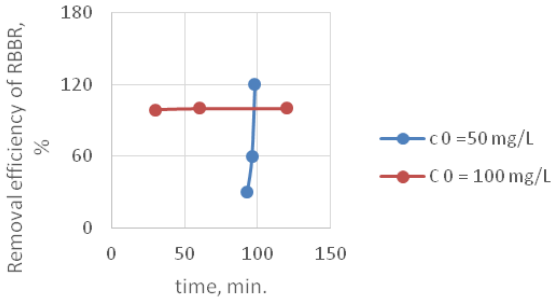

Fig. 11. *The data obtained in experiments with the initial concentration of dye solution Remazol Brilliant Blue R RBBR (C_0 = 50 and 100 mg / L) at pH = 10 and the temperature of 25 °C, on the bentonite sample NaB-S1* [23]

It can be observed that at a concentration of 100 mg / L, the adsorption process is very fast, so that the total removal of the dye takes place in a contact time of 30 min. The comparison of the two sets of samples shows that in case of lower initial concentration (50 mg / L) kinetics of the process is slower, but adsorption efficiency in the first 30 min. of contact is over 90% [23].

In the past few years, an enormous amount of research has been conducted on biosorbents. Uptake capacities of various bio adsorbents for dyes removal are presented in Table 2.

THE ANNALS OF "DUNAREA DE JOS" UNIVERSITY OF GALATI
FASCICLE IX. METALLURGY AND MATERIALS SCIENCE
Nº. 2 - 2021, ISSN 2668-4748; e-ISSN 2668-4756
Article DOI: https://doi.org/10.35219/mms.2021.2.08

Table 2. *Uptake capacities of various bio adsorbents for dyes removal*

Adsorbent	Organic pollutant - dye	Amount adsorbed	References
Orange peel waste	Toluidine blue	314.3 mg/g	[24]
Bentonite	Remazol Brilliant Blue R	198.3 mg/g	[23]
Grapefruit peel	Crystal violet	254.16 mg/g	[25]
Cucumis sativa fruit peel	Malachite green	36.23 mg/g	[26]
Pomelo peel	Methylene blue	133 mg/g	[27]
Activated carbon from pomelo peels	Malachite green	178.43 mg/g	[28]
Coffee wastes carbon and red mud composite	Reactive red	139.5 mg/g	[29]
Sodium alginate and wastes of oil extraction from almond peanut composite	Methyl blue	222.8 mg/g	[30]

3. Conclusions

The pollution of industrial wastewater with heavy metals and dyes is a highly important environmental problem, because of the propagation of the pollution and because of its unfavourable consequences. Sustainable wastewater treatment is one of the foremost challenges of this century.

In the past few years, an enormous amount of research has been conducted on biosorbents. The current review focused on the preparation and applications of waste biomass and zeolite adsorbents for the sequestration of heavy metals and dyes.

Biosorbents, agricultural waste materials and lignocelluloses waste biomass have been widely used for dye and heavy metal sequestration from wastewater.

Due to the low cost and good absorption capacity, the sorbents derived from waste products are promising biosorbent materials. Tea consumption is global and tea waste can be easily purchased, so it can be stated that tea waste has a high potential for applications in wastewater treatment. Carrot residues are also biodegradable and low-cost biosorbents with a good potential to remove heavy metals.

Use of bentonite to the treatment of wastewater containing reactive dyes in aqueous solutions was also presented in this study. The use of bentonite as an inexpensive sorbent for the removal of Remazol Brilliant Blue R (RBBR) from synthetic aqueous solutions was studied in batch conditions. The influence of some parameters such as: pH, initial dye concentration, sorbent mass on sorption kinetics for dye removal were investigated. The research studies presented in this chapter show that bentonite is an effective adsorbent for the removal of Remazol Brilliant Blue R dye from aqueous solutions. There is a variety of aspects that should be taken into account for achieving maximum removal of both dyes and heavy metals. Achieving a combinatorial optimality between the biosorption parameters and removal efficiency remains a challenging task for the researchers.

The reviewed literature proved that instead of many chemicals, non-hazardous materials can be used as heavy metal and dyes removers from wastewaters and industrial effluents to overcome water pollution. The use of non-conventional, low-cost biosorbents has many benefits, including low investment cost, simplicity of operation and a remarkable performance.

Appendices and Nomenclature

Clinoptillolite (CLP)
Carrot residues (CR)
Green tea waste (TW)
Remazol Brilliant Blue R (RBBR)

References

[1]. Ata S., Hamid W., Rukh S., Hamid S., Syed A., Din I., Mohsin I., Turkish Journal of Biochemistry, 37 (3), p. 272-279, 2012.
[2]. Amarasinghe B. M., Williams R. A., Chemical Engineering Journal, 132, p. 299-309, 2007.
[3]. Eslamzadeh T., Nasernejad B., Bonakdar Pour B., Zamani A., Esmaail B. M., Iranian Journal of Science & Technology, Transaction A, 28 (A1), p. 161-167, 2004.
[4]. El-Ashtoukhya E.-S. Z., Amina N. K., Abdelwahabb O., Desalination, 223, p. 162-173, 2008.
[5]. Wingenfelder U., Nowack B., Furrer G., Schulin R., Water Research 39, 200, p. 3287-3297.
[6]. Horsfall M., Spiff A., Acta Chim. Slov., 52, p. 174-181, 2005.
[7]. Tunali S., Cabuk A., Akar T., Chemical Engineering Journal, 115, p. 203-211, 2006.

[8]. Yadav S., Yadav A., **Bagotia N., Sharma A., Kumar S.**, Journal of Water Process Engineering, 42, 102148, 2021.
[9]. Cay S., Uyanik A. Ozajik, Sep. Purif. Technol. 38, p. 273-280, 2004.
[10]. Egila J. N., Dauda B., Jimoh T., African Journal of Biotechnology, 9(48), p. 8192-8198, 2010.
[11]. Razmovski R., Ciban M., Ecological Engineering, 34, p. 179-186, 2008.
[12]. Mondal M. K., Journal of Environmental Management, 90, p. 3266-3271, 2009.
[13]. Ibrahima H., Jamila T., Hegazyb E., Journal of Hazardous Materials, 182, p. 842-847, 2010.
[14]. Ozdes D., Duran C., Senturk H., Journal of Environmental Management, 92, p. 3082-3090, 2011.
[15]. Suteu D., Zaharia C., Chemical Bulletin of "Politehnica" University of Timisoara, Romania, Series of Chemistry and Environmental Engineering, 56(70), p. 85, 2011.
[16]. Jacob J. S., Roberto L.-R., Rivera J., Ocampo R., Cerino-Cordova F., Sustainable Environment Research, 27, p. 32, 2017.
[17]. Subramani S. E., Thinakaran N., Process Safety and Environmental Protection, 106, p. 1, 2017.
[18]. Auta M., Hameed B. H., Chem. Eng. J., 175, p. 233, 2011.
[19]. Malik R., Ramteke D. S., Wate S. R., Waste Management, 27, p. 1129, 2007.
[20]. Paul S. A., Chavan S. K., Oriental Jr. Chem., 27, p. 4, 2011.
[21]. Singha B., Das S. K., Colloids and Surfaces B, 107, p. 97, 2013.
[22]. Bondarev A., Pantea O., Mihai S., Calin C., Gheorghe C. G., REV.CHIM., 67 (4), p. 728-733, 2016.
[23]. Bombos D., Ganea R., Matei V., Marinescu C., Bondarev A., Mihai S., Natu T., Tamas I., REV. CHIM. (Bucharest), 65 (8), p. 976-982, 2014.
[24]. Lafi R., Rezma S., Hafiane A., *Removal of toluidine blue from aqueous solution using orange peel waste (OPW)*, Desalin. Water Treat., p. 1-12, 2014.
[25]. Owamah H., Chukwujindu I., Asiagwu A., *Biosorptive capacity of yam peels waste for the removal of dye from aqueous solutions*, Civil Environ. Res., 3, p. 36-47, 2013.
[26]. Santhi T., Manonmani S., *Malachite green removal from aqueous solution by the peel of Cucumis sativa fruit*, Clean Soil Air Water, 39, p. 162-170, 2011.
[27]. Hou S., *Adsorption properties of pomelo peels against methylene blue in dye wastewater*, Adv. Mater. Res., 634-638, p. 178-181, 2013.
[28]. Bello O. S., Ahmad M. A., Semire B., *Scavenging malachite green dye from aqueous solutions using pomelo (Citrus grandis) peels: kinetic, equilibrium and thermodynamic studies*, Desalin. Water Treat., p. 1-15, 2014.
[29]. Bello K., Sarojini B. K., Narayana B., Rao A., Byrappa K., *A study on adsorption behavior of newly synthesized banana pseudo-stem derived superabsorbent hydrogels for cationic and anionic dye removal from effluents*, Carbohydr. Polym., 181, p. 605-615, 2018.
[30]. Erfani M., Javanbakht V., *Methylene Blue removal from aqueous solution by a biocomposite synthesized from sodium alginate and wastes of oil extraction from almond peanut*, Int. J. Biol. Macromol., 114, p. 244-255, 2018.

MANUSCRISELE, CĂRŢILE ŞI REVISTELE PENTRU SCHIMB, PRECUM ŞI ORICE CORESPONDENŢE SE VOR TRIMITE PE ADRESA:

MANUSCRIPTS, REVIEWS AND BOOKS FOR EXCHANGE COOPERATION, AS WELL AS ANY CORRESPONDANCE WILL BE MAILED TO:

LES MANUSCRIPTS, LES REVUES ET LES LIVRES POUR L'ECHANGE, TOUT AUSSI QUE LA CORRESPONDANCE SERONT ENVOYES A L'ADRESSE:

MANUSCKRIPTEN, ZIETSCHRITFTEN UND BUCHER FUR AUSTAUCH SOWIE DIE KORRESPONDENZ SID AN FOLGENDE ANSCHRIFT ZU SEDEN:

After the latest evaluation of the journals by the National Center for Science Policy and Scientometrics (**CENAPOSS**), in recognition of its quality and impact at national level, the journal will be included in the B^+ category, 215 code (http://cncsis.gov.ro/userfiles/file/CENAPOSS/Bplus_2011.pdf).

The journal is already indexed in:

DOAJ: https://doaj.org/

SCIPIO-RO: http://www.scipio.ro/web/182206

EBSCO: http://www.ebscohost.com/titleLists/a9h-journals.pdf

Google Academic: https://scholar.google.ro

Index Copernicus: https://journals.indexcopernicus.com

Crossref: https://search.crossref.org/

The papers published in this journal can be viewed on the website: http://www.gup.ugal.ro/ugaljournals/index.php/mms

Name and Address of Publisher:
Contact person: Elena MEREUȚĂ
Galati University Press - GUP
47 Domneasca St., 800008 - Galati, Romania
Phone: +40 336 130139
Fax: +40 236 461353
Email: gup@ugal.ro

Name and Address of Editor:
Prof. Dr. Eng. Marian BORDEI
"Dunarea de Jos" University of Galati, Faculty of Engineering
111 Domneasca St., 800201 - Galati, Romania
Phone: +40 336 130208
Phone/Fax: +40 336 130283
Email: mbordei@ugal.ro

AFFILIATED WITH:

- THE ROMANIAN SOCIETY FOR METALLURGY
- THE ROMANIAN SOCIETY FOR CHEMISTRY
- THE ROMANIAN SOCIETY FOR BIOMATERIALS
- THE ROMANIAN TECHNICAL FOUNDRY SOCIETY
- THE MATERIALS INFORMATION SOCIETY (ASM INTERNATIONAL)

Edited under the care of the FACULTY OF ENGINEERING

Annual subscription (4 issues per year)

Fascicle DOI: https://doi.org/10.35219/mms

Volume DOI: https://doi.org/10.35219/mms.2021.2

Editing date: 15.06.2021
Number of issues: 200
Printed by Galati University Press (accredited by CNCSIS)
47 Domneasca Street, 800008, Galati, Romania